

การพัฒนาสารประกอบพอร์ไฟริน-พอลิไดอะเซทิลีนเป็นสารไวแสงในเซลล์สุริยะชนิดสารอินทรีย์

นาย ชวัลวิทย์ เจริญประยูร

วิทยานิพนธ์นี้เป็นส่วนหนึ่งของการศึกษาตามหลักสูตรปริญญาวิทยาศาสตรมหาบัณฑิต

สาขาวิชาปิโตรเคมีและวิทยาศาสตร์พอลิเมอร์

คณะวิทยาศาสตร์ จุฬาลงกรณ์มหาวิทยาลัย

ปีการศึกษา 2553

ลิขสิทธิ์ของจุฬาลงกรณ์มหาวิทยาลัย

DEVELOPMENT OF PORPHYRIN-POLYDIACETYLENE COMPOUNDS AS  
PHOTOSENSITIZERS IN ORGANIC SOLAR CELLS

Mr. Chawanwit Reanprayoon

A Thesis Submitted in Partial Fulfillment of the Requirements  
for the Degree of Master of Science Program in Petrochemistry and Polymer Science  
Faculty of Science  
Chulalongkorn University  
Academic Year 2010  
Copyright of Chulalongkorn University

Thesis Title                    DEVELOPMENT OF PORPHYRIN-POLYDIACETYLENE  
  COMPOUNDS AS PHOTSENSITIZERS IN ORGANIC  
  SOLAR CELLS

By                                    Mr. Chawanwit Reanprayoon

Field of Study                    Petrochemistry and Polymer Science

Thesis Advisor                    Assistant Professor Patchanita Thamyongkit, Ph.D.

Thesis Co-advisor                Associate Professor Mongkol Sukwattanasinitt, Ph.D.

---

Accepted by the Faculty of Science, Chulalongkorn University in Partial  
Fulfillment of the Requirements for the Master's Degree

..... Dean of the Faculty of Science  
(Professor Supot Hannongbua, Dr.rer.nat.)

THESIS COMMITTEE

.....Chairman  
(Assistant Professor Warinthorn Chavasiri, Ph.D.)

..... Thesis Advisor  
(Assistant Professor Patchanita Thamyongkit, Ph.D.)

.....Thesis Co-Advisor  
(Associate Professor Mongkol Sukwattanasinitt, Ph.D.)

.....Examiner  
(Associate Professor Voravee Hoven, Ph.D.)

.....External Examiner  
(Nantanit Wanichacheva, Ph.D.)

ชวัลวิทย์ เจริญประยูร : การพัฒนาสารประกอบพอร์ไฟริน-พอลิไดอะเซทิลีนเป็น  
 สารไวแสงในเซลล์สุริยะชนิดสารอินทรีย์. (DEVELOPMENT OF PORPHYRIN-  
 POLYDIACETYLENE COMPOUNDS AS PHOTSENSITIZERS IN  
 ORGANIC SOLAR CELLS) อ.ที่ปรึกษาหลัก : ผศ. ดร.พัชณิตา ธรรมมงคลกิจ, อ.ที่  
 ปรึกษาร่วม : รศ.ดร. มงคล สุขวัฒนาสินินิทธิ, 89 หน้า.

สารประกอบพอร์ไฟรินเป็นสารที่มักใช้เป็นตัวเลือกสำหรับเซลล์สุริยะเนื่องจากมีค่าการ  
 ดูดกลืนแสงที่สูง สมบัติทางกายภาพเชิงแสงที่สามารถปรับได้ และความเป็นไปได้ในการ  
 ปรับเปลี่ยนโครงสร้างทางโมเลกุล งานวิจัยนี้ได้สังเคราะห์พอร์ไฟรินที่มีหมู่แทนที่ที่ตำแหน่งมีโซ  
 เป็นหมู่ไดอะเซทิลีน ที่มีและไม่มีหมู่เกาะพื้นผิวชนิดคาร์บอกซิล การนำพอลิไดอะเซทิลีนมาต่อ  
 กับโครงสร้างของพอร์ไฟรินถูกคาดว่าจะช่วยเพิ่มการดูดกลืนแสงในช่วง 500–600 นาโนเมตร  
 ซึ่งเป็นช่วงแสงที่พอร์ไฟรินดูดกลืนได้น้อย ทำให้โมเลกุลเรียงตัวเป็นฟิล์มที่มีระเบียบมากขึ้น และ  
 มีความสามารถในการละลายที่สูงขึ้น พอร์ไฟรินที่มีไดอะเซทิลีนต่อที่ตำแหน่งมีโซทั้ง 4 ตำแหน่ง  
 จะถูกนำไปใช้ในเซลล์สุริยะแบบ Bulk heterojunction ส่วนในกรณีที่พอร์ไฟรินมีไดอะเซทิลีนต่อที่  
 ตำแหน่งมีโซ 3 ตำแหน่ง ตำแหน่งมีโซที่เหลือจะถูกแทนที่ด้วยหมู่เกาะพื้นผิวชนิดคาร์บอกซิล  
 และสารประกอบนี้จะถูกนำมาใช้ในเซลล์สุริยะชนิดสีย้อม นอกจากนี้ สารประกอบเปรียบเทียบกับที่  
 มีหมู่แทนที่ที่ตำแหน่งมีโซ เป็นสายโซ่แอลคิลสายยาวชนิดอิมิตัวยังถูกสังเคราะห์และนำมา  
 ศึกษาเปรียบเทียบกับอนุพันธ์ที่มีไดอะเซทิลีนอีกด้วย

สาขาวิชา ปิโตรเคมีและวิทยาศาสตร์พอลิเมอร์ ปลายมือชื่อนิติ.....  
 ปีการศึกษา.....2553..... ปลายมือชื่ออ.ที่ปรึกษาวิทยานิพนธ์หลัก.....  
 ปลายมือชื่ออ.ที่ปรึกษาวิทยานิพนธ์ร่วม.....

# # 5072249223 : PETROCHEMISTRY AND POLYMER SCIENCE

KEYWORDS : PORPHYRIN / POLYDIACETYLENE / PHOTOSENSITIZER /  
ORGANIC SOLAR CELL.

CHAWANWIT REANPRAYOON : DEVELOPMENT OF PORPHYRIN-  
POLYDIACETYLENE COMPOUNDS AS PHOTOSENSITIZERS IN  
ORGANIC SOLAR CELLS. ADVISOR : ASST. PROF. PATCHANITA  
THAMYONGKIT, Ph.D. CO-ADVISOR : ASSOC. PROF. MONGKOL  
SUKWATTANASINITT , Ph.D., 89 pp.

Porphyritic compounds have been known to be potential candidate for organic solar cells, owing to their large molar absorption coefficients, tunable photophysical properties, and amenability to molecular modification. In this research, synthesis of a series of diacetylene meso-substituted porphyrins with and without carboxyl anchoring group was pursued. The incorporation of polydiacetylene in the porphyritic structure is expected to provide enhanced absorption at 550–600 nm where the porphyrin has limited absorptivity, improved film uniformity and enhanced solubility. The porphyrin bearing diacetylene units at all 4 meso positions will be used in bulk heterojunction solar cell.

In case of the porphyrin having 3 diacetylene chains, the remaining meso position will be replaced by a carboxyl anchoring group and the compound will be used in dye-sensitized solar cells. Furthermore, benchmark compounds bearing long saturated alkyl meso-substituents were also synthesized and investigated in comparison with the diacetylene containing derivatives.

Field of Study: Petrochemistry and Polymer science Student's Signature:.....

Academic Year: .....2010.....

Advisor's Signature:.....

Co-advisor's Signature:.....

## ACKNOWLEDGEMENTS

I would like to begin by thanking Assistant Professor Dr. Patchanita Thamyongkit, Associate Professor Dr. Mongkol Sukwattanasinitt and Associate Professor Dr. Amorn Petsom for being the best advisors anyone could ever ask for. There are no words that can express the depth of gratitude that I have towards them. They have supported me whole heartedly in everything that I set out to improve the synthetic skills, believe in me even at the moments of my life when I was down and help me to get back on my feet.

I am also grateful to Assistant Professor Dr. Warinthorn Chavasiri, for serving as the chairman, and Associate Professor Dr. Voravee Hoven, Associate Professor Dr. Mongkol Sukwattanasinitt and Dr. Nantanit Wanichacheva for serving as members of my thesis committee, and all for their valuable suggestion and comments.

I thank Center of Petroleum, Petrochemicals, and Advanced Materials and Graduate School of Chulalongkorn University, Marie Curie International Incoming Fellowship (PIIF-GA-2008-220272), Thailand Research Fund-Master Research Grants-Window II (TRF-MRG-WII 515S043) for partial financial support to conduct this research.

I also thank Research Centre for Bioorganic Chemistry (RCBC) for warm welcome into their family, great experience and laboratory facilities. I feel blessed and very privileged to have joined a group with great members who supported me throughout this course.

Finally, I am grateful to my family for their love, understanding, and great encouragement throughout the entire course of my study.

# CONTENTS

	<b>Page</b>
<b>ABSTRACT (THAI)</b> .....	iv
<b>ABSTRACT (ENGLISH)</b> .....	v
<b>ACKNOWLEDGEMENTS</b> .....	vi
<b>CONTENTS</b> .....	vii
<b>LIST OF FIGURES</b> .....	ix
<b>LIST OF SCHEMES</b> .....	xii
<b>LIST OF CHARTS</b> .....	xiii
<b>LIST OF ABBREVIATIONS</b> .....	xiv
<b>CHAPTER I INTRODUCTION</b> .....	1
1.1 Objectives of Research.....	4
1.2 Scope of Research.....	4
<b>CHAPTER II THEORY AND LITERATURE REVIEWS</b> .....	6
<b>THEORY</b> .....	6
2.1 Organic Solar Cells.....	6
2.2 Bulk Heterojunction Solar Cell.....	7
2.3 Dye-sensitized Solar Cells.....	9
2.4 Measurements for Solar Cell Performance.....	10
2.5 Molecular Design of Photosensitizers.....	11
2.6 Porphyrin.....	12
2.7 Polydiacetylene.....	14
<b>LITERATURE REVIEWS</b> .....	15
<b>CHAPTER III EXPERIMENTAL</b> .....	18
3.1 Chemicals.....	18
3.2 Analytical Instruments.....	19
3.3 Experimental Procedure.....	19
3.3.1 5,10,15,20-Tetra(4-carboxyphenyl)porphyrin ( <b>3</b> ).....	19
3.3.2 1-amino-10,12-pentacosadiyne ( <b>8</b> ).....	20
3.3.3 Synthesis of Compound <b>1</b> via Acid Chloride Formation.....	21
3.3.4 Synthesis of Compound <b>1</b> and <b>2</b> via Succinimide Formation.....	21
3.3.5 Compounds <b>Zn-1</b> and <b>Zn-2</b> .....	22

	<b>Page</b>
3.3.6 tetracosan-1-amine ( <b>13</b> ).....	23
3.3.7 Synthesis of Compounds <b>14</b> , <b>15</b> , <b>Zn-14</b> and <b>Zn-15</b> .....	24
<b>CHAPTER IV RESULTS AND DISCUSSION</b> .....	26
4.1 Synthesis of Porphyrin-diacetylene Compounds for Organic Solar Cells.....	26
4.2 Synthesis of Benchmark Compounds of Compounds <b>Zn-1</b> and <b>Zn-2</b>	30
4.3 Polymerization of Porphyrin-diacetylene Compound <b>Zn-1</b> .....	32
4.4 Study of the Polymerization of Porphyrin-diacetylene using Raman Spectroscopy.....	33
4.5 Photophysical and Electrochemical Properties.....	33
4.5.1 Compound <b>Zn-1</b> . ....	33
4.5.2 Compound <b>Zn-2</b> . ....	36
<b>CHAPTER V CONCLUSION</b> .....	39
<b>REFERENCES</b> .....	40
<b>APPENDICES</b> .....	44
Appendix A.....	45
Appendix B.....	74
<b>VITA</b> .....	89



## LIST OF FIGURES

Figure		Page
2-1	Chemical structures and abbreviations of some conjugated organic molecules. (a) poly(acetylene) or PA, (b) poly(para-phenylene-vinylene) or PPV (c) a substituted PPV (MDMO-PPV) (d) poly(3-hexyl thiophene) or P3HT (e) a C <sub>60</sub> derivative PCBM. In each compound, one can identify a sequence of alternating single and double bonds.....	7
2-2	Structural design for a thin film photovoltaic device.....	8
2-3	Energy diagram of bulk heterojunction solar cells.....	9
2-4	Schematic mechanism of DSSC.....	10
2-5	Photocurrent-photovoltage curve of the organic solar cell.....	11
2-6	The ways of anchoring of photosensitizer on nanocrystalline TiO <sub>2</sub> surface.....	12
2-7	Structures of naturally occurring porphyrin derivatives.....	13
2-8	UV-Visible absorption spectrum of porphyrin.....	14
2-9	The topological polymerization of diacetylene monomer.....	15
2-10	Synthesis of tetracarboxyphenylporphyrin (TCPP) using Alder's method.....	15
2-11	Porphyrin-DA molecule and time dependence of the UV-Vis spectral change upon UV irradiation.....	16
2-12	Binding geometry of tetrachelate porphyrin on metal oxide surface....	17
4-1	UV-visible spectra of a <b>Zn-1</b> film before (solid line) and after radiation (dashed line) at 254 nm.....	32
4-2	Raman spectra of <b>Zn-1</b> .....	33
4-3	Comparative energy diagram of compound <b>Zn-1</b> -based BHJ-SC.....	34
4-4	Photoluminescence study of the films .....	35
4-5	A schematic cell structure of BHJ-SC based on <b>Zn-1</b> .....	35
4-6	Comparative energy diagram of compound <b>Zn-2</b> -based DSSC.....	37

<b>Figure</b>		<b>Page</b>
4-7	A schematic cell structure of a DSSC based on <b>Zn-2</b> .....	38
A-1	<sup>1</sup> H-NMR spectrum of compound <b>3</b> .....	46
A-2	<sup>1</sup> H-NMR spectrum of compound <b>7</b> .....	47
A-3	<sup>1</sup> H-NMR spectrum of compound <b>8</b> .....	48
A-4	Mass spectrum of compound <b>1</b> via acid chloride formation.....	49
A-5	Mass spectrum of an ester derivative of compound <b>2</b> .....	50
A-6	<sup>1</sup> H-NMR spectrum of compound <b>1</b> via succinimide formation.....	51
A-7	Mass spectrum of compound <b>1</b> via succinimide formation.....	52
A-8	<sup>1</sup> H-NMR spectrum of compound <b>2</b> .....	53
A-9	Mass spectrum of compound <b>2</b> .....	54
A-10	<sup>1</sup> H-NMR spectrum of compound <b>Zn-1</b> .....	55
A-11	<sup>13</sup> C-NMR spectrum of compound <b>Zn-1</b> .....	56
A-12	Mass spectrum of compound <b>Zn-1</b> .....	57
A-13	<sup>1</sup> H-NMR spectrum of compound <b>Zn-2</b> .....	58
A-14	<sup>13</sup> C-NMR spectrum of compound <b>Zn-2</b> .....	59
A-15	Mass spectrum of compound <b>Zn-2</b> .....	60
A-16	<sup>1</sup> H-NMR spectrum of compound <b>12</b> .....	61
A-17	<sup>13</sup> C-NMR spectrum of compound <b>12</b> .....	62
A-18	Mass spectrum of compound <b>12</b> .....	63
A-19	<sup>1</sup> H-NMR spectrum of compound <b>13</b> .....	64
A-20	<sup>13</sup> C-NMR spectrum of compound <b>13</b> .....	65
A-21	Mass spectrum of compound <b>13</b> .....	66
A-22	Mass spectrum of compound <b>14</b> .....	67
A-23	Mass spectrum of compound <b>15</b> .....	68
A-24	<sup>1</sup> H-NMR spectrum of compound <b>Zn-14</b> .....	69

<b>Figure</b>		<b>Page</b>
A-25	Mass spectrum of compound <b>Zn-14</b> .....	70
A-26	<sup>1</sup> H-NMR spectrum of compound <b>Zn-15</b> .....	71
A-27	<sup>13</sup> C-NMR spectrum of compound <b>Zn-15</b> .....	72
A-28	Mass spectrum of compound <b>Zn-15</b> .....	73
B-1	Absorption spectrum of compound <b>1</b> .....	75
B-2	Emission spectrum of compound <b>1</b> .....	76
B-3	Absorption spectrum of compound <b>2</b> .....	77
B-4	Emission spectrum of compound <b>2</b> .....	78
B-5	Absorption spectrum of compound <b>Zn-1</b> .....	79
B-6	Emission spectrum of compound <b>Zn-1</b> .....	80
B-7	Absorption spectrum of compound <b>Zn-2</b> .....	81
B-8	Emission spectrum of compound <b>Zn-2</b> .....	82
B-9	Absorption spectrum of compound <b>Zn-14</b> .....	83
B-10	Emission spectrum of compound <b>Zn-14</b> .....	84
B-11	Absorption spectrum of compound <b>15</b> .....	85
B-12	Emission spectrum of compound <b>15</b> .....	86
B-13	Absorption spectrum of compound <b>Zn-15</b> .....	87
B-14	Emission spectrum of compound <b>Zn-15</b> .....	88

**LIST OF SCHEMES**

<b>Scheme</b>		<b>Page</b>
4-1	Synthesis of compound <b>1</b> via acid chloride formation.....	27
4-2	Synthesis of compounds <b>1</b> and <b>2</b> via succinimide formation.....	29
4-3	Synthesis of compound <b>13</b> .....	30
4-4	Synthesis of compounds <b>Zn-14</b> and <b>Zn-15</b> .....	31

**LIST OF CHARTS**

<b>Chart</b>		<b>Page</b>
1-1	Target porphyrin-diacetylene compounds.....	4
4-1	Ion fragment of a) <b>Zn-1</b> and b) <b>Zn-2</b> .....	28

**LIST OF ABBREVIATIONS**

$\lambda_{\text{abs}}$	:	absorption wavelength
calcd	:	calculated
$^{13}\text{C-NMR}$	:	carbon-13 nuclear magnetic resonance spectroscopy
$\delta$	:	chemical shift
$\text{CHCl}_3$	:	chloroform
$J$	:	coupling constant
$^{\circ}\text{C}$	:	degree Celsius
$\text{CDCl}_3$	:	deuterated chloroform
d	:	doublet (NMR)
$\lambda_{\text{em}}$	:	emission wavelength
$\lambda_{\text{ex}}$	:	excitation wavelength
g	:	gram (s)
Hz	:	hertz (s)
HOMO	:	Highest Occupied Molecular Orbital
h	:	hour (s)
LUMO	:	Lowest Unoccupied Molecular Orbital
MS	:	mass spectrometry
MALDI-TOF-MS	:	matrix-assisted laser desorption ionization mass spectrometry
max	:	maximum
$\lambda_{\text{max}}$	:	maximum wavelength
$\text{CH}_2\text{Cl}_2$	:	methylene chloride
$\mu\text{L}$	:	microliter (s)
mg	:	milligram (s)
mL	:	milliliter (s)
mmol	:	millimole (s)
min	:	minute
$\epsilon$	:	molar absorptivity
m	:	multiplet (NMR)

nm	:	nanometer
NMR	:	nuclear magnetic resonance spectroscopy
obsd	:	observed
ppm	:	parts per million
PCBM	:	Phenyl-C61-butyric acid methyl ester
PEDOT:PSS	:	Polyethylenedioxythiophene:polystyrenesulfonate
P3HT	:	Poly(3-hexyl thiophene)
<sup>1</sup> H-NMR	:	proton nuclear magnetic resonance spectroscopy
S	:	singlet (NMR)
TEA	:	triethylamine
t	:	triplet (NMR)
UV/Vis	:	ultraviolet and visible spectroscopy

# CHAPTER I

## INTRODUCTION

When the economic growth and population are rapidly increased, demands of energy become one of the top problems in the world. The energy consumption is made up of about 86% fossil fuels, 6% hydroelectricity, 6% nuclear power and tiny fraction from biomass and solar energy sources.<sup>(1)</sup> Fossil fuels are causing environmental pollution. Nuclear energy from nuclear fission is considered very dangerous and limited due to lack of safety support. Therefore, development of using renewable energy has become an important topic for scientists, and solar energy is one of the most popular sources of choice.

Solar collectors and modules are designed to capture the sun energy and change it into more usable forms such as heat or electricity. Sunlight can be converted directly to electricity by devices called a photovoltaic cell or solar cell. Four generations of solar cell can separate by types of photoactive materials. The first generation of solar cells is based on single crystal silicon (c-Si). The advantages of this generation are high carrier mobilities, broad spectral absorption range, and having small band gap (1.1 eV). However, disadvantages of c-Si solar cell are requiring the expensive manufacturing technologies and high energy process for affording c-Si, and environmental hazard. The second generation of solar cells uses thin-film deposits of semiconductors for reduces mass of material. General semiconductors to employ in this cell are amorphous silicon deposited on stainless-steel ribbon, polycrystalline silicon or cadmium telluride (CdTe) deposited on glass, and copper indium gallium diselenide (CIGS) alloy. The cells in this generation are lower manufacturing costs, reduced mass, and allow fitting panels on light or flexible materials. The problems of this generation are, however, lower efficiencies when compared with silicon, and amorphous silicon is not stable. The third generation is using a semiconductor very different from the previous semiconductor devices. The devices in the third generation include nanocrystal solar cells, photoelectrochemical cells, dye-sensitized solar cells, and polymer solar cells. Nanocrystal solar cells based on a silicon substrate with a coating of nanocrystals, and silicon substrate with small grains of



quantum dots, is a semiconductor nanostructure and using for the confines the motion of conduction band electrons, valence band holes or excitons. Thin-film of nanocrystals is obtained by a process known as “spin-coating”, and solar cells having high current potential. Photoelectrochemical cell has a consists of a semiconductor photoanode and a metal cathode immersed in an electrolyte such as  $K_3Fe(CN)_6/K_4Fe(CN)_6$  and iodide/triiodide. The charge separation of these cells is not solely provided by the semiconductor, but works in concert with the electrolyte. The Grätzel cells are a dye-sensitized photoelectrochemical cells, and photoelectrons provided from separate photosensitive dye. These cells using ruthenium metal organic complexes as photosensitizers, and having overall peak power production represents a conversion efficiency of about 10–12%.<sup>(2)</sup> Grätzel photoelectrochemical cell has attractive replacement for existing technologies in “low density” applications like the rooftop solar collectors, and working even in low-light conditions. The disadvantages are the low efficiencies when compared with silicon (c-Si) solar cells and the efficiency is decreased over time due to the environmental effects. The photoelectrochemical cells suffer from degradation of the electrodes from the electrolyte. This type of cell is often included in dye sensitized solar cells (DSSCs), wherein the dye molecules occurred photoexcitation, photocurrent is produced from charge separation to the electrode. This cell is similar to Grätzel cell except the electrolyte is replaced with a conductive polymer. The typical DSSC used titanium dioxide coated and sintered on a transparent semi-conducting oxide (ITO), and employ the polymeric conductor such as PEDOT or PEDOT:TMA, which carries electrons from the counter electrode to the oxidized dye. The last type in this generation is polymer solar cells or bulk heterojunction solar cell (BHJ-SC) which is the organic solar cells using an organic polymer and/or organic molecule as light absorber molecules. These cells do not need to use electrolyte solution as same as DSSCs. The advantages of these cells are lightweight, disposable, inexpensive to fabricate, flexible, and designable on the molecular level. These cells are given the energy band gap about 2 eV, and show the efficiency near 5%. In polymer cells are low material cost, and solution is processable. The last generation of solar cell is hybrid between nanocrystal/polymer cells. This cell using of polymers with nanoparticles mixed together

to make a single multispectrum layer and significant advances in hybrid solar cells gave followed the development of elongated nanocrystal rods and branched nanocrystals. This cell was using the Si, In, CuInS<sub>2</sub>, CdSe in solid state nanocrystals, and embedded in light absorbing polymer, *i.e.* P3HT. The p-type, polymeric conductor, such as PEDOT:PSS carries “holes” to the counter electrode is coated on a transparent semi-conducting oxide (ITO). The advantages of this generation are lower material cost, printable nanocrystals on a polymer film, and improved the conversion efficiency. However, the efficiencies are lower compared to silicon (c-Si) solar cells and degradation of potential similar to polymer cells.

Porphyrins are a class of naturally occurring macrocyclic aromatic compounds. Due to their large  $\pi$ -conjugation system, porphyrins exhibit high stability and high absorptivity at about 400–500 nm. Porphyrins have proven to be useful in several application, such as photocatalysis,<sup>(3)</sup> various medical applications,<sup>(4)</sup> and optoelectronic devices,<sup>(5)</sup> etc.

Polydiacetylene (PDA) is an ene-yne conjugated polymer consisting of double and triple bonds in its backbone. It is normally prepared via a topological 1,4-addition polymerization of diacetylene monomer by heat, UV-light or  $\gamma$  rays.<sup>(6)</sup> PDA possesses several interesting optical properties, including solvatochromism, thermochromism and mechanochromism. Polydeacetylene have strong absorption at 550–600 nm where porphyrins generally have relatively low absorptivity.

This research focuses on the development of organic polymers containing porphyrin and polydiacetylene as photosensitizing materials for DSSC and BHJ-SC. The corporation of polydiacetylene, obtained from photopolymerization of diacetylene compound, in the structure provides thermal stability and strong absorption at 550–600 nm which is the region porphyrins have limited absorptivity. According to a previous study,<sup>(7)</sup> the porphyrins are expected to serve as a template for the photopolymerization of diacetylene while the polydiaceylene should increase the solubility of the molecule and broaden the absorption range.

## 1.1 Objective of Research

The objective of this research is the development of organic polymers containing porphyrin and polydiacetylene as photosensitizing materials for organic solar cells (Chart 1-1).

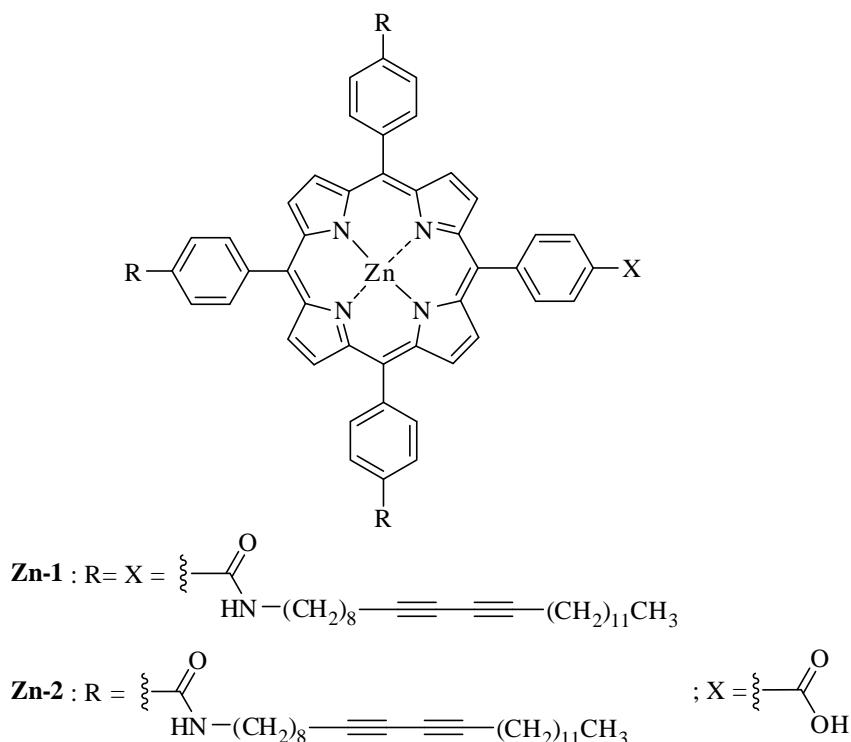


**Chart 1-1:** Target porphyrin-diacetylene compounds.

## 1.2 Scope of Research

The scope of this research covers the synthesis of porphyrins containing 3–4 diacetylene chains at the meso positions via amido linkages. The porphyrin bearing diacetylene units at all 4 meso positions will be used in BHJ-SCs. In case of the porphyrin having 3 diacetylene chains, the remaining meso position will be replaced by a carboxyl anchoring group and the compound will be used in DSSCs. Moreover, two derivatives of these porphyrins bearing  $\text{C}_{24}$ -saturated alkyl chains will be also synthesized as benchmark compounds. These compounds will be fully characterized by spectroscopic techniques, *i.e.* matrix-assisted laser desorption ionization mass

spectrometry (MALDI-TOF-MS),  $^1\text{H}$ -NMR and  $^{13}\text{C}$ -NMR spectroscopy, and absorption and emission spectrophotometry. In addition, their photo physical and electrochemical properties, and the performance of the solar cells based on these compounds will be investigated.

## CHAPTER II

### THEORY AND LITERATURE REVIEWS

#### THEORY

##### 2.1 Organic Solar Cells

Organic materials had been intensively developed in the direction to get a long-term technology providing solar cells that have large area, high conversion efficiency, economically effective production and are environmentally friendly. Organic semiconductors are a less expensive alternative to inorganic semiconductors like Si as having extremely high optical absorption coefficients which offer the possibility for the production of very thin solar cells. Additional attractive features of organic photovoltaics are the possibilities for flexible devices which can be fabricated using high throughput, low temperature approaches that employ well established printing techniques in a roll-to-roll process.<sup>(8,9)</sup> This possibility of using flexible plastic (or polymer) substrates in an easily scalable high-speed printing process can reduce the balance of system cost for organic photovoltaics, resulting in a shorter energetic pay-back time.

The electronic structure of all organic semiconductors is based on conjugated  $\pi$ -electrons. A conjugated organic system is made of an alternation between single and double carbon-carbon bonds. Single bonds are known as  $\sigma$ -bonds and are associated with localized electrons, and double bonds contain a  $\sigma$ -bond and a  $\pi$ -bond. The  $\pi$ -electrons are much more mobile than the  $\sigma$ -electrons, they can jump from site to site between carbon atoms thanks to the mutual overlap of  $\pi$ -orbitals along the conjugation path, which causes the wave functions to delocalize over the conjugated backbone. The  $\pi$ -bands are either empty (called Lowest Unoccupied Molecular Orbital - LUMO) or filled with electrons (called Highest Occupied Molecular Orbital - HOMO). The band gap of these materials ranges from 1 to 4 eV. This  $\pi$ -electron system has all the essential electronic features of organic materials: light absorption and emission, charge generation and transport. Figure 2-1 shows several examples of well-known conjugated organic molecules.

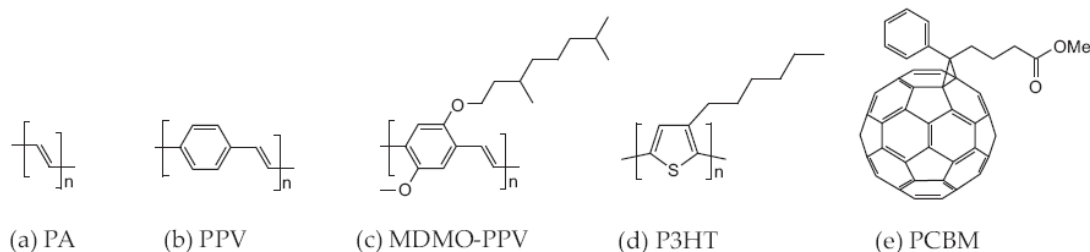


**Figure 2-1:** Chemical structures and abbreviations of some conjugated organic molecules: (a) poly(acetylene) or PA, (b) poly(*para*-phenylene-vinylene) or PPV (c) a substituted PPV (MDMO-PPV) (d) poly(3-hexyl thiophene) or P3HT (e) a C<sub>60</sub> derivative PCBM. In each compound, one can identify a sequence of alternating single and double bonds.

According to the types of solar cells described in Chapter 1, this research focuses on the synthesis of the photoactive compounds for BHJ-SCs and Grätzel cells or DSSCs. The detailed device structure and operation of these two cells are explained here in the following sections.

## 2.2 Bulk Heterojunction Solar Cell

A typical bulk heterojunction solar cell consists of a photoactive layer sandwiched between two different electrodes, one of which should be transparent in order to allow the incoming photons to reach the photoactive layer, as seen in Figure 2-2. This photoactive layer is based on a single, a bi-layer, or a mixture of two (or more) components. Upon light absorption the charge carriers are generated inside the photoactive layer and due to the presence of an electric field, provided by the asymmetrical ionization energies/work functions of the electrodes (anode and cathode), these charges are transported and collected into the external circuit. In this way, an organic solar cell converts light into electricity.

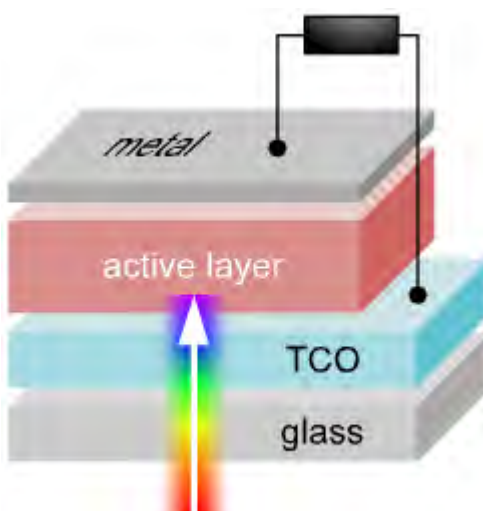


**Figure 2-2:** Structural design for a thin film photovoltaic device.<sup>(10)</sup>

Most of the developments that have improved the performance of organic PV devices are based on donor/acceptor heterojunctions. The idea behind a heterojunction is to use two materials with different electron affinities and ionization potentials. In the planar of heterojunction, the organic donor/acceptor interface separates excitons much more efficient than an organic/metal interface in the single layer device. The energy diagram of bulk heterojunction solar cells is shown in the Figure 2-3. Sunlight photons which are absorbed inside the device excite the donor molecule, directing to the creation of excitons. In some cases, the acceptor phase can also absorb light. The electron starts to diffuse within the donor phase (HOMO to LUMO) to LUMO of acceptor phase and cathode by order. At the same time, the hole is transporting to the anode. Subsequently, the separated free electrons (and electron-holes) are transported with the support of the internal electric field, caused by the use of electrodes with different work functions, towards the cathode (anode) where they are collected by the electrodes and driven into the external circuit.

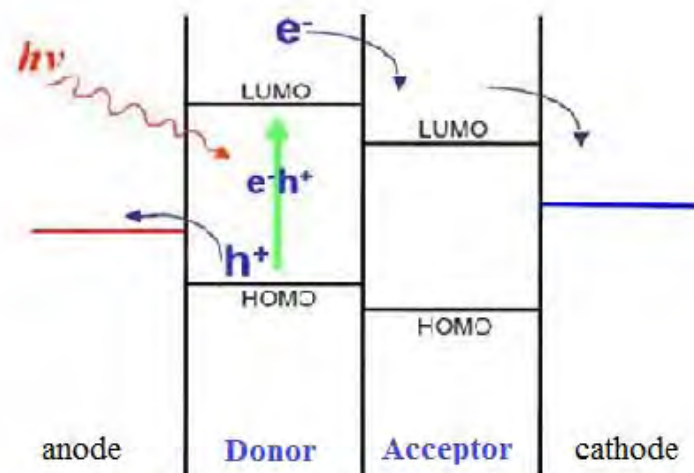


**Figure 2-3:** Energy diagram of bulk heterojunction solar cells.

### 2.3 Dye-Sensitized Solar Cells

A dye-sensitized solar cell (DSSC) can be considered as a hybrid version of photogalvanic cells and solar cells based on semiconductor electrodes. The cell consists of a dye-coated semiconductor electrode and a counter electrode arranged in a sandwich configuration and the inter-electrode space is filled with an electrolyte containing a redox mediator as shown in Figure 2-4.<sup>(11,12)</sup> In several researches, the researchers used a polypyridine complex of Ru as a dye sensitizer, nanocrystalline  $\text{TiO}_2$  as a semiconductor and an  $\text{I}_2/\text{I}_3^-$  solution as a redox mediator.<sup>(13)</sup> The reactions occur in a dye sensitized solar cell are schematically illustrated in Figure 2-4. Optical excitation of the dye with visible light leads to excitation of the dye to an excited state that undergoes electron transfer, injecting electrons into the conduction band of the semiconductor. The oxidized dye is subsequently reduced back to the ground state by the electron donor present in the electrolyte. The electrons in the conduction band collect at the electrode and subsequently pass through the external circuit to arrive at the counter electrode where they effect the reverse reaction of the redox mediator.<sup>(11,12)</sup>



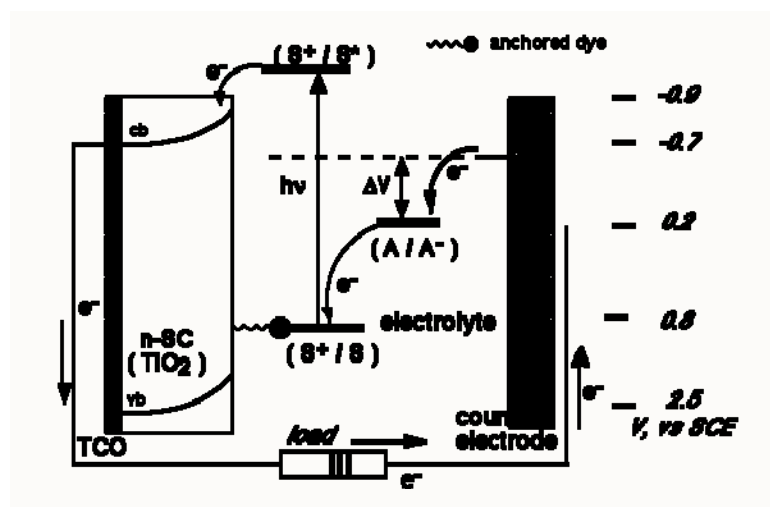


Figure 2-4: Schematic mechanism of DSSC.<sup>(14)</sup>

## 2.4 Measurements for Solar Cell Performance

The solar cell performance is given by two key parameters, one is the incident photon to current conversion efficiency (IPCE) for monochromatic radiation and the other is overall white light-to-electrical conversion efficiency ( $\eta$ ). The IPCE value is the ratio of the observed photocurrent divided by the incident photon flux, uncorrected for reflective losses during optical excitation through the conducting glass electrode.

$$\text{IPCE} = \frac{\text{no. of electron flowing through the external circuit}}{\text{no. of photons incident}} \quad (1)$$

The IPCE value can be considered as the effective quantum yield of the device. It is the product of three factors: (a) light harvesting efficiency (depend on the spectral and photophysical properties of the dye), (b) the charge injection (depend on the excited state redox potential and the exciton lifetime), and (c) the charge collection efficiency (depend on the structure and morphology of the  $\text{TiO}_2$  or ITO layer). The overall efficiency of the photovoltaic cell can be obtained as a product of the short circuit photocurrent density ( $J_{sc}$ ), the open circuit voltage ( $V_{oc}$ ), the fill factor (FF) and the intensity of the incident light ( $I_s$ ) according to the following equation.

$$\eta = (J_{sc} V_{oc} \text{FF})/I_s \quad (2)$$

$J_{sc}$  and  $V_{oc}$  are determined from the photocurrent-photovoltage curve of the cell (Figure 2-5). The FF was calculated according to equation 1,

$$FF = J_{max}V_{max}/ J_{sc}V_{oc} \quad (3)$$

where  $J_{max}$  and  $V_{max}$  were determined from the point of the curve that the product of J and V is maximum.

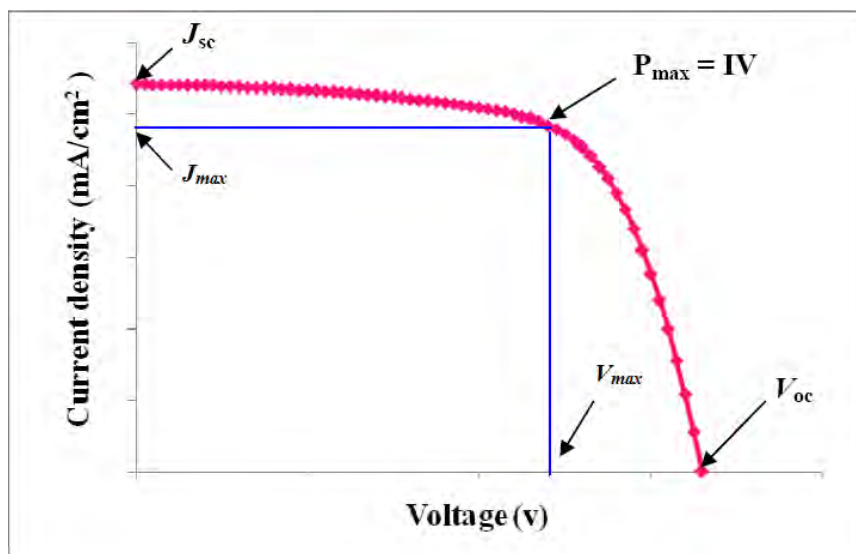


**Figure 2-5:** Photocurrent-photovoltage curve of the organic solar cell.

## 2.5 Molecular Design of Photosensitizers

There are several factors for design molecule of dyes for organic solar cell:

a) Spectra properties to ensure maximal visible light absorption

The dye should absorb all of the visible and near IR photons of the sunlight incident on earth. This research, for example, uses porphyrins having strong absorption at 420 nm and PDA exhibiting strong absorption at 550–600 nm where the porphyrins have limited absorption.

b) Redox properties in ground and excited states

Efficient charge injection from the excited state of the dye into the conduction band of  $TiO_2$  depends on the redox potential of the dye in the excited state. The energy level of the excited state should be higher than conduction band of the  $TiO_2$  to minimize energetic losses during the electron transfer reaction.

c) Anchoring group<sup>(15)</sup>

Dye sensitizer must carry attachment groups such as carboxylate or phosphonate to firmly graft it on the semiconductor oxide surface. Figure 2-6 showed different ways of anchoring of the dye via carboxylate onto the  $\text{TiO}_2$  surface (M).

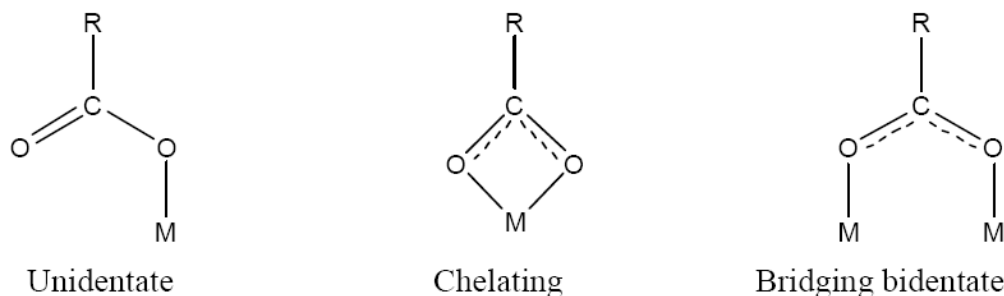


**Figure 2-6:** The ways of anchoring of photosensitizer on nanocrystalline  $\text{TiO}_2$  surface.

#### d) Solubility

The dye should be soluble in common organic solvents for loading of the dye into device.

## 2.6 Porphyrins

The porphyrins are a class of naturally occurring macrocyclic aromatic compounds and are ubiquitous in our world. On account of their large  $\pi$ -conjugated system, all porphyrins are intensely colored. As such, they have been called the pigments and the colors of life. This auspicious designation reflects their importance in numerous biological functions. Indeed, life as we understand it relies on the full range of biological processes that are either performed by or catalyzed by porphyrin-containing substances. Complexes of many metals with various porphyrins play a key role in biological activities as for instance iron complexes in the haemoprotein and cytochrome C, magnesium complexes in the chlorophylls, and a cobalt complex in Vitamin  $\text{B}_{12}$  (Figure 2-7).

In haemoglobins and myoglobins, haem is the prosthetic group which is responsible for oxygen transport and storage in living tissues. Furthermore, haem can also be found in cytochrome C to function in an array of reactions as a single electron carrier in the electron transport chain and as a catalyst for redox reactions.<sup>(16)</sup> The reduction of one of the pyrrole units on the porphyrin ring leads to the formation of a

class of porphyrin derivatives called “Chlorins”. Chlorophylls are chlorin pigments which are structurally similar to and produced through the same metabolic pathway as haem. They are found abundantly in green plants as photosynthetic reaction centers which convert light energy into chemical energy while producing oxygen along the way.

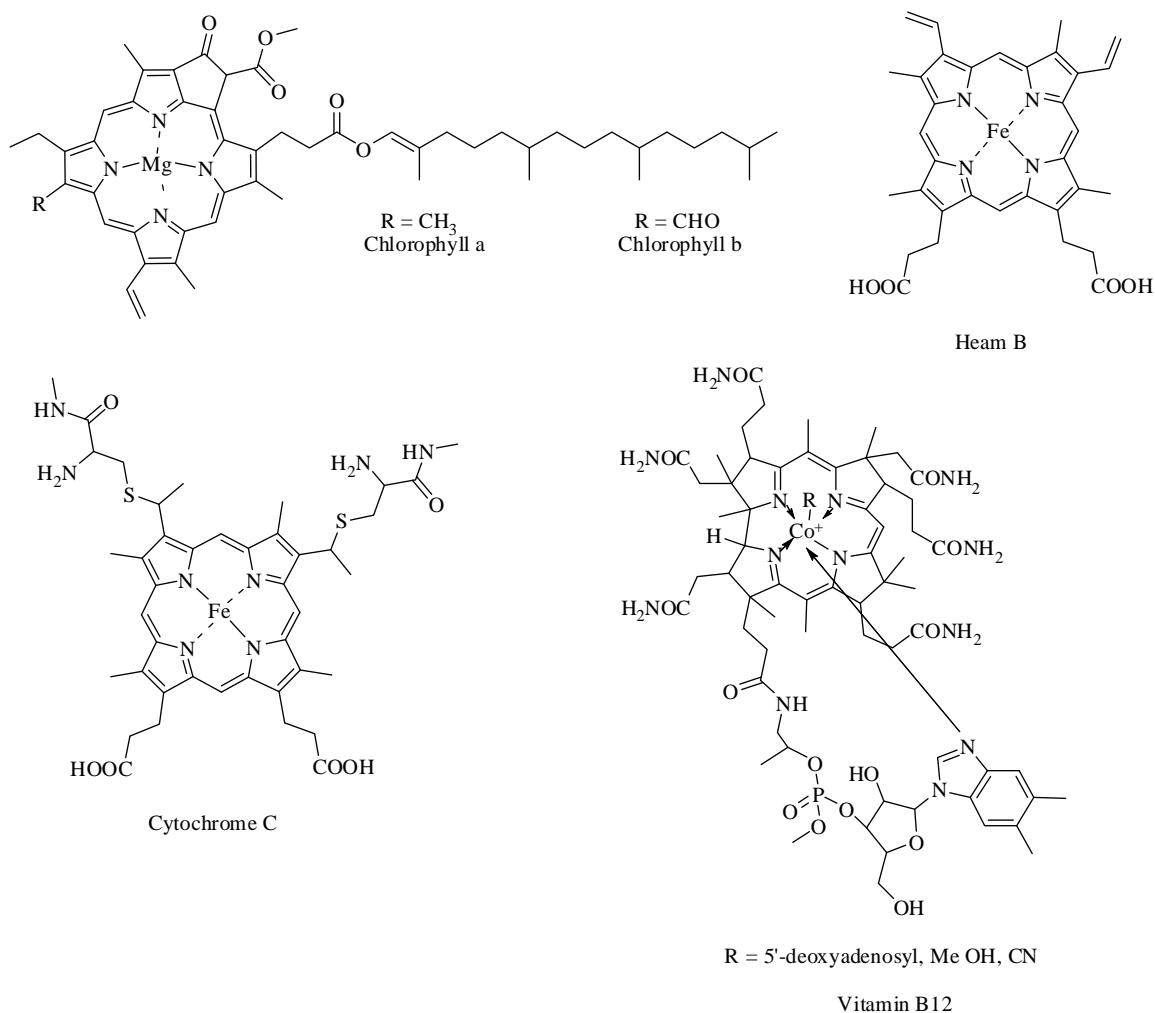


**Figure 2-7:** Structures of naturally occurring porphyrin derivatives.

Nowadays, these molecules remain of fundamental interest to chemists and biochemists. In recent years, a number of porphyrin derivatives have been synthesized and studied to determine and imitate the electron or energy transfer mechanisms of natural photosynthetic reaction centers and light harvesting complexes.<sup>(17)</sup> In addition, porphyrin derivatives have been widely proven heretofore in relation to photocatalysts,<sup>(18)</sup>

optical sensors,<sup>(19)</sup> organic semiconductors,<sup>(20)</sup> and optoelectronic devices such as photovoltaic cells,<sup>(5)</sup> organic light emitting diodes.<sup>(21)</sup>

Porphyrin and their derivatives are highly absorbing strongly in the visible region near 420 nm, known as a Soret band, and several weaker absorption bands, known as Q bands, between 450–700 nm (Figure 2-8). A variation in the peripheral substituents of the porphyrin ring normally results in a change in the intensity and wavelength of the absorption bands. A disrupted porphyrin macrocycle results in the disappearance of the Soret band. Each tetrapyrrolic system is unique and therefore different in color. Naturally occurring porphyrins are dark, red while chlorin that are reduced tetrapyrrolic systems are dark green or blue green.

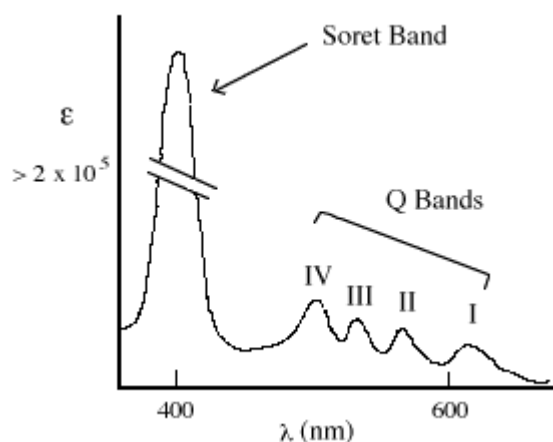


**Figure 2-8:** UV-Visible absorption spectrum of porphyrin.

## 2.7 Polydiacetylene

Poly(diacetylene) (PDA) is one of polymers that has been extensively investigated since 1969 due to its excellent optical, electrical, and sensing properties. One of the most important properties of PDA arises from its mode of polymerization, topological photopolymerization.<sup>(22)</sup> The topological polymerization is a polymerization of diacetylene monomers which were aligned within a suitable position<sup>(23)</sup> (Figure 2-9). Upon UV irradiation at 254 nm, well aligned diacetylene (DA) can undergo 1,4-photopolymerization to form conjugate polymer with alternating ene-yne backbone structure. The resulting polymer is intensely colored, typically a deep blue. PDAs show different phases such as well-known blue ( $\lambda_{\text{max}}$ : ~640 nm) and red ( $\lambda_{\text{max}}$ : ~530 nm)

phases. Moreover, the blue phase can change to the red phase upon external stimuli, such as pH, temperature, solvent, mechanical stress and ligandreceptor interaction.<sup>(24)</sup>

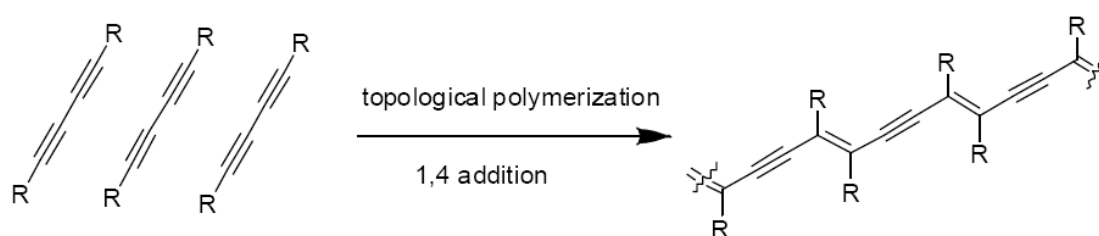


**Figure 2-9:** The topological polymerization of diacetylene monomer.

### Literature reviews

Adler, A. D. *et al.*<sup>(25)</sup> reported the use of refluxing propionic acid instead of sealed tubes chemistry to reproducibly synthesize a 20–25% yield of 5,10,15,20-tetra(4-carboxyphenyl)porphyrin (TCPP). This trivial procedure concerned the addition of equimolar amounts of pyrrole and benzaldehyde to refluxed propionic acid; after heating for about one half hour, the mixture was allowed to cool and the product TPP was filtered off (Figure 2-10). This procedure has been widely used when large amounts of porphyrins are needed and the corresponding aldehydes are able to survive under the condition of refluxed propionic acid.

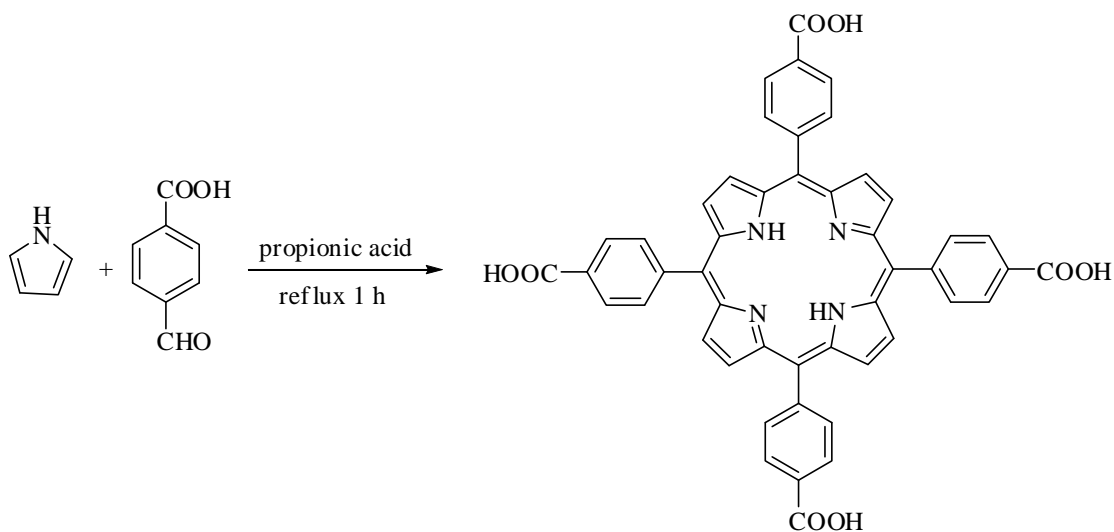


**Figure 2-10:** Synthesis of tetracarboxyphenylporphyrin (TCPP) using Alder's method.

Shirakawa, M. *et al.*<sup>(7)</sup> described the use of porphyrin units as a backbone in polymerization of porphyrin-DA compound (Figure 2-11). Aggregation binding of porphyrin was found and used in one dimension polymerization of DA. Increase in absorption intensity at about 580 and 620 nm upon UV radiation indicated transformation from porphyrin-diacetylene to porphyrin-PDA.

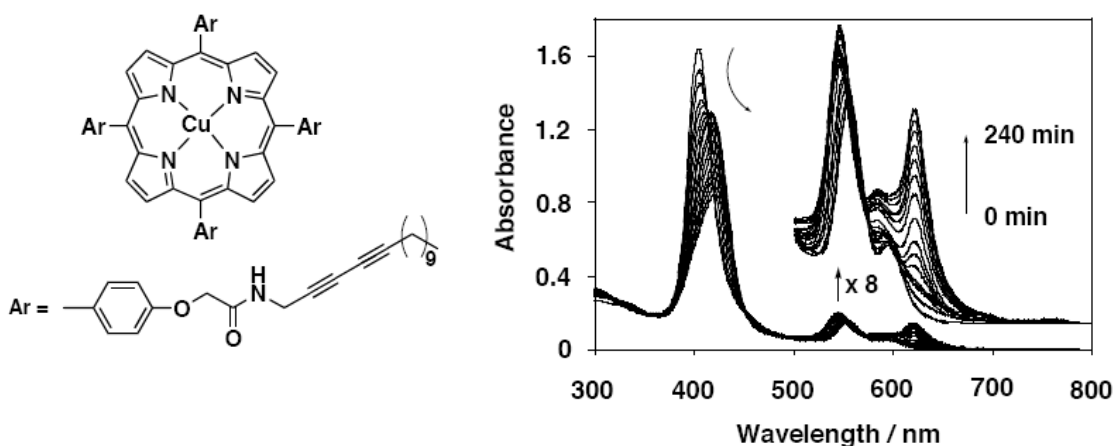


**Figure 2-11:** Porphyrin-DA molecule and time dependence of the UV-Vis spectral change upon UV irradiation.

Rochford, J. *et al.*<sup>(15)</sup> studied the effect of anchoring group at para and meta position of phenyl meso substituents of tetrachelate porphyrin on binding geometry and photoelectrochemical and photophysical properties. Figure 2-12 shows ideal binding behavior of the porphyrin carboxyl groups on metal oxide surfaces (such as TiO<sub>2</sub>, ZnO) with bidentate chelating mode. The result revealed that the para derivative exhibited less efficient electronic communication with the metal oxide surface compared to the meta one due to the potential aggregation of the porphyrins.

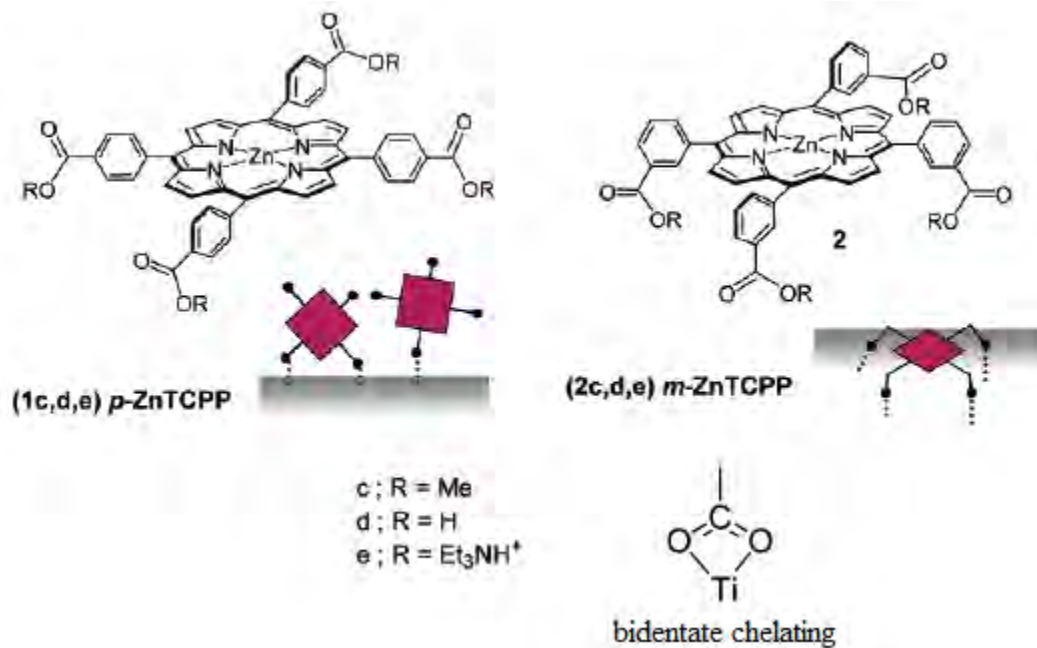


**Figure 2-12:** Binding geometry of tetrachelate porphyrin on metal oxide surface.



## CHAPTER III

### EXPERIMENTAL

#### 3.1 Chemical

1. Pyrrole : Aldrich
2. 4-carboxybenzaldehyde : Fluka
3. Propionic acid : Fluka
4. 10,12-pentacosadiynoic acid : GFS
5. Lignoceric acid : TCI
6. Thionyl chloride : Fluka
7. 25% Ammonia solution : MERCK
8. Lithium aluminium hydride : Aldrich
9. Diethyl ether : Lab-Scan
10. n-Hexane, commercial grade : Lab-Scan
11. Methylene Chloride, commercial grade : Lab-Scan
12. 1-ethyl-3-(3-dimethylaminopropyl)carbodiimide hydrochloride : Fluka
13. *N*-hydroxysuccinimide : Fluka
14. Triethylamine : Sigma-Aldrich
15. Sodium sulfate anhydrous : Sigma-Aldrich
16. Sodium hydroxide : MERCK
17. Methanol : MERCK
18. Ethanol : Labscan
19. Tetrahydrofuran : Lab-Scan
20. sodium hydrogen carbonate : MERCK
21. Magnesium sulfate anhydrous : Aldrich
22. Zinc acetate dihydrate : Aldrich
23. Hexadeuterated Dimethyl sulfoxide : MERCK

24. Deuterated chloroform	: Lab-Scan
25. Oxalyl chloride	: MERCK
26. Diisopropylethylamine	: Aldrich
27. Dimethylformamide	: Aldrich
28. Sodium chloride	: MERCK
29. Citric acid	: Aldrich
30. Octadeuterated Tetrahydrofuran	: MERCK

### 3.2 Analytical Instruments

$^1\text{H}$ -NMR and  $^{13}\text{C}$ -NMR spectra were obtained in deuterated chloroform ( $\text{CDCl}_3$ ) or hexadeuterated dimethyl sulfoxide ( $\text{DMSO-}d_6$ ) using Varian Mercury and Bluker NMR spectrometer operated at 400 MHz for  $^1\text{H}$  and 100 MHz for  $^{13}\text{C}$  nuclei (Varian Company, CA, USA and Bluker company, Germany). Chemical shifts ( $\delta$ ) are reported in parts per million (ppm) relative to the residual  $\text{CHCl}_3$  peak (7.26 ppm for  $^1\text{H}$ -NMR and 77.0 ppm for  $^{13}\text{C}$ -NMR). Coupling constants ( $J$ ) are reported in Hertz (Hz).

UV/vis spectra were recorded on a Perkin-Elmer (Lamda 2) UV-Visible spectrophotometer (Varian, USA) and tetrahydrofuran was used as solvent.

Fluorescence spectra were measured in toluene using a Perkin-Elmer LS45 luminescence spectrometer.

Raman spectra were performed on a Perkin-Elmer 1760 FT-IR spectrophotometer (Thermo Fisher Scientific company, USA) with an Nd:YAG laser source and a Raman sample compartment attached to the FT-IR instrument.

Mass analysis was conducted with a Microflex MALDI-TOF MS (Bruker Daltonics, Germany) by using dithranol as a matrix.

### 3.3 Experimental Procedure

#### 3.3.1 5,10,15,20-Tetra(4-carboxyphenyl)porphyrin (3)

Following a literature procedure<sup>(25)</sup> with slight modification, 4-carboxybenzaldehyde (0.9436 g, 6.285 mmol) was dissolved in propionic acid and pyrrole (0.4201 g, 6.262 mmol) was added. The reaction mixture was refluxed for 1 h.

After cooling to room temperature, the reaction mixture was cooled in a refrigerator (4 °C) overnight for precipitation. After that, the precipitate was washed with cold acetone and dried under vacuum to obtain compound **3** as a purple solid (280.3 mg, 23%). <sup>1</sup>H-NMR (DMSO-*d*<sub>6</sub>) δ -2.90 (s, 2H), 8.02 (s, 2H), 8.35 (dd, *J* = 21.1, 8.1 Hz, 16H), 8.85 (s, 6H) (**Figure A-1**). Other spectral data are consistent with these reported in the literature.

### 3.3.2 1-amino-10,12-pentacosadiyne (**8**)

Following a previously published procedure<sup>(26)</sup> with slight modification, a mixture of 10,12-pentacosadiynoic acid (0.9998 g, 2.669 mmol) and thionyl chloride (1.800 g, 15.13 mmol) in tetrahydrofuran (4 mL) was refluxed for 1 h. The remaining thionyl chloride was removed under reduced pressure to obtain 10,12-pentacosadiynoyl chloride as an orange oil, which was used in the next step without further purification. This oil was added to cold aqueous ammonia (25 %w/w, 20 mL) and stirred for 3 h. The product was extracted with CH<sub>2</sub>Cl<sub>2</sub> (3 x 50 mL). The organic fractions were combined and dried over anhydrous magnesium sulfate. After the removal of solvent under reduced pressure, hexane (30 mL) was added into the resulting yellow solid. The mixture was sonicated for 10 min and then placed in a refrigerator (4 °C) overnight for precipitation. The precipitate was filtered off and washed with cold hexane and dried under vacuum to obtain 10,12-pentacosadiynoyl amide as a colorless solid (0.8389 g, 83%). <sup>1</sup>H-NMR (CDCl<sub>3</sub>) δ 0.87 (t, *J* = 6.4 Hz, 3H), 1.00–1.42 (m, 28H), 1.50 (t, *J* = 7.6 Hz, 4H), 2.22 (t, *J* = 8.0 Hz, 2H), 2.23 (t, *J* = 7.2 Hz, 4H) (**Figure A-2**). Other spectral data are consistent with these reported in the literature. A solution of 10,12-pentacosadiynoyl amide (0.8389 g, 2.245 mmol) in diethyl ether (20 mL) was reacted with LiAlH<sub>4</sub> (0.8394 g, 22.12 mmol) at 0 °C for 17 h. After that, LiAlH<sub>4</sub> was deactivated by adding water (1.00 mL), 15 % NaOH (1.00 mL) and then 3.00 mL water. The reaction mixture was filtered and concentrated to dryness. 1-Amino-10,12-pentacosadiyne (**7**) was obtained as a colorless solid (0.7764 g, 96%). <sup>1</sup>H-NMR (CDCl<sub>3</sub>) δ 0.87 (t, 3H, *J* = 13.2 Hz), 1.41 (m, 28H), 2.23 (t, *J* = 14.0 Hz, 4H), 2.67 (t, *J* = 13.6 Hz, 2H) (**Figure A-3**). Other spectral data are consistent with these reported in the literature.

### 3.3.3 Synthesis of Compound 1 Via Acid Chloride Formation

Following a previously published procedure<sup>(27)</sup> with slight modification, a solution of compound **3** (0.055 g, 0.070 mmol) in dry methylene chloride (10 mL) was reacted with oxalyl chloride (a 2 M solution in methylene chloride, 1.50 mL, 3.00 mmol) and dimethylformamide (1  $\mu$ L). The resulting mixture was stirred under nitrogen atmosphere at room temperature for 24 h. After the removal of solvent under reduced pressure, green crude acid chloride **4** was redissolved in dry methylene chloride (10 mL) and then treated with amine **8** (0.200 g, 0.560 mmol) and diisopropylethylamine (1 mL). The reaction mixture was stirred under nitrogen atmosphere at room temperature for 24 h. After that, methylene chloride (200 mL) was added, and the resulting mixture was washed with a 10% aqueous citric acid solution (100 mL), a 1 M aqueous sodium hydroxide solution (100 mL), and then a saturated aqueous solution of sodium chloride (50 mL). The organic phase was dried over Na<sub>2</sub>SO<sub>4</sub> and concentrated to dryness. The resulting crude product was purified by column chromatography [silica, methylene chloride:methanol (100:2)], affording compound **1** as a purple solid (0.090 g, 54%). MALDI-TOF-MS *m/z* obsd 2158.333 [ $M^+$ ] calcd 2157.240 ( $M = C_{148}H_{202}N_8O_4$ ) (**Figure A-4**). Other characterization data are consistent with those of compound **1** obtained via a succinimide formation as described below.

Unfortunately, this method afforded ester derivative of compound **2** instead of the desirable compound **2**. MALDI-TOF-MS *m/z* obsd 1842.747 [ $M^+$ ], calcd 1815.622 ( $M = C_{123}H_{159}N_7O_5$ ) (**Figure A-5**).

### 3.3.4 Synthesis of Compound 1 and 2 via Succinimide Formation

Following previously published procedure<sup>(28)</sup> with slight modification, compound **3** (0.1341 g, 0.1696 mmol) was stirred in THF (10 mL) and *N*-hydroxysuccinimide (NHS) (0.1283 g, 1.115 mmol, 6 equiv.), 1-ethyl-3-(3-dimethylaminopropyl)carbodiimide hydrochloride (EDC·HCl) (0.2217 g, 1.156 mmol, 7 equiv.) were added. The reaction mixture was stirred at reflux temperature for 2 d and the solvent was then removed under reduce pressure. The resulting crude containing compound **9** was dissolved in THF (10 mL) and treated with compound **8** (0.5651 g,

1.571 mmol, 9 equiv.) and triethylamine (5 mL). The reaction mixture was stirred at reflux temperature for 1 d. After the solvent was removed under reduced pressure, the crude mixture was purified by column chromatography [silica, DCM : EtOH : TEA (96 : 3 : 1)]. Compounds **1** (0.0980 g, 27%) and compound **2** (0.1006 g, 33%) were obtained as purple solids. Both compounds were used in the Zn-metallation without further purification.

Compound **1**:  $^1\text{H-NMR}$  ( $\text{CDCl}_3$ )  $\delta$  -2.82 (s, 2H), 0.88 (s, 12H), 1.02–1.72 (m, 108H), 1.74–2.01 (m, 16H), 2.27 (s, 16H), 3.56–3.86 (m, 8H), 5.01 (s, 8H), 6.20–6.78 (m, 8H), 6.83–7.20 (m, 12H), 7.69 (s, 2H), 8.15–8.20 (s, 2H), 8.27–8.32 (m, 2H), 8.80–8.85 (m, 2H) (**Figure A-6**); MALDI-TOF-MS  $m/z$  obsd 2158.056 [ $\text{M}^+$ ], calcd 2157.240 ( $\text{M} = \text{C}_{148}\text{H}_{202}\text{N}_8\text{O}_4$ ) (**Figure A-7**);  $\lambda_{\text{abs}}$  417, 514, 548, 590, 647 nm (**Figure B-1**);  $\lambda_{\text{em}}$  ( $\lambda_{\text{ex}} = 417$  nm) 649, 715 nm (**Figure B-2**).

Compound **2**:  $^1\text{H-NMR}$  ( $\text{CDCl}_3$ )  $\delta$  -2.83 (s, 2H), 0.88 (t,  $J = 6.7$  Hz, 9H), 1.04–1.57 (m, 93H), 2.15–2.29 (m, 12H), 3.16–3.28 (m, 6H), 5.02 (s, 6H), 6.98 (s, 6H), 7.81 (s, 6H), 8.16 (d,  $J = 7.5$  Hz, 2H), 8.28 (d,  $J = 7.7$  Hz, 2H), 8.33–8.73 (m, 8H), 8.82 (s, 6H) ppm (**Figure A-8**); MALDI-TOF-MS  $m/z$  obsd 1817.311 [ $\text{M}^+$ ], calcd 1815.622 ( $\text{M} = \text{C}_{123}\text{H}_{159}\text{N}_7\text{O}_5$ ) (**Figure A-9**);  $\lambda_{\text{abs}}$  419, 514, 548, 593, 648 nm (**Figure B-3**);  $\lambda_{\text{em}}$  ( $\lambda_{\text{ex}} = 419$  nm) 651, 712 nm (**Figure B-4**).

### 3.3.5 Compounds Zn-1 and Zn-2

Following a previously published procedure,<sup>(29)</sup> a solution of compound **1** (0.0980 g, 0.0454 mmol) in  $\text{CHCl}_3$  (3 mL) was treated with a solution of zinc acetate dihydrate (0.0503 g, 0.2291 mmol) in methanol (1 mL). The reaction mixture was stirred at room temperature for 3 h and then extracted with  $\text{CH}_2\text{Cl}_2/\text{H}_2\text{O}$ . The organic phase was dried over anhydrous magnesium sulfate and concentrated to dryness. The resulting crude was purified by washing and sonication with hexane and then methanol to afford compound **Zn-1** as a purple solid (0.0577 g, 57%).  $^1\text{H NMR}$  ( $\text{CDCl}_3$ )  $\delta$  0.77–0.94 (m, 12H), 1.10–1.76 (m, 128), 2.25 (m, 16H), 3.50–3.63 (m, 16H), 6.36–6.51 (m, 4H), 8.06 (d,  $J = 7.6$  Hz, 8H), 8.26 (d,  $J = 7.9$  Hz, 8H), 8.88 (s, 8H) (**Figure A-10**);  $^{13}\text{C-NMR}$  ( $\text{CDCl}_3$ )  $\delta$  14.1, 19.2, 22.7, 25.7, 27.1, 28.3, 28.4, 28.8, 28.9, 29.0, 29.10, 29.3, 29.4, 29.5, 29.6, 29.7,

29.8, 31.9, 32.8, 40.4, 63.1, 65.2, 65.3, 120.2, 125.1, 132.1, 134.1, 134.5, 145.9, 149.9, 167.6 (**Figure A-11**); MALDI-TOF-MS  $m/z$  obsd 1373.070 [(M-C<sub>61</sub>H<sub>110</sub>)<sup>+</sup>], 2220.831 [M<sup>+</sup>], calcd 2220.633 [M<sup>+</sup>], (M = ZnC<sub>148</sub>H<sub>200</sub>N<sub>8</sub>O<sub>4</sub>) (**Figure A-12**);  $\lambda_{\text{abs}}$  426, 557, 596 nm (**Figure B-5**);  $\lambda_{\text{em}}$  ( $\lambda_{\text{ex}}$  = 424 nm) 607, 649 nm (**Figure B-6**).

A solution of compound **2** (0.1006 g, 0.0554 mmol) in chloroform (3 mL) was reacted with a solution of zinc acetate dihydrate (0.0632 g, 0.2879 mmol) in methanol (1 mL) at room temperature for 3 h. The resulting mixture was extracted with CH<sub>2</sub>Cl<sub>2</sub>/H<sub>2</sub>O. The organic phase was dried over anhydrous magnesium sulfate and concentrated to dryness. The resulting crude was purified by washing and sonication with hexane and then methanol to afford compound **Zn-2** as a purple solid (0.0805 g, 77%). <sup>1</sup>H NMR (CDCl<sub>3</sub>)  $\delta$  0.89 (t,  $J$  = 7.3 Hz, 9H), 1.97–1.56 (m, 90H), 1.99–2.05 (m, 12H), 3.43 (m, 12H), 5.12–5.26 (m, 6H), 6.86–6.90 (m, 3H), 8.06–8.16 (m, 8H), 8.20–8.31 (m, 8H), 8.80–8.90 (m, 8H) (**Figure A-13**); <sup>13</sup>C NMR (CDCl<sub>3</sub>)  $\delta$  14.1, 19.2, 22.7, 25.5, 26.8, 26.9, 27.0, 28.3, 28.4, 28.7, 28.8, 28.9, 29.0, 29.1, 29.2, 29.3, 29.5, 29.6, 30.1, 31.9, 35.4, 35.9, 36.5, 36.7, 39.6, 40.2, 40.6, 62.7, 65.3, 127.1, 137.4, 158.5, 166.6, 171.9 (**Figure A-14**); MALDI-TOF-MS  $m/z$  obsd 1373.194 [(M-C<sub>37</sub>H<sub>63</sub>)<sup>+</sup>], 1881.103 [M<sup>+</sup>] calcd 1879.017 [M<sup>+</sup>], (M = ZnC<sub>123</sub>H<sub>157</sub>N<sub>7</sub>O<sub>5</sub>) (**Figure A-15**);  $\lambda_{\text{abs}}$  425, 557, 598 nm. (**Figure B-7**);  $\lambda_{\text{em}}$  ( $\lambda_{\text{ex}}$  = 425 nm) 605, 651 nm (**Figure B-8**).

### 3.3.6 Tetracosan-1-amine (**13**)

Following a previously published procedure<sup>(26)</sup> with slight modification, a mixture of lignoceric acid (**10**, 1.0021 g, 2.718 mmol) and thionyl chloride (1.800 g, 15.13 mmol) in tetrahydrofuran (4 mL) was refluxed for 1 h. The remaining thionyl chloride was removed under reduced pressure to obtain tetracosanoyl chloride (**11**) as an orange brown oil, which was used in the next step without further purification. This oil was added to cold aqueous ammonia (25% w/w, 20 mL) and stirred for 3 h. The mixture was extracted with CH<sub>2</sub>Cl<sub>2</sub> (3 x 50 mL) and the organic phase was collected and dried over anhydrous magnesium sulfate. After the removal of solvent under reduced pressure, the resulting yellow crude was treated with hexanes (30 mL). The mixture was then sonicated for 10 min and placed in a refrigerator (4 °C) overnight for precipitation. The resulting

precipitate was filtered and washed with cold hexane and dried under vacuum to obtain tetracosanamide (**12**) as a colorless solid (0.8022 g, 80%).  $^1\text{H-NMR}$  ( $\text{CDCl}_3$ )  $\delta$  0.87 (t,  $J$  = 6.7 Hz, 3H), 1.00–1.40 (m, 40H), 2.29 (t,  $J$  = 7.6 Hz, 2H), 4.10 (t,  $J$  = 6.1 Hz, 2H) (**Figure A-16**);  $^{13}\text{C-NMR}$  ( $\text{CDCl}_3$ )  $\delta$  14.1, 22.7, 25.0, 26.1, 29.2, 29.3, 29.4, 29.5, 29.6, 29.7, 31.9, 34.3, 44.5, 63.3, 173.7 (**Figure A-17**); MALDI-TOF-MS  $m/z$  obsd 367.934 cald 367.652 [ $\text{M}^+$ ], ( $\text{M} = \text{C}_{24}\text{H}_{49}\text{NO}$ ) (**Figure A-18**). A solution of compound **12** (0.8022 g, 2.182 mmol) in diethyl ether (20 mL) was reacted with  $\text{LiAlH}_4$  (0.8054 g, 21.23 mmol) at 0 °C for 17 h. After that,  $\text{LiAlH}_4$  was deactivated by adding water (1.00 mL), 15 % NaOH (1.00 mL) and then water (3.00 mL), the mixture was filtered and concentrated under reduced pressure, leading to tetracosan-1-amine (**13**) as a colorless solid (0.5148 g, 67%).  $^1\text{H-NMR}$  ( $\text{CDCl}_3$ )  $\delta$  0.87 (t,  $J$  = 6.8 Hz, 3H), 1.00–1.43 (m, 42H), 1.61–1.51 (m, 2H), 2.67 (t,  $J$  = 7.0 Hz, 2H), 3.63 (t,  $J$  = 6.6 Hz, 2H) (**Figure A-19**);  $^{13}\text{C-NMR}$  ( $\text{CDCl}_3$ )  $\delta$  14.1, 22.7, 25.8, 26.9, 29.4, 29.5, 29.6, 29.7, 31.9, 32.8, 33.8, 42.2, 63.0 (**Figure A-20**); MALDI-TOF-MS  $m/z$  obsd 353.835 cald 353.668 [ $\text{M}^+$ ], ( $\text{M} = \text{C}_{24}\text{H}_{51}\text{N}$ ) (**Figure A-21**).

### 3.3.7 Synthesis of Compounds Zn-14 and Zn-15

Following a previously published procedure<sup>(29)</sup> with slightly modification, a solution of compound **3** (0.1488 g, 0.1882 mmol) in THF (10 mL) was treated with NHS (0.2165 g, 1.881 mmol, 10 equiv.) and EDC·HCl (0.2177 g, 2.177 mmol, 12 equiv.). The reaction mixture was stirred at reflux temperature for 2 d and then the solvent was removed under reduce pressure. The crude mixture was redissolved in THF (10 mL) and the resulting solution was treated with compound **13** (0.8150 g, 2.304 mmol, 12 equiv.) and triethylamine (5 mL). The reaction mixture was stirred at refluxing temperature for 1 d and then the solvent was removed under reduce pressure. Column chromatography [silica, DCM : EtOH : TEA (96 : 3 : 1)] afforded compounds **14** (0.0172 g, 4%) and **15** (0.0164 g, 5%) as purple solids. Compound **14** was characterized with MALDI-TOF-MS:  $m/z$  obsd 2135.371 [ $\text{M}^+$ ], calcd 2133.386 ( $\text{M} = \text{C}_{144}\text{H}_{226}\text{N}_8\text{O}_4$ ) (**Figure A-22**). Compound **15**: MALDI-TOF-MS  $m/z$  obsd 1800.122 [ $\text{M}^+$ ], calcd 1797.733 ( $\text{M} = \text{C}_{120}\text{H}_{177}\text{N}_7\text{O}_5$ ) (**Figure A-23**);

Compound **14** (0.0172 g, 0.0081 mmol) was redissolved in  $\text{CHCl}_3$  (3 mL) and treated with a solution of zinc acetate dihydrate (0.0448 g, 0.2041 mmol) in methanol (1 mL). The reaction mixture was stirred at room temperature for 3 h and then extracted with  $\text{CH}_2\text{Cl}_2/\text{H}_2\text{O}$ . The organic phase was dried over anhydrous magnesium sulfate and concentrated to dryness. The resulting crude was purified by washing and sonication with hexane and then methanol to afford compound **Zn-14** as a purple solid (0.0157 g, 89%).  $^1\text{H-NMR}$  ( $\text{CDCl}_3$ )  $\delta$  0.85 (s, 12H), 0.93–1.65 (m, 160H), 1.78–1.92 (m, 8H), 3.74 (t,  $J = 6.6$  Hz, 8H), 5.02 (s, 8H), 6.56 (s, 4H), 7.83 (s, 8H), 7.97–8.22 (m, 4H), 8.14 (d,  $J = 8.8$  Hz, 2H), 8.28 (d,  $J = 8.4$  Hz, 2H), 8.90 (s, 8H) (**Figure A-24**). Due to the low solubility of Zn-14, a  $^{13}\text{C-NMR}$  spectrum could not be obtained. MALDI-TOF-MS  $m/z$  obsd 2198.746 [ $\text{M}^+$ ], calcd 2196.781, ( $\text{M} = \text{ZnC}_{144}\text{H}_{224}\text{N}_8\text{O}_4$ ) (**Figure A-25**);  $\lambda_{\text{abs}}$  426, 556, 597 nm (**Figure B-9**);  $\lambda_{\text{em}}$  ( $\lambda_{\text{ex}} = 426$  nm) 605, 651 nm (**Figure B-10**).

A solution of compound **15** (0.0179 g, 0.0100 mmol) in chloroform (3 mL) was reacted with a solution of zinc acetate dihydrate (0.0452 g, 0.2059 mmol) in methanol (1 mL) at room temperature for 3 h. The resulting mixture was extracted by  $\text{CH}_2\text{Cl}_2/\text{H}_2\text{O}$ . The organic phase was dried over anhydrous magnesium sulfate and the resulting crude was concentrated under reduced pressure. The resulting crude was purified by washing and sonication with hexane and then methanol to afford compound **Zn-15** as a purple solid (0.0157 g, 85%).  $^1\text{H-NMR}$  ( $\text{CDCl}_3$ )  $\delta$  0.74–0.93 (m, 12H), 0.99–1.68 (m, 112H), 1.77–1.85 (m, 8H), 3.62–3.77 (m, 8H), 5.02 (s, 6H), 6.56 (s, 4H), 7.75 (s, 8H), 8.04–8.10 (m, 4H), 8.36–8.48 (m, 4H), 8.81–8.95 (m, 8H) ppm (**Figure A-26**);  $^{13}\text{C-NMR}$  ( $\text{CDCl}_3$ )  $\delta$  11.4, 14.1, 22.7, 29.5, 29.7, 30.3, 31.2, 125.5 (**Figure A-27**); MALDI-TOF-MS  $m/z$  obsd 1862.492 [ $\text{M}^+$ ], calcd 1861.127 ( $\text{M} = \text{ZnC}_{120}\text{H}_{175}\text{N}_7\text{O}_5$ ) (**Figure A-28**);  $\lambda_{\text{abs}}$  426, 556, 597 (**Figure B-13**);  $\lambda_{\text{em}}$  ( $\lambda_{\text{ex}} = 426$  nm) 605, 651 nm (**Figure B-14**).



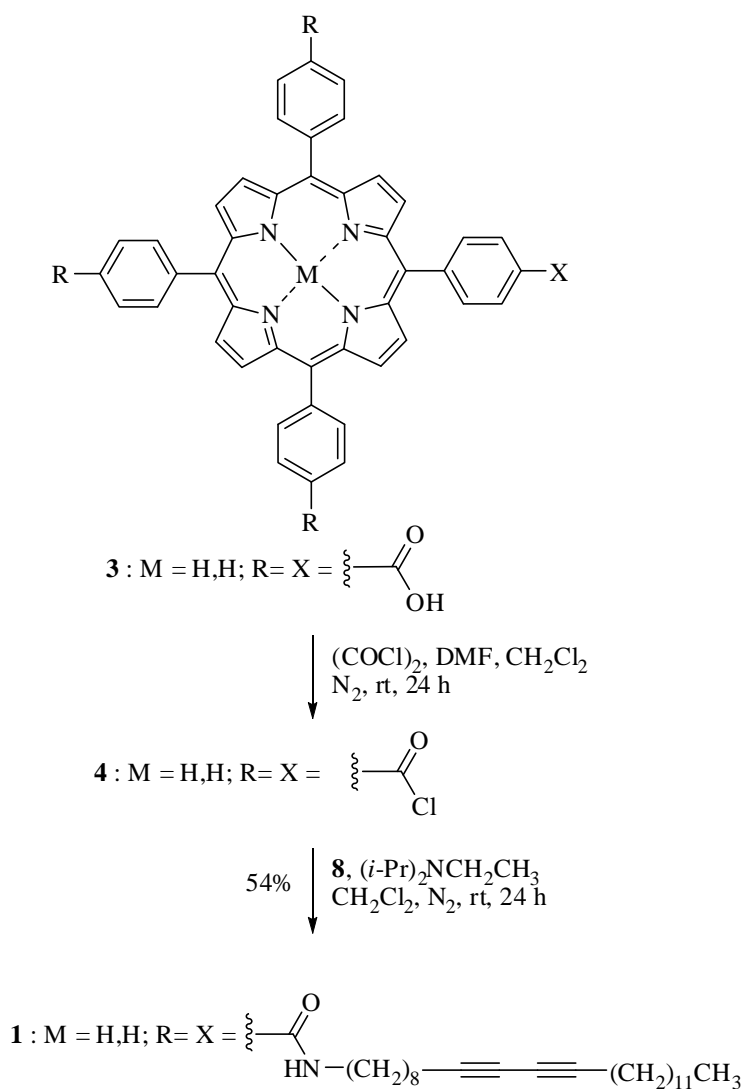
## CHAPTER IV

### RESULTS AND DISCUSSION

Key concepts of the molecular design of organic light sensitizers in this project are (i) the collaboration between highly photoactive porphyrin and polydiacetylene as a co-absorber for broad absorption range, and (ii) the use of surface anchoring groups to enhance electronic communication between the chromophore and the electrode surface. Synthesis of the photoactive compounds are shown as follows.

#### 4.1 Synthesis of Porphyrin-diacetylene Compounds for Organic Solar Cells

The first attempt for synthesizing target compounds **Zn-1** and **Zn-2** is summarized in Scheme 4-1. Compound **3** was reacted with oxalyl chloride to provide compound **4**. After that, compound **4** was reacted with compound **8** to obtain compound **1** in 54%. Instead of the desired compound **2**, its amide derivative was obtained. This is attributed to the side reaction of the remaining acid chloride functional group and (*i*-Pr)<sub>2</sub>NCH<sub>2</sub>CH<sub>3</sub>. Therefore, this method is suitable for preparing compound **1** only.



**Scheme 4-1:** Synthesis of compound **1** via acid chloride formation.

An alternative reaction condition was investigated for synthesizing compound **2**. Compound **3** was reacted with NHS and EDC·HCl to yield compound **9** (Scheme 4-2). After that, compound **9** was reacted with nine equivalents of compound **8** to give compound **1** and **2** in 27% and 33%, respectively. Due to its hygroscopic property, compound **9** was used in the next step without chromatographic purification. When six to eight equivalents of compound **8** were employed to condense with compound **9**, compound **2** was obtained in 80% as a single product. Mass spectrum of compound **1**

(MW = 2157.240) exhibited the molecular ion peak at  $m/z$  2158.056 and that of compound **2** (MW = 1815.622) at  $m/z$  1815.993. Beside the molecular ion peaks, mass spectra of **Zn-1** and **Zn-2** showed a fragment ion peak at  $m/z$  1373.070 (**Zn-1**, Chart 4-1a) and 1373.194 (**Zn-2**, Chart 4-1b), possibly resulting from the fragmentation of 2 *N*-alkyl substituents and a part of the alkyl chain. Zn-metallation of compounds **1** and **2** was performed by a reaction with zinc acetate dihydrate in  $\text{CHCl}_3/\text{MeOH}$ . The completion of metalation was indicated by the absence of an emission peak at about 720 nm and the disappearance of  $^1\text{H-NMR}$  peak of the inner protons at  $\delta$  -2.89 ppm for compound **1** and -3.07 ppm for compound **2**. All of compounds are satisfactorily soluble in common organic solvents, such as  $\text{CH}_2\text{Cl}_2$ ,  $\text{CHCl}_3$ , THF.

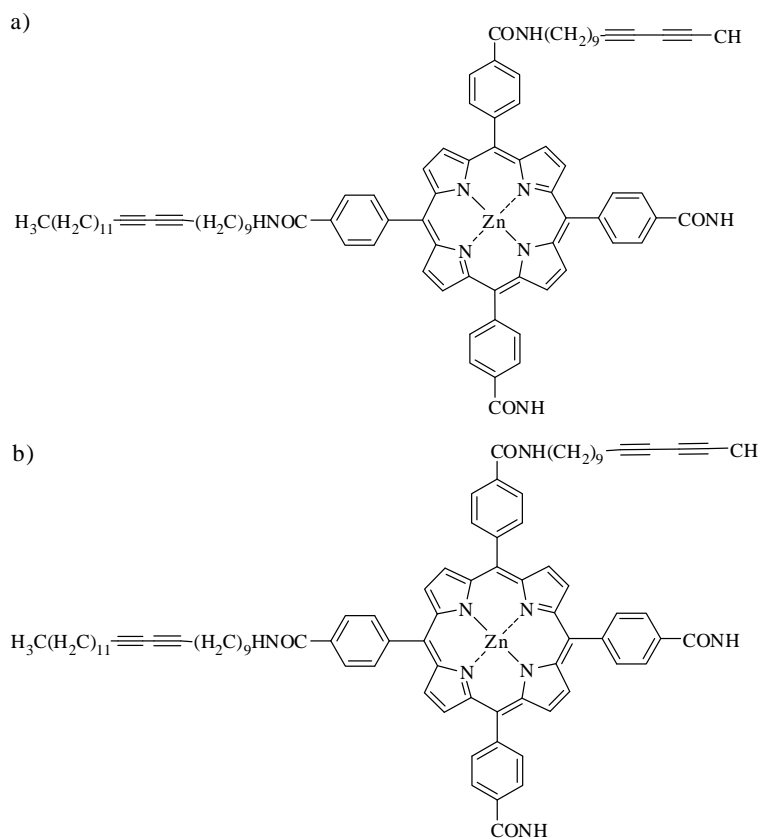
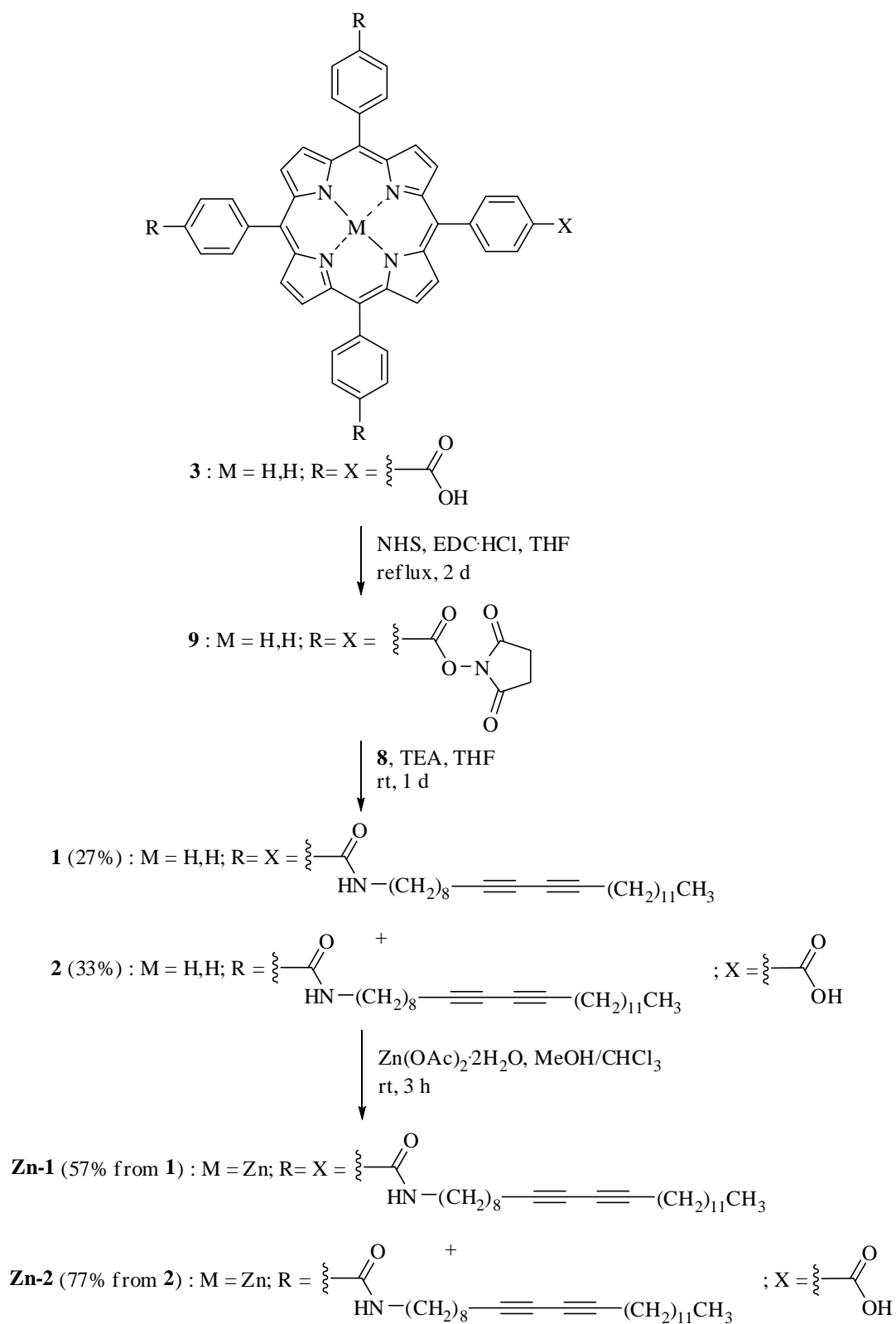
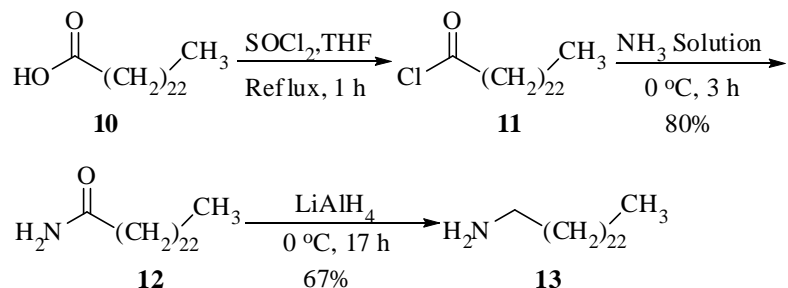


**Chart 4-1:** Ion fragment of a) **Zn-1** and b) **Zn-2**.



**Scheme 4-2:** Synthesis of compounds **Zn-1** and **Zn-2** via succinimide formation.

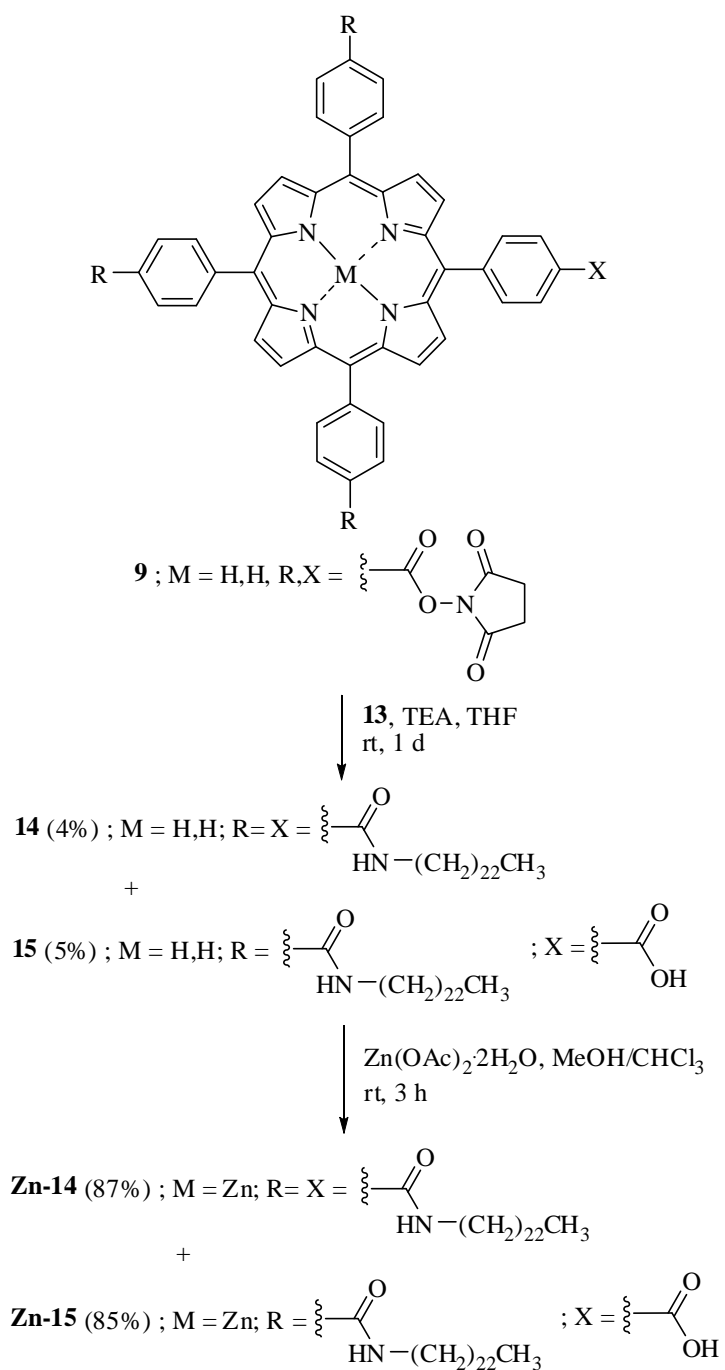
In the similar manner to the preparation of compound **8**,<sup>(26)</sup> compound **10** was reacted with thionyl chloride to obtain compound **11**. Compound **11** was reacted with a 25% NH<sub>4</sub>OH solution leading to compound **12** in 80% yield (from **10**). After that, compound **12** was reduced by LiAlH<sub>4</sub> to afford compound **13** in 67% yield (Scheme 4-3).



**Scheme 4-3:** Synthesis of compound **13**.

#### 4.2 Synthesis of Benchmark Compounds Zn-1 and Zn-2

Synthesis of the benchmark compounds **Zn-1** and **Zn-2**<sup>(28)</sup> started with condensation of compound **9** with an excess amount of **13**, affording **14** and **15** in 4% and 5%, respectively (Scheme 4-4). The lower yields of **14** and **15** compared with those of compounds **1** and **2** are attributed to lower solubility of compound **13** compared with that of **8**. Zn-metallation of compounds **14** and **15** were quantitatively carried out by a reaction with a solution of zinc acetate dihydrate in CHCl<sub>3</sub>/MeOH. The completion of the metallation was confirmed by emission spectrophotometry and <sup>1</sup>H-NMR spectroscopy as mentioned above. All of compounds are satisfactorily soluble in common organic solvents, such as CH<sub>2</sub>Cl<sub>2</sub>, CHCl<sub>3</sub>, THF, etc. Compound **Zn-14** found peak at m/z 1373.070 and compound **Zn-15** at m/z 1373.194 could be resulted from the molecular ion losing 2 *N*-alkyl substituents and 1 short alkyl chain the structure of the possible fragments are shown in chart 4-1.



**Scheme 4-4:** Synthesis of compounds **Zn-14** and **Zn-15**.

### 4.3 Polymerization of Porphyrin-diacetylene Compound Zn-1

According to a previous study,<sup>(7)</sup> porphyrin-diacetylene compound was photopolymerized upon a radiation at 254 nm and the increase in absorption was observed at 550–650 nm. To perform the photopolymerization of **Zn-1**, a **Zn-1** film was prepared by drop-casting a solution of **Zn-1** in THF (2.318 mM, 1 mL) on a glass substrate (1.0 cm x 3.5 cm) and the sample was left in the dark at room temperature until the solvent completely evaporized. After that, the resulting film sample was exposed to 254 nm radiation for 10 min. However, based on absorption spectrophotometry, the film did not give a significant change of absorption in the region of 550–650 nm (Figure 4-1), indicating the inefficient photopolymerization of DA chains on **Zn-1**. An attempt to use toluene as a solvent and allow the film to slowly form in a closed chamber was failed to give the expected distinctive polymerization. This observation indicates that the chosen film preparation condition may not afford the ordered orientation of the molecule and, hence, the film formation technique has to be improved.

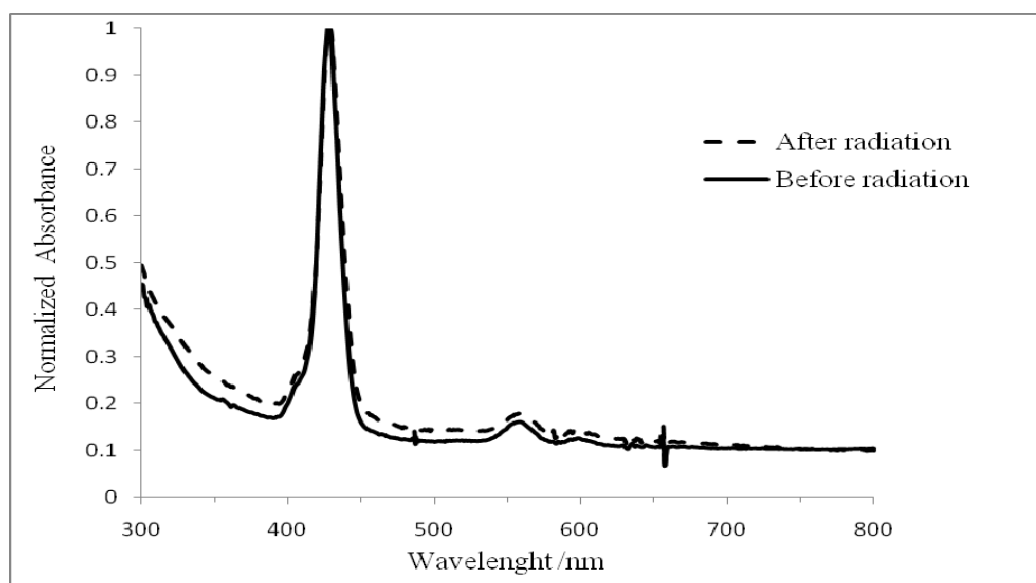


**Figure 4-1:** UV-visible spectra of a **Zn-1** film before (solid line) and after radiation (dashed line) at 254 nm.

#### 4.4 Study of the Polymerization of Porphyrin-diacetylene using Raman Spectroscopy

The polymerization of the porphyrin-diacetylene upon UV-irradiation was evidenced by the disappearance of the C≡C stretching peak at 2117 cm<sup>-1</sup> in the Raman spectra (Figure 4-2). The double and the triple bond stretching peaks of the ene-yne conjugate appeared at 1446 and 2080 cm<sup>-1</sup>, respectively. It is interesting to note that these ene-yne conjugate signals were also observed in the spectrum before UV-irradiation at 1446 and 2074 cm<sup>-1</sup>. This is probably due to partial polymerization caused by the irradiation of the laser source used in the Raman spectroscopy.

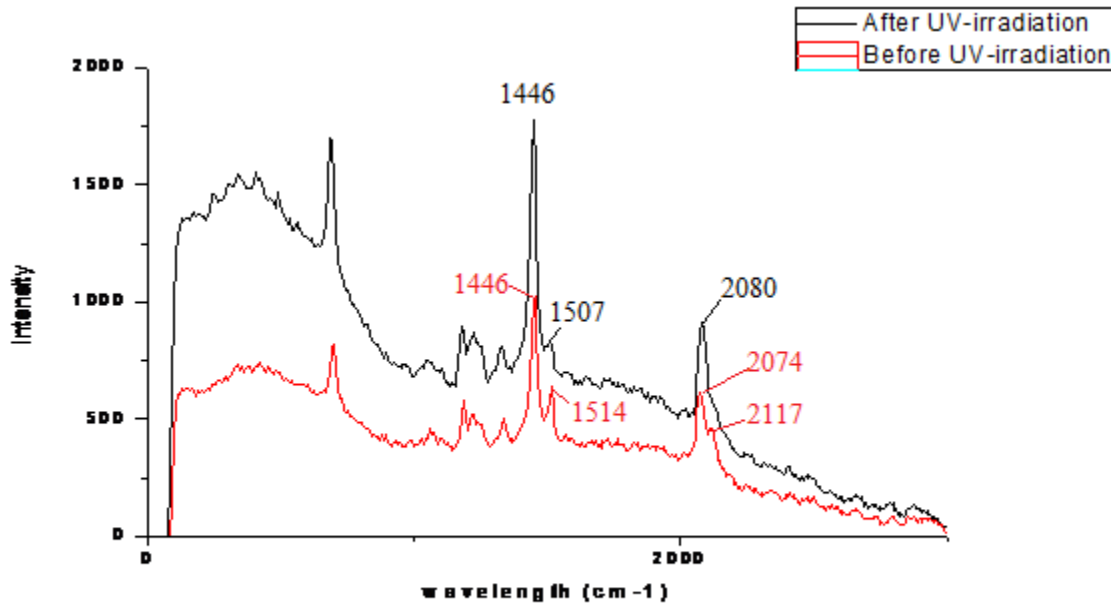


Figure 4-2: Raman spectra of **Zn-1**.

#### 4.5 Photophysical and Electrochemical Properties

##### 4.4.1 Compound Zn-1

Electrochemical properties of compound **Zn-1** was determined by mean of cyclic voltammetry in MeCN containing 0.1 M Bu<sub>4</sub>NPF<sub>6</sub> by using a ITO-coated glass working electrode, Pt wire counter electrode and Ag/AgCl quasi-reference electrode (QRE) with



scan rate of 50 mV/s. The resulting redox potentials were externally calibrated with ferrocene/ferrocenium couple of which the potential of 0.40 V vs NHE was used. The result indicated that the estimated energy gap of compound **Zn-1** was 2.2 eV with the HOMO level of  $-5.6$  eV and the LUMO level of  $-3.4$  eV. When consider together with ITO conduction band (CB), PEDOT:PSS Fermi level (FL), HOMO-LUMO level of P3HT and PCBM and Al work function (WF), the HOMO-LUMO level of **Zn-1**, the HOMO-LUMO levels of **Zn-1** should be able to serve as a either donor or acceptor for the solar cells (Figure 4-3).

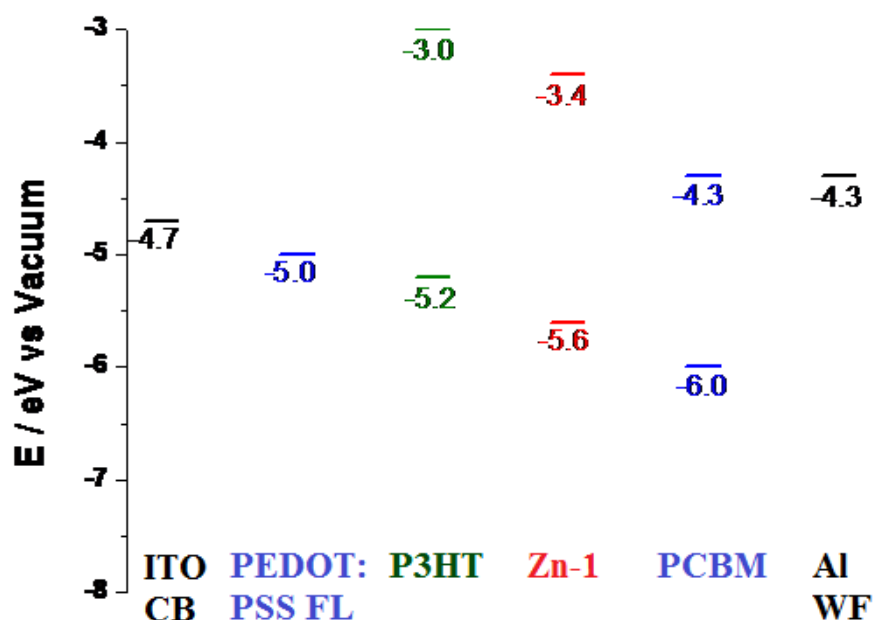


**Figure 4-3:** Comparative energy diagram of compound **Zn-1**-based BHJ-SC.

In order to prove the ability of compound **Zn-1** for serving as a donor or an acceptor material, a photoluminescence study of compound **Zn-1**:PCBM (1:1) and P3HT:**Zn-1** (1:1) blended films was performed. The result in Figure 4-4 revealed that porphyrin emission was completely quenched by PCBM, indicating the efficient charge transfer from compound **Zn-1** (donor) to PCBM (acceptor). However, such emission quenching was not observed in the case of a P3HT:**Zn-1** film, indicating that the charge transfer from P3HT (donor) to **Zn-1** (acceptor) was not efficient. Therefore, the

PCBM:**Zn-1** blended film was employed as a photoactive layer in the bulk heterojunction solar cell, whose fabrication and study are explained below.

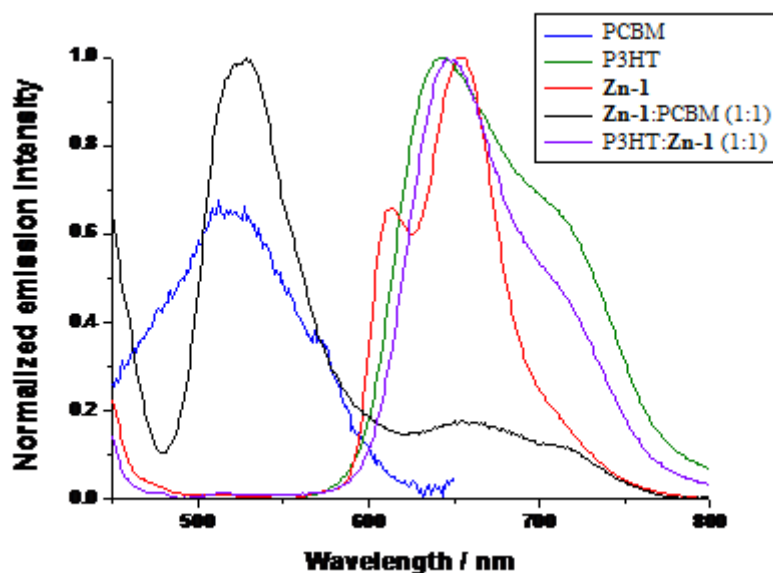


**Figure 4-4:** Photoluminescence study of the films.

Following a literature procedure<sup>(30)</sup> with slight modification, the bulk heterojunction solar cells containing the **Zn-1:PCBM** was fabricated. The schematic structure of the device is shown in Figure 4-5.

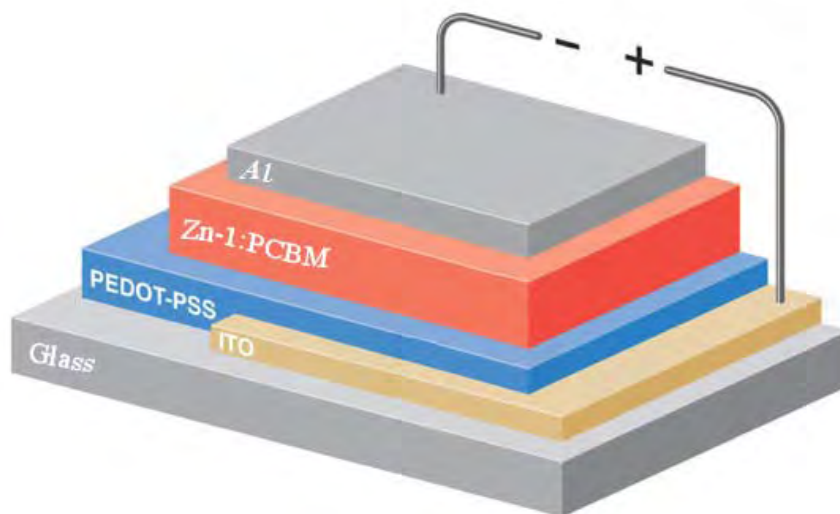


**Figure 4-5:** A schematic cell structure of a BHJ-SC based on **Zn-1**.

In the cell fabrication, Following a literature procedure<sup>(30)</sup> with slight modification the thickness and type of a metal top contact, PEDOT:PSS and ITO-coated glass were initially kept constant. The **Zn-1**:PCBM ratio was varied and two different film formation techniques, *i.e.* drop-casting or spin-coating, were performed by using a homogeneous **Zn-1**:PCBM mixed solution or individual solutions in a stepwise manner. The resulting cell efficiency was found to be 0.1–0.2%. Due to its higher reproducibility compared to the drop-casting technique, the spin-coating was employed for further study. Although it is unclear how the porphyrin and diacetylene alkyl long chain oriented in the blended film with PCBM, the presence of the diacetylene alkyl long chain substituents affected the film morphology somehow in a positive way, resulting in a photovoltaic effect. Such an effect was not observed when *meso*-tetraphenylporphyrinatozinc (II) (**Zn-TPP**), which has similar energy gap and HOMO-LUMO levels. Further improvement of the device efficiency can be expected when other cell parameters, for example, types of top contact and PEDOT:PSS, and film formation technique are optimized.

#### 4.5.2 Compound **Zn-2**

Electrochemical properties of compound **Zn-2** was determined by mean of cyclic voltammetry by using the same measurement set up as that described for **Zn-1**. The result indicated that the estimated energy gap of compound **Zn-2** was 2.3 eV with the HOMO level of 0.9 eV and the LUMO level of –1.4 eV. When consider together with TiO<sub>2</sub> conduction band (CB), HOMO-LUMO level of **Zn-2** and **2** should be able to serve as a photosensitizers for the solar cells (Figure 4-6).

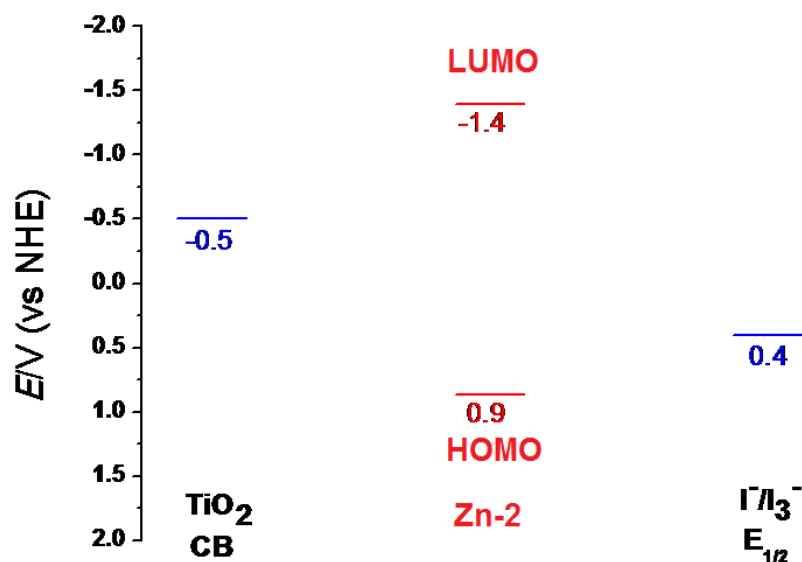


**Figure 4-6:** Comparative energy diagram of a **Zn-2**-based DSSC.

Following a literature procedure<sup>(31)</sup> with slight modification, the DSSCs based on Compound **Zn-2** were fabricated and investigated (Figure 4-7). As a result, the efficiency of the resulting DSSC was found to be 1.1% and slightly improved to 1.2% upon storage in the dark at ambient atmosphere overnight. Upon light soaking under 1 SUN for 45 min, the efficiency was increased to 1.8% and became 2.0% when the light soaking was continued for additional 4 h. After overnight light soaking, the efficiency did not significantly change. Interestingly, unlike most of organic compounds, DSSC based on compound **Zn-2** showed the reversible light soaking effect, which means the device efficiency was decreased when the device was kept in the dark and increased again when it was soaked by light. To determine whether this behavior stems from the long alkyl chain or the presence of diacetylene unit, which might be partially photopolymerized, the synthesis of the benchmark compound **Zn-15** and the study of **Zn-15**-based DSSC are required and will be reported elsewhere.

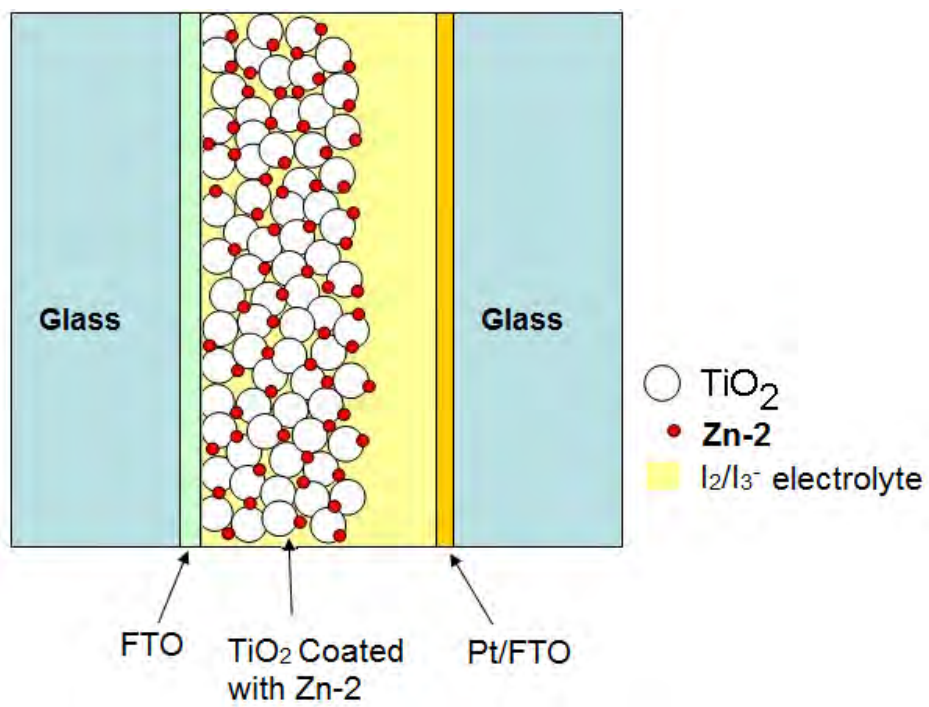


**Figure 4-7:** A schematic cell structure of a DSSC based on **Zn-2**.

## CHAPTER V

### CONCLUSION

The desirable porphyrin-diacetylene compounds and their benchmark derivatives were successfully synthesized by using amidation of porphyrin bearing succinimide groups and alkylamine compounds as a key reaction. The resulting compounds were fully characterized by spectroscopic techniques. Based on HOMO-LUMO levels of compound **Zn-1** obtained from cyclic voltammetry analysis and photoluminescence of **Zn-1**:PCBM and P3HT:**Zn-1** blended film, the photovoltaic effect should be possible in a bulk-heterojunction solar cell based on **Zn-1**. **Zn-1**-based bulk-heterojunction solar cells were fabricated and up to 0.2% energy conversion efficiency was obtained. Cyclic voltametric study of **Zn-2** also showed the electron transfer in a dye-sensitized solar cell based on **Zn-2** possible. The devices were fabricated and found to give up to 2.0% energy conversion efficiency upon light-soaking.

## REFERENCES

- [1] World energy resources and consumption. Wikipedia [Online]. 2010, Available from : [http://en.wikipedia.org/wiki/World\\_energy\\_resources\\_and\\_consumption](http://en.wikipedia.org/wiki/World_energy_resources_and_consumption) [2011, May]
- [2] O' Regan, B., and Gratzel, M. A Low Cost, High-Efficiency Solar Cell Based on Dyesensitized Colloidal TiO<sub>2</sub> Film. Nature 353 (October 1991): 737–740.
- [3] Nango, M., and others. Molecular Assembly of Zn Porphyrin Complexes onto a Gold Electrode using Synthetic Light-Harvesting Model Polypeptides. Tetrahedron Lett. 48 (November 2007): 8468–8471.
- [4] Maeda, C., Kamada, T., Aratani, N., and Osuka, A. Chiral Self-Discriminative Self-Assembling of *meso-meso* Linked Diporphyrins. Coord. Chem. Rev. 251 (March 2007): 2743–2752.
- [5] Granstrom, M., Petritsch, K., Arias, A. C., Lux, A., Anderson, M. R., and Friend, R. H. Laminated Fabrication of Polymeric Photovoltaic Diodes. Nature 395 (September 1998): 257-260.
- [6] Lim, C., Sandman, D. J., and Sukwattanasinitt, M. Topological Polymerization of *tert*-Butylcalix[4]arenes Containing Dienes. Macromolecules 41 (November 2007): 675–681.
- [7] Shirakawa, M., Fujita, N., and Shinkai, S. A Stable Single Piece of Unimolecularly  $\pi$ -Stacked Porphyrin Aggregate in a Thixotropic Low Molecular Weight Gel: A One-Dimensional Molecular Template for Polydiacetylene Wiring up to Several Tens of Micrometers in Length. J. Am. Chem. Soc. 127 (March 2005): 4164–4165.
- [8] Shaheen, S. E., Radspinner R., Peyghambarian, N., and Jabbour, G. E. Fabrication of Bulk Heterojunction Plastic Solar Cells by Screen Printing. Appl. Phys. Lett. 79 (August 2001): 2996–2998.
- [9] Gustafsson G., Cao, Y., Treacy, G. M., Klavetter, F., Colaneri, N., and Heeger, A. J. Flexible Light-Emitting-Diodes Made From Soluble Conducting Polymers. Nature 357 (June 1992): 477–479.

- [10] University of Würzburg. Research : Optoelectronics [Online]. 2011, Available from : <http://www.physik.uni-wuerzburg.de/EP6/research-oe.html> [2011, Mar]
- [11] Gratzel, M., and Kalyanasundaram, K. Applications of Functionalized Transition Metal Complexes in Photonic and Optoelectronic Devices. Coord. Chem. Rev. 177 (October 1998): 347–414.
- [12] Hagfeldt, A., and Gratzel, M. Molecular Photonics. Acc. Chem. Res. 33 (June 1999): 269–277.
- [13] Hara, K., and other. Influence of Electrolyte on the Photovoltaic Performance of a Dye Sensitized TiO<sub>2</sub> Solar Cell Base on a Ru(II)terpyridyl Complex Photosensitizer. Sol. Energy Mater. Sol. Cells 85 (January 2005): 21–30.
- [14] Supramolecular Materials Group. Dye-Sensitized Solar Cells [Online]. 2011, Available from : <http://140.109.91.205/en/research/DSSC.htm> [2011, Mar]
- [15] Rochford, J., Chu, D., Hagfeldt, A., and Galoppini, E. Tetrachelate Porphyrin Chromophores for Metal Oxide Semiconductor Sensitization: Effect of the Spacer Length and Anchoring Group Position. J. Am. Chem. Soc. 129 (March 2007): 4655–4665.
- [16] Thunell, S. Porphyrins, Porphyrin Metabolism and Porphyrias I. Update. Scand. J. Clin. Lab. Invest. 60 (November 2000): 509–540.
- [17] Graca, M., Vicente, H., Jaquinod, L., and Smith, K. M. Oligomeric Porphyrin Arrays. Chem. Commun. 18 (May 1999): 1771–1782.
- [18] Rahiman, A. K., Rajesh, K., Bharathi, K. S., Sreedaran, S., and Narayanan, V. Catalytic Oxidation of Alkenes by Manganese(III) Porphyrin-Encapsulated Al, V, Si-Mesoporous Molecular Sieves. Inorg. Chim. Acta. 362 (April 2009): 1491–1500.
- [19] Fang, Z., and Liu, B. A Cationic Porphyrin-Based Self-Assembled Film for Mercury Ion Detection. Tetrahedron Lett. 49 (February 2008): 2311–2315.
- [20] Kathiravan, A., Kumar, P. S., Renganathan, R., and Anandan, S. Photoinduced Electron Transfer Reactions Between *meso*-Tetrakis(4-sulfonatophenyl) porphyrin and Colloidal Metal-Semiconductor Nanoparticles. Colloids



- and Surfaces A: Physicochem. Eng. Aspects. 333 (February 2009): 175–181.
- [21] Salaneck, W. R., and other. Electroluminescence in Conjugated Polymers. Nature 397 (January 1999): 121–128.
- [22] Zhong, L., Zhu, X., Duan, P., and Liu, M. Photopolymerization and Formation of a Stable Purple Langmuir-Blodgett Film Based on the Gemini-type Amphiphilic Diacetylene Derivatives. J. Phys. Chem. B. 114 (June 2010): 8871–8878.
- [23] Li, F., and other. Photopolymerization of Self-Assemble Monolayers of Diacetylenic Alkylphosphonic Acid on Group-III Nitride Substrates. Langmuir 26 (May 2010): 10725–10730.
- [24] Okada, S., peng, S., Spevak, W., and Charych, D. Color and Chromism of Polydiacetylene Vesicles. Acc. Chem. Res. 31 (July 1997): 229–239.
- [25] Adler, A. D., Longo F. R., Finarelli J. D., Goldmacher J., Assour J., and Korsakoff L. A Simplified Synthesis for meso-Tetraphenylporphin. J. Org. Chem. 32 (August 1966): 476.
- [26] Howarth N. M., Lindsell W. E., Murray E., and Preston P. N. Lipophilic Peptide Nucleic Acids Containing a 1,3-Diyne Function : Synthesis, Characterization and Production of Derived Polydiacetylene Liposomes. Tetrahedron 61 (July 2005): 8875–8887.
- [27] Gradl S. N., Felix J. P., Lsacoff E. Y., Garcia M. L., and Trauner D. Protein Surface Recognition by Rational Design: Nanomolar Ligands for Potassium Channels. J. Am. Chem. Soc. 125 (September 2003): 12668–12669.
- [28] Kew, S. J., and Hall, E. A. H. Structural Effect of Polymerisation and Dehydration on Bolaamphiphilic Polydiacetylene Assemblies. J. Mater. Chem. 16 (April 2006): 2039–2047.
- [29] Jiao, J., Thamyongkit P., Schmidt I., Lindsey J., and Bocian D. F. Characterization of Porphyrin Surface Orientation in Monolayers on Au(111) and Si(100) Using Spectroscopically Labeled Molecules. J. Phys. Chem. C. 111 (June 2007): 12693–12704.
- [30] Troshin, P. A., and other. Material Solubility-Photovoltaic Performance Relationship in the Design of Novel Fullerene Derivatives for Bulk

Heterojunction Solar Cells. Adv. Funct. Mater. 19 (February 2009): 779–788.

- [31] Grätzel, M. and other. Fabrication of thin film dye sensitized solar cells with solar to electric power conversion efficiency over 10%. Thin. Sol. Films. 516 (June 2007): 4613–4619.

## **APPENDICES**

## **APPENDIX A**

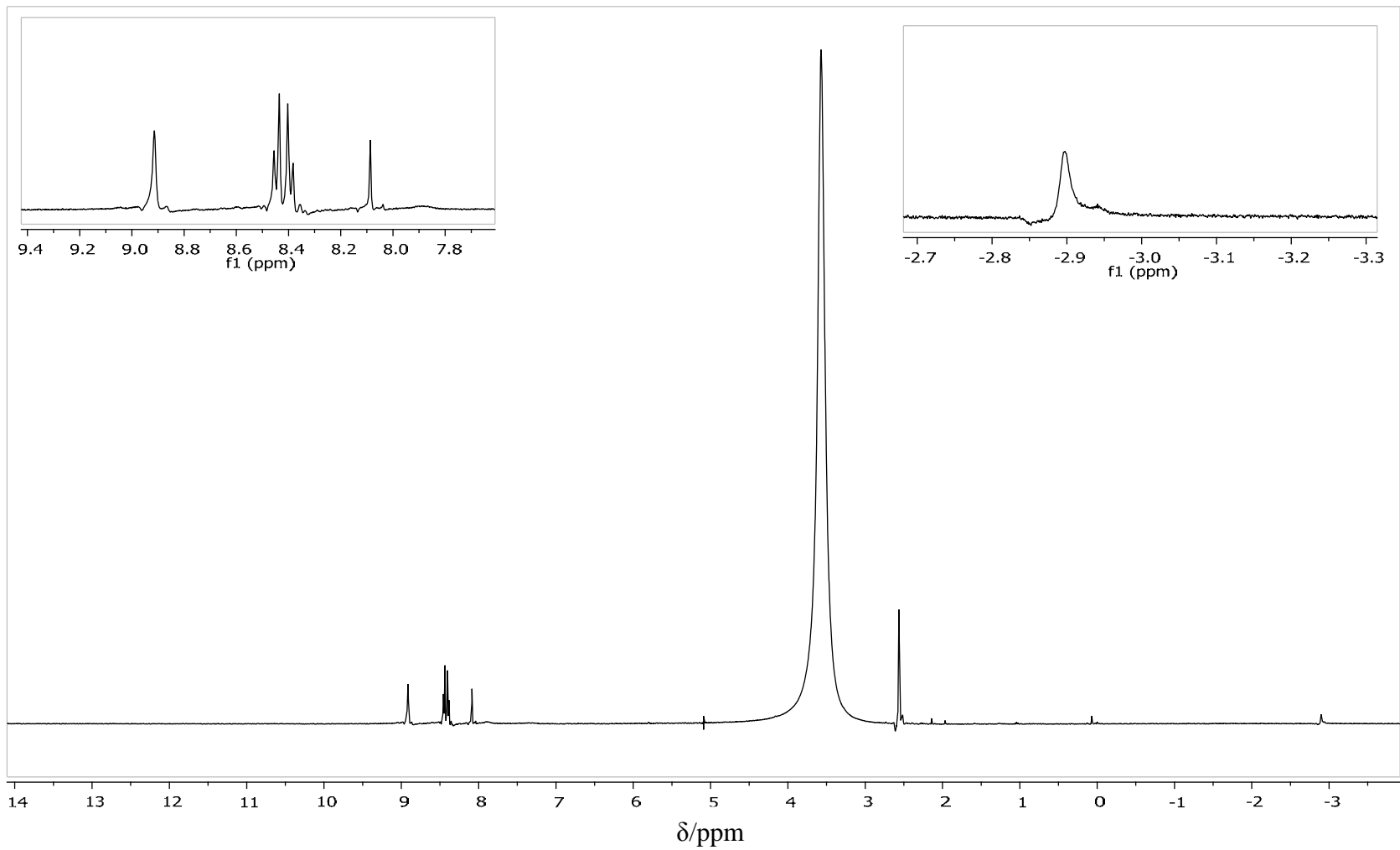


**Figure A-1:**  $^1\text{H-NMR}$  spectrum of compound 3.

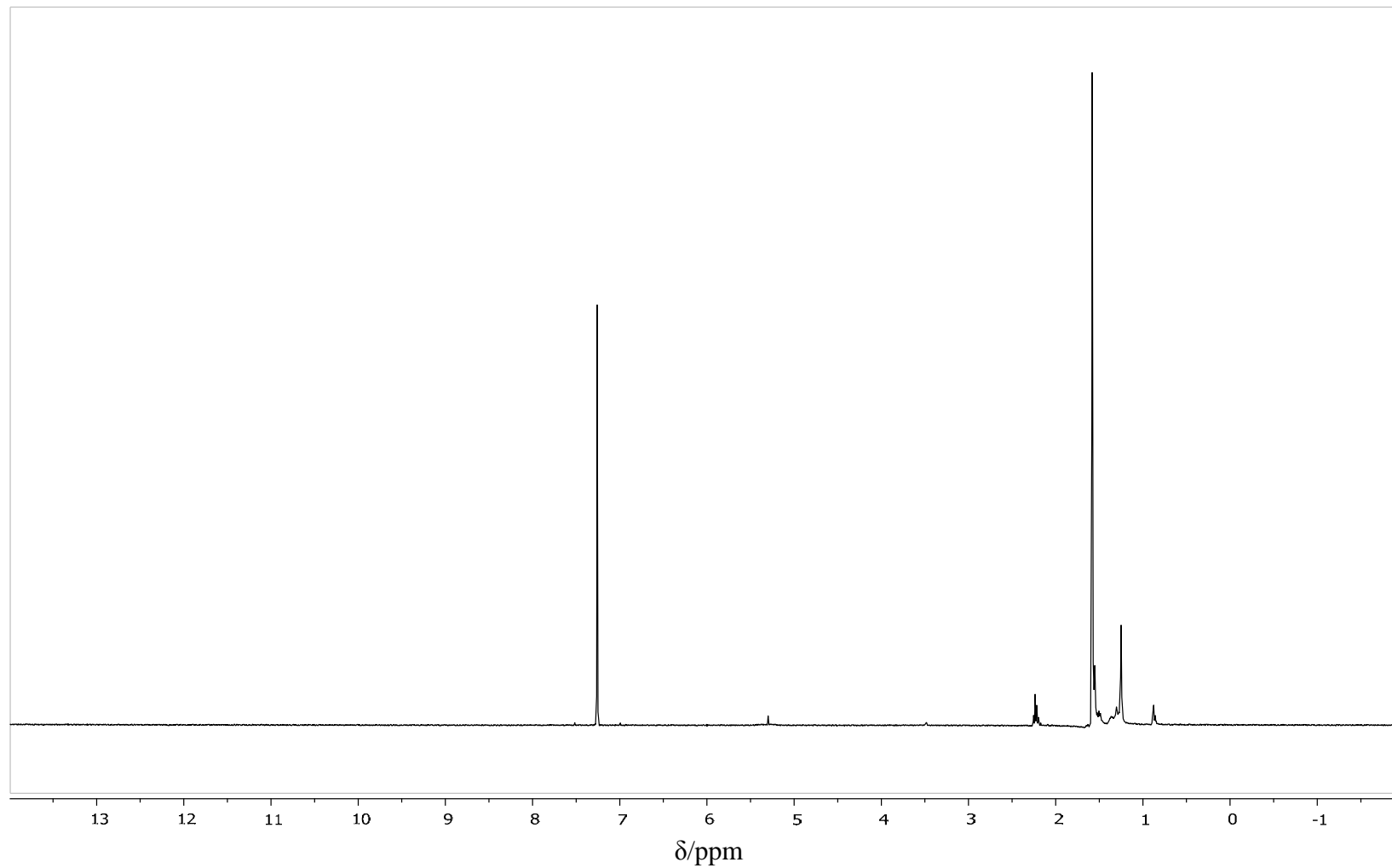


**Figure A-2:**  $^1\text{H-NMR}$  spectrum of compound 7.

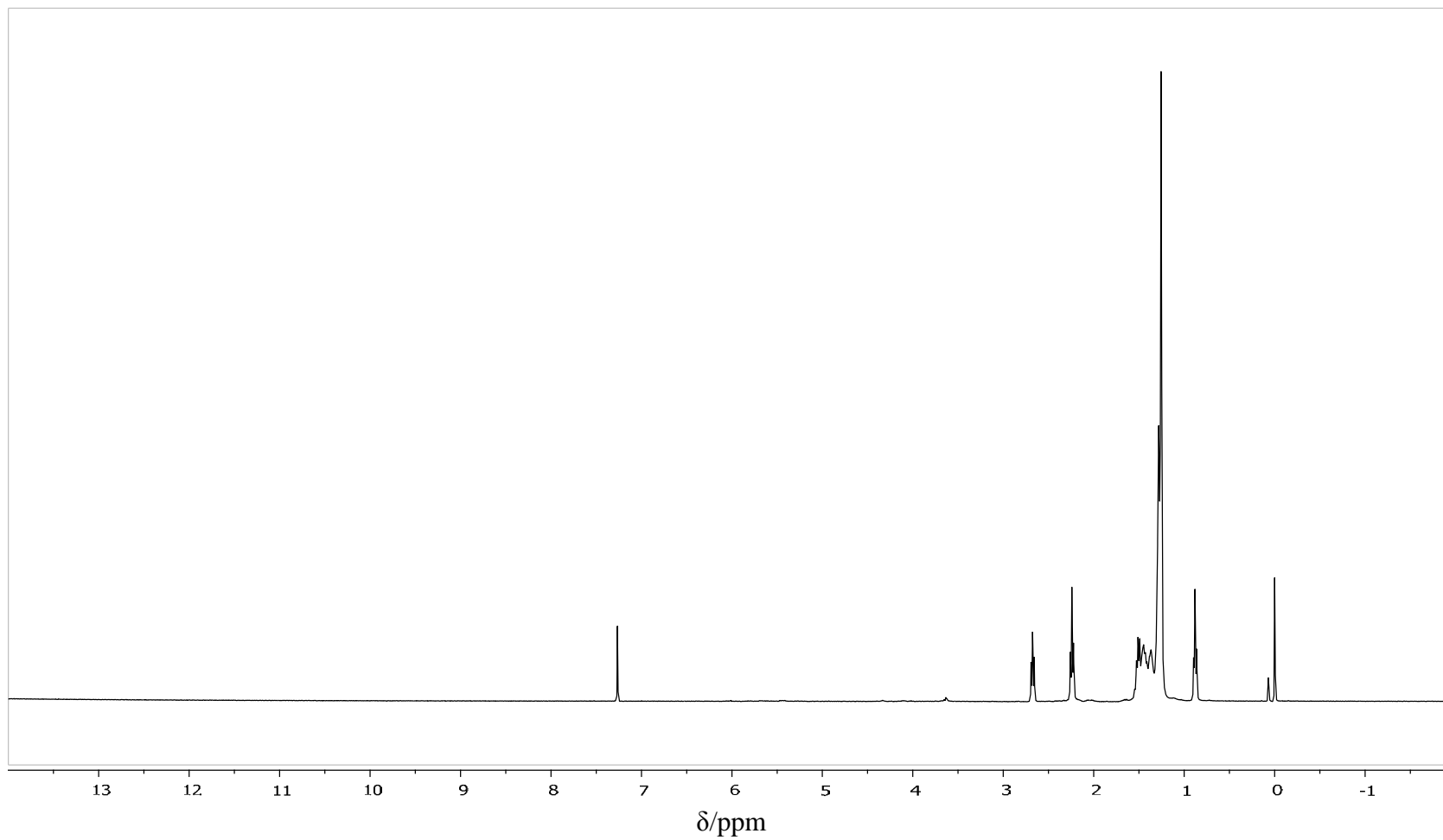


**Figure A-3:** <sup>1</sup>H-NMR spectrum of compound **8**.

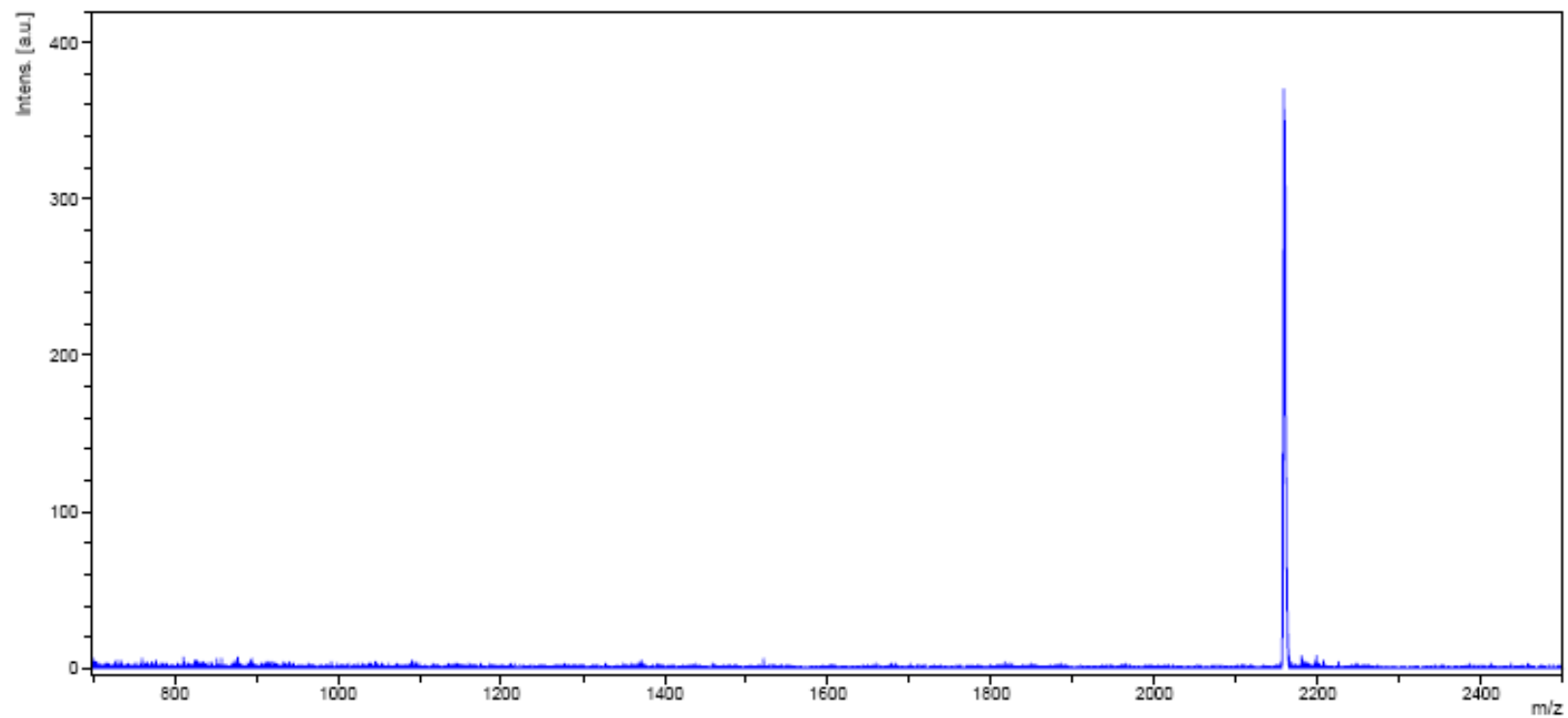


**Figure A-4:** Mass spectrum of compound **1** via acid chloride formation.



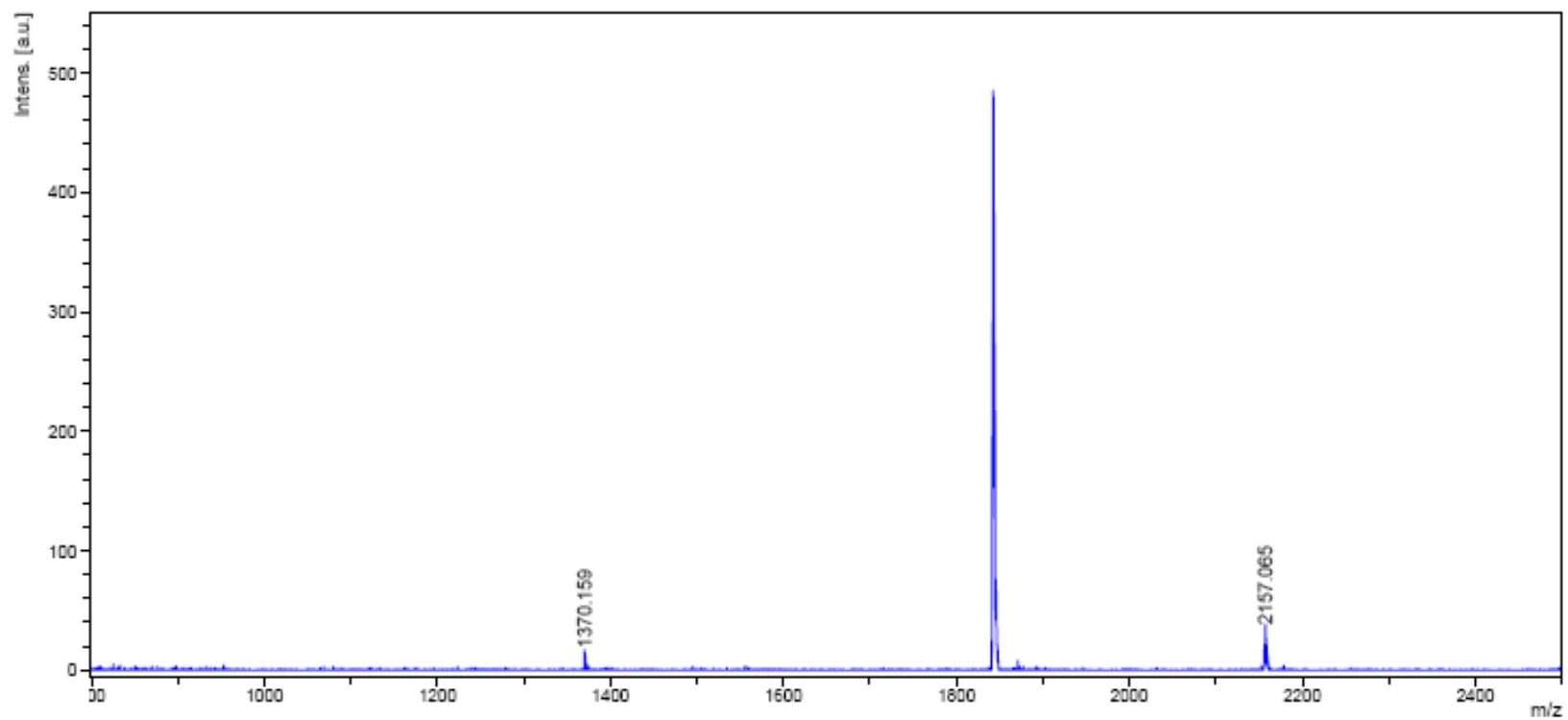


**Figure A-5:** Mass spectrum of ester derivative of compound 2.

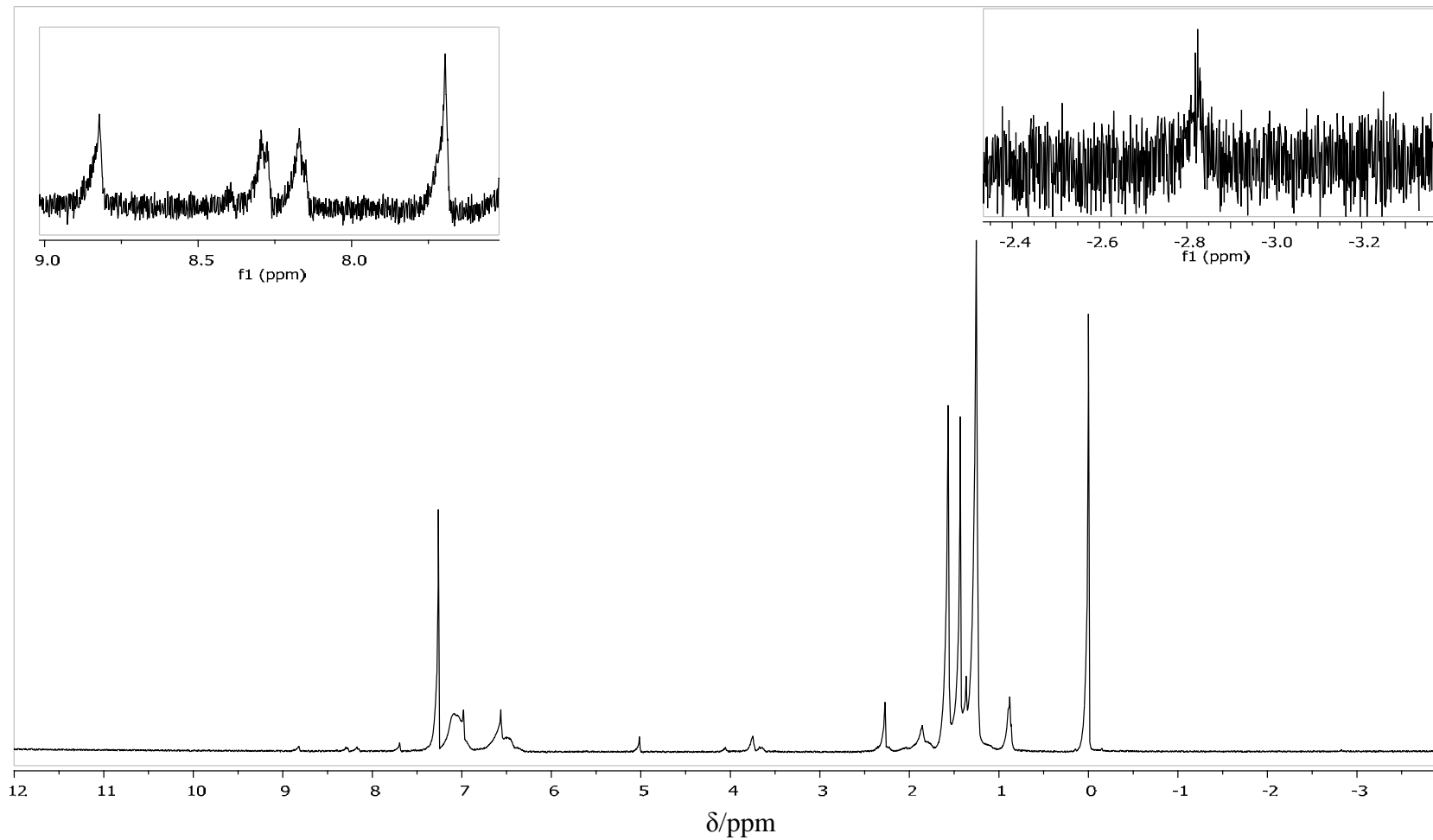


**Figure A-6:**  $^1\text{H-NMR}$  spectrum of compound **1** via succinimide formation.

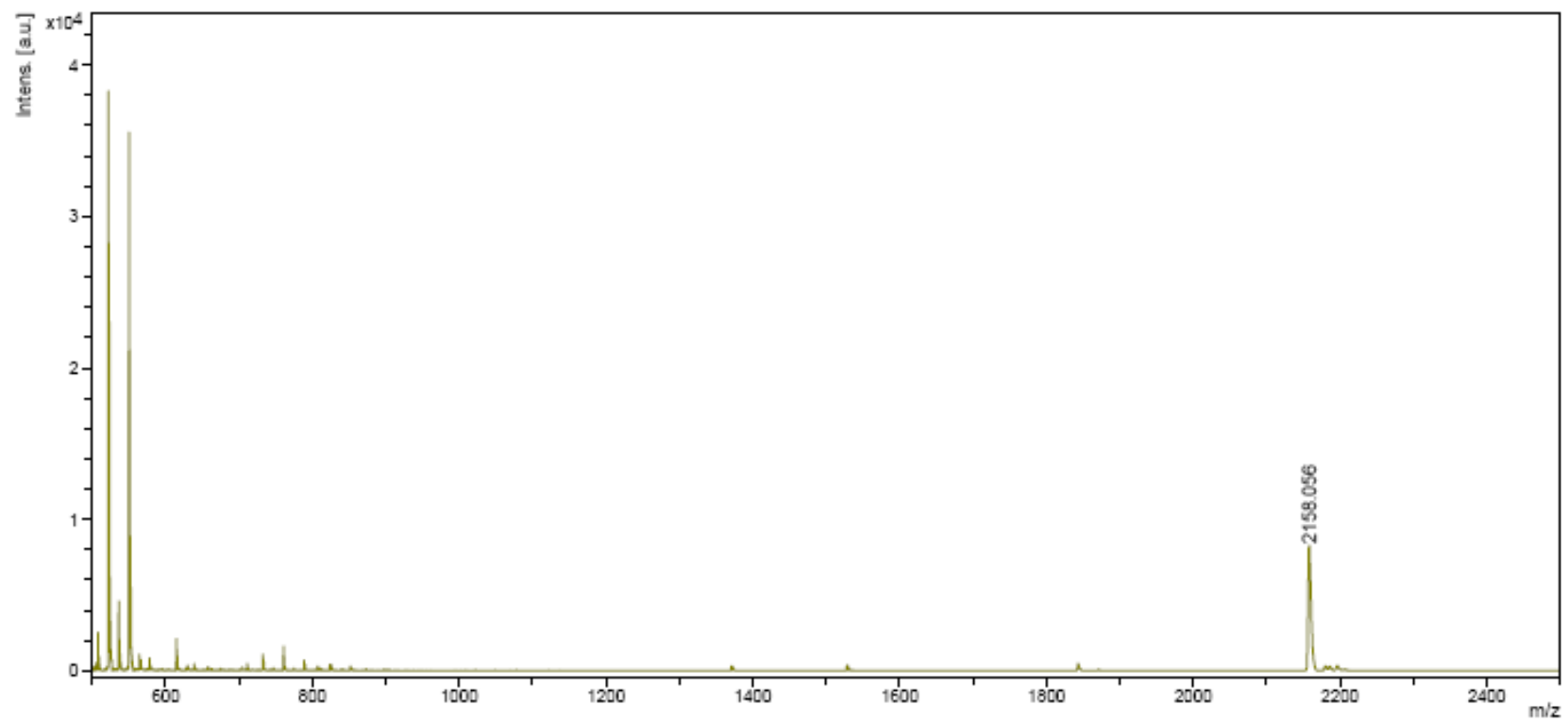


**Figure A-7:** Mass spectrum of compound **1** via succinimide formation.

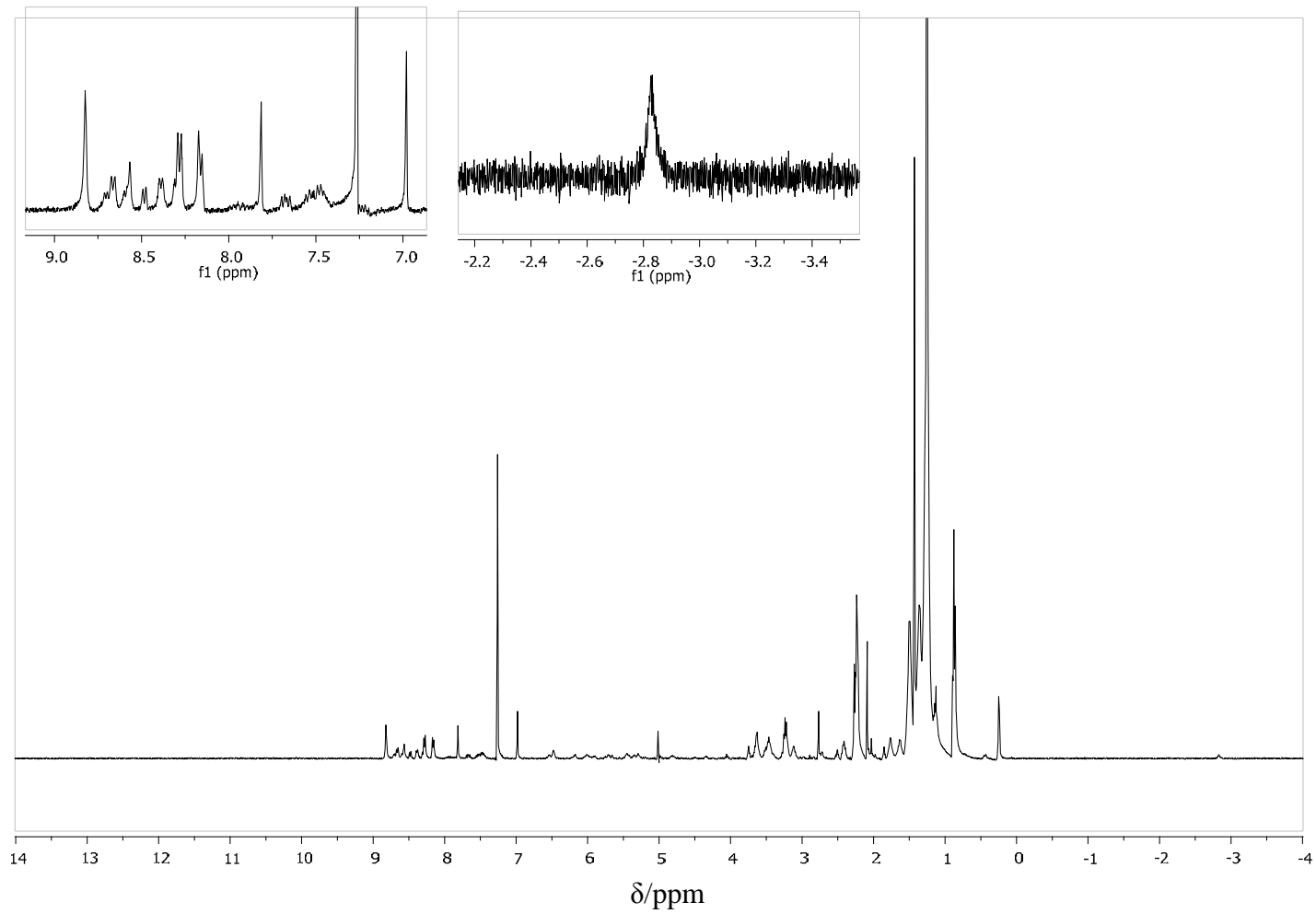


**Figure A-8:**  $^1\text{H-NMR}$  spectrum of compound 2.

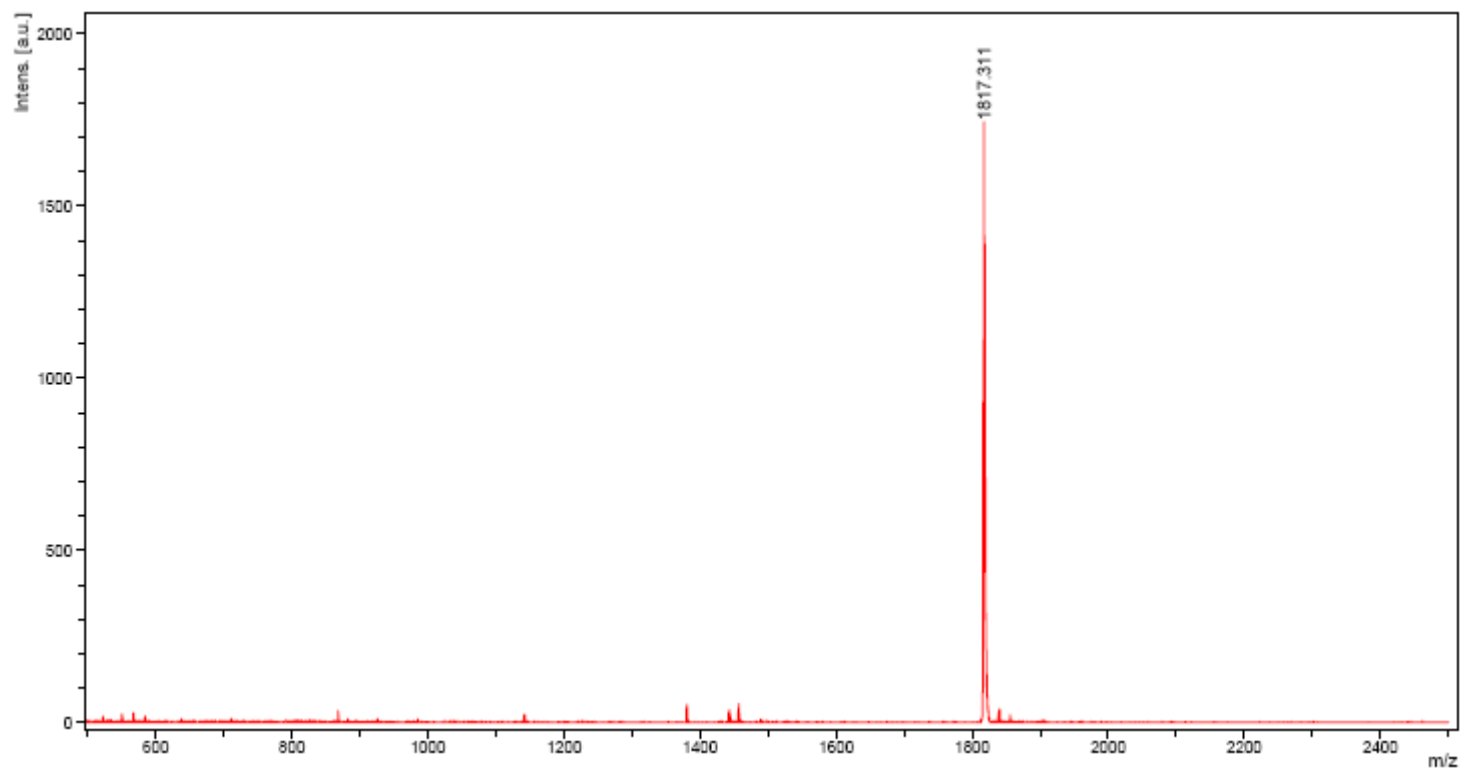


**Figure A-9:** Mass spectrum of compound 2.

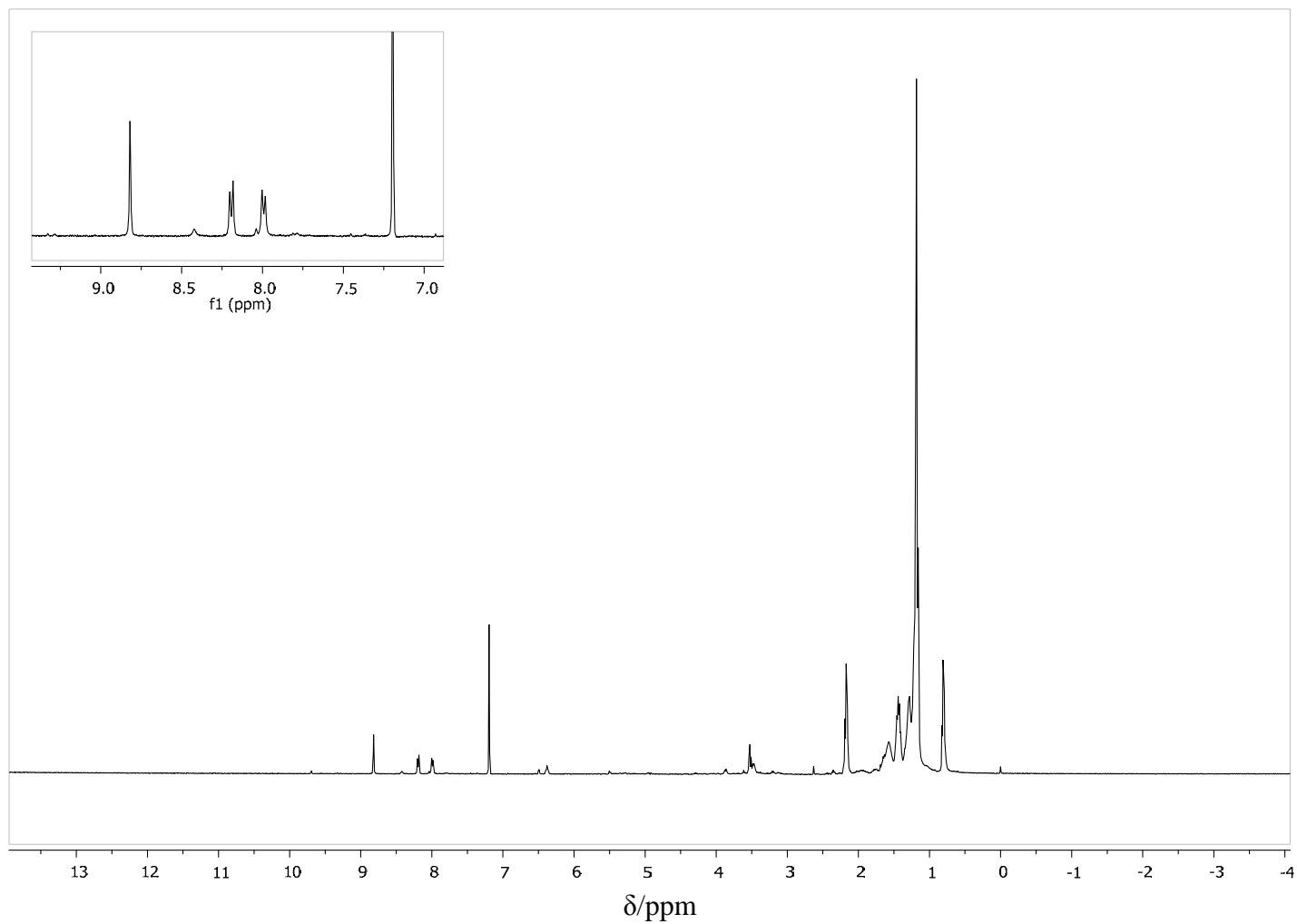


**Figure A-10:**  $^1\text{H-NMR}$  spectrum of compound Zn-1.

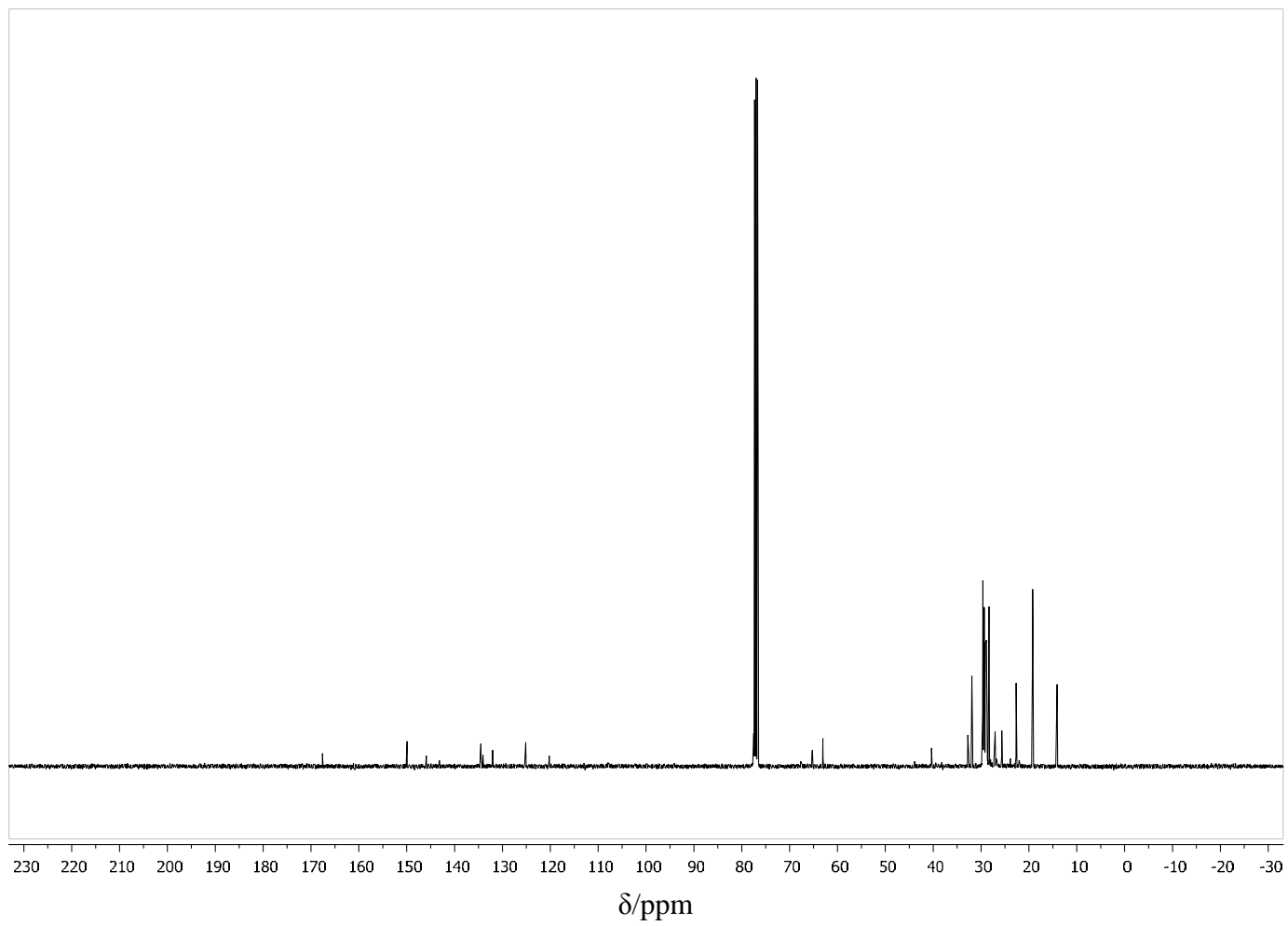


**Figure A-11:**  $^{13}\text{C}$ -NMR spectrum of compound Zn-1.

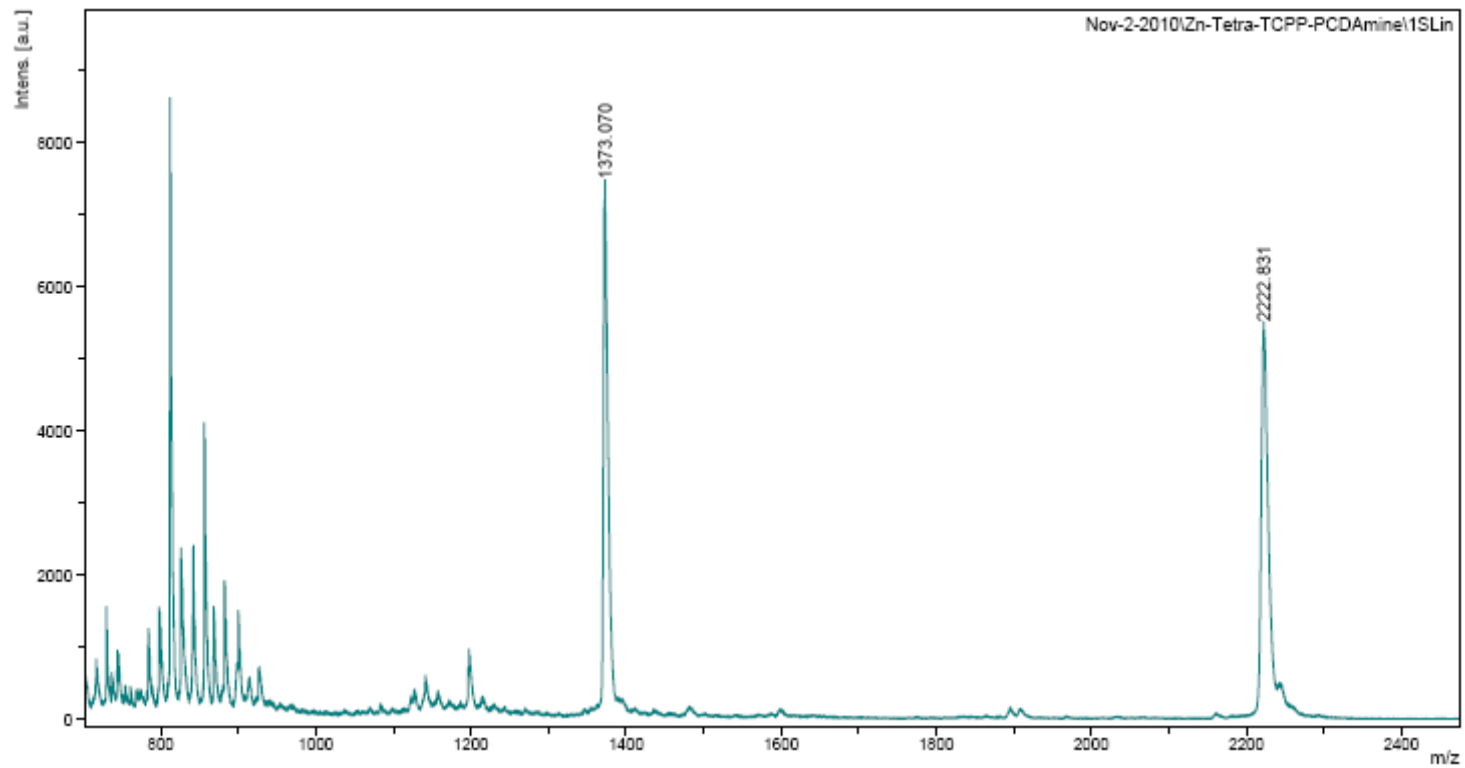


**Figure A-12:** Mass spectrum of compound **Zn-1**.



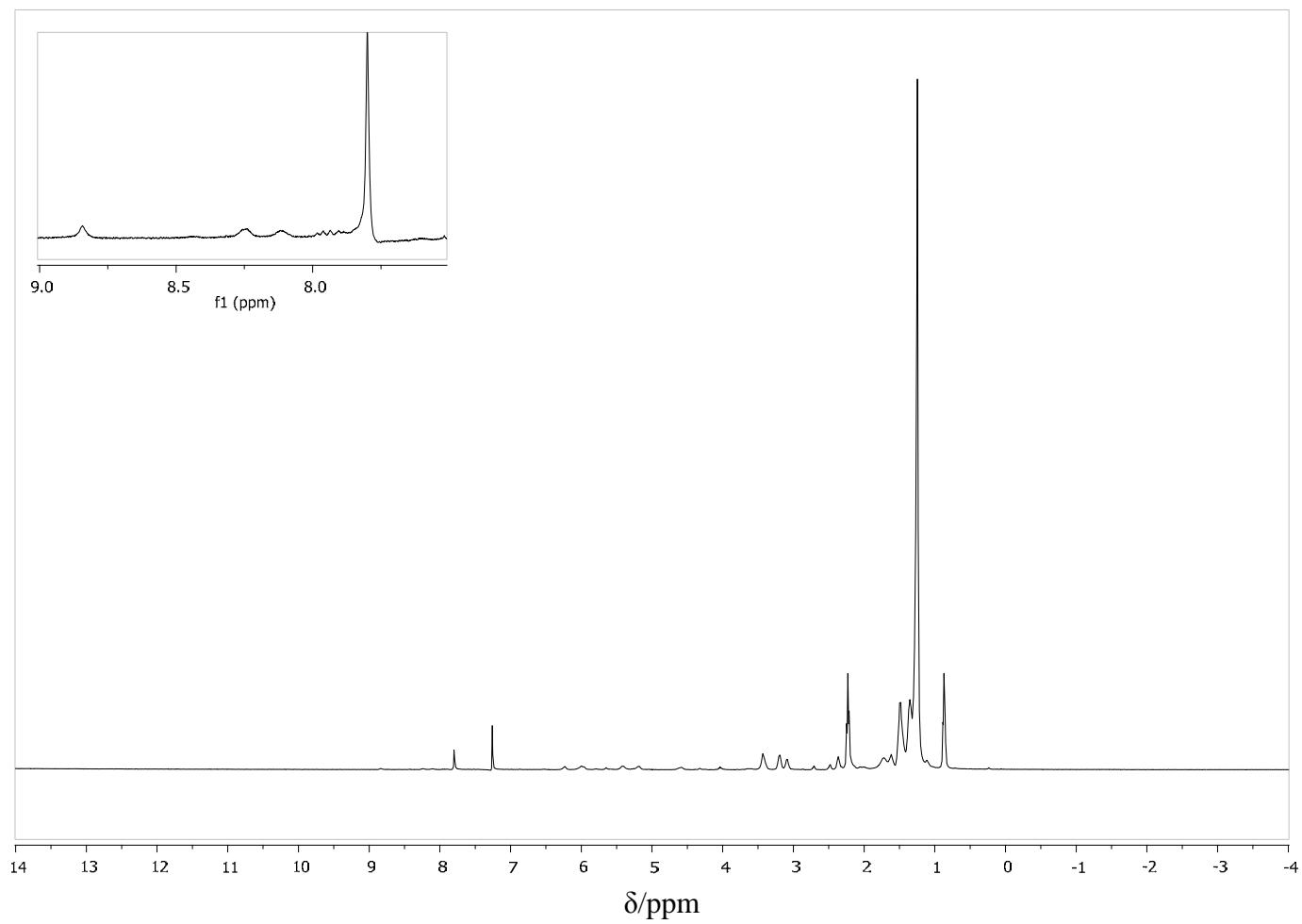


**Figure A-13:**  $^1\text{H-NMR}$  spectrum of compound **Zn-2**.

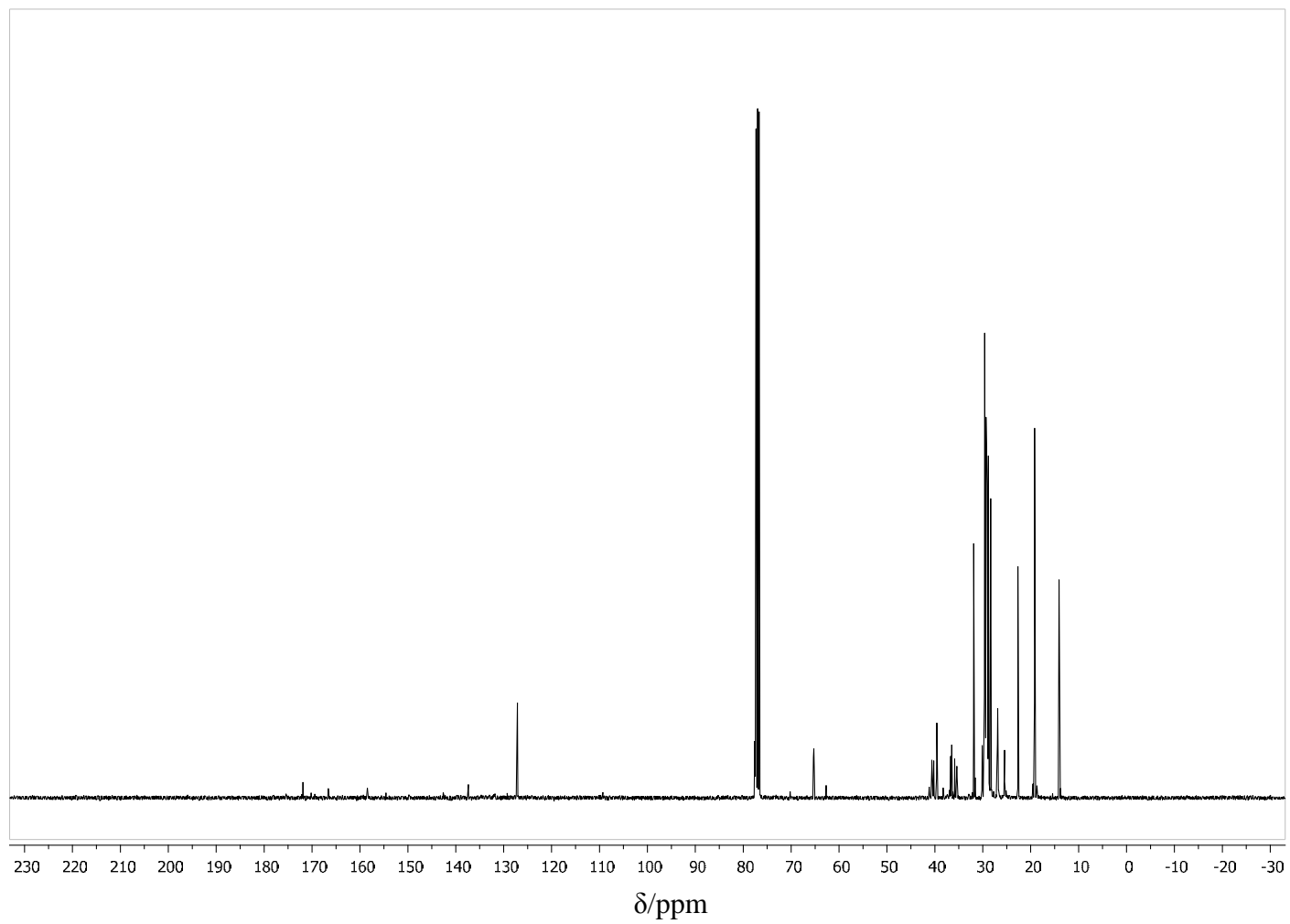


**Figure A-14:**  $^{13}\text{C}$ -NMR spectrum of compound **Zn-2**.

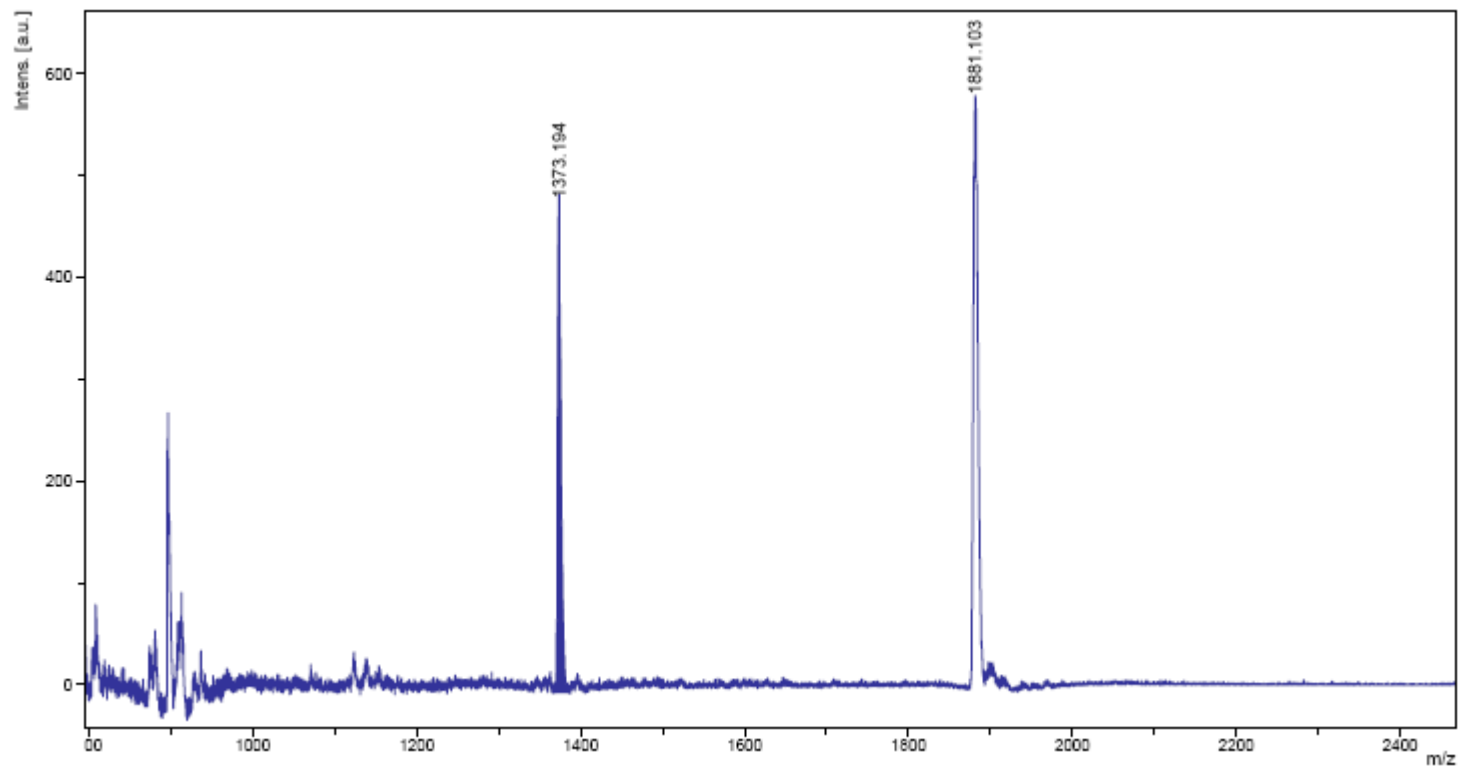


**Figure A-15:** Mass spectrum of compound **Zn-2**.

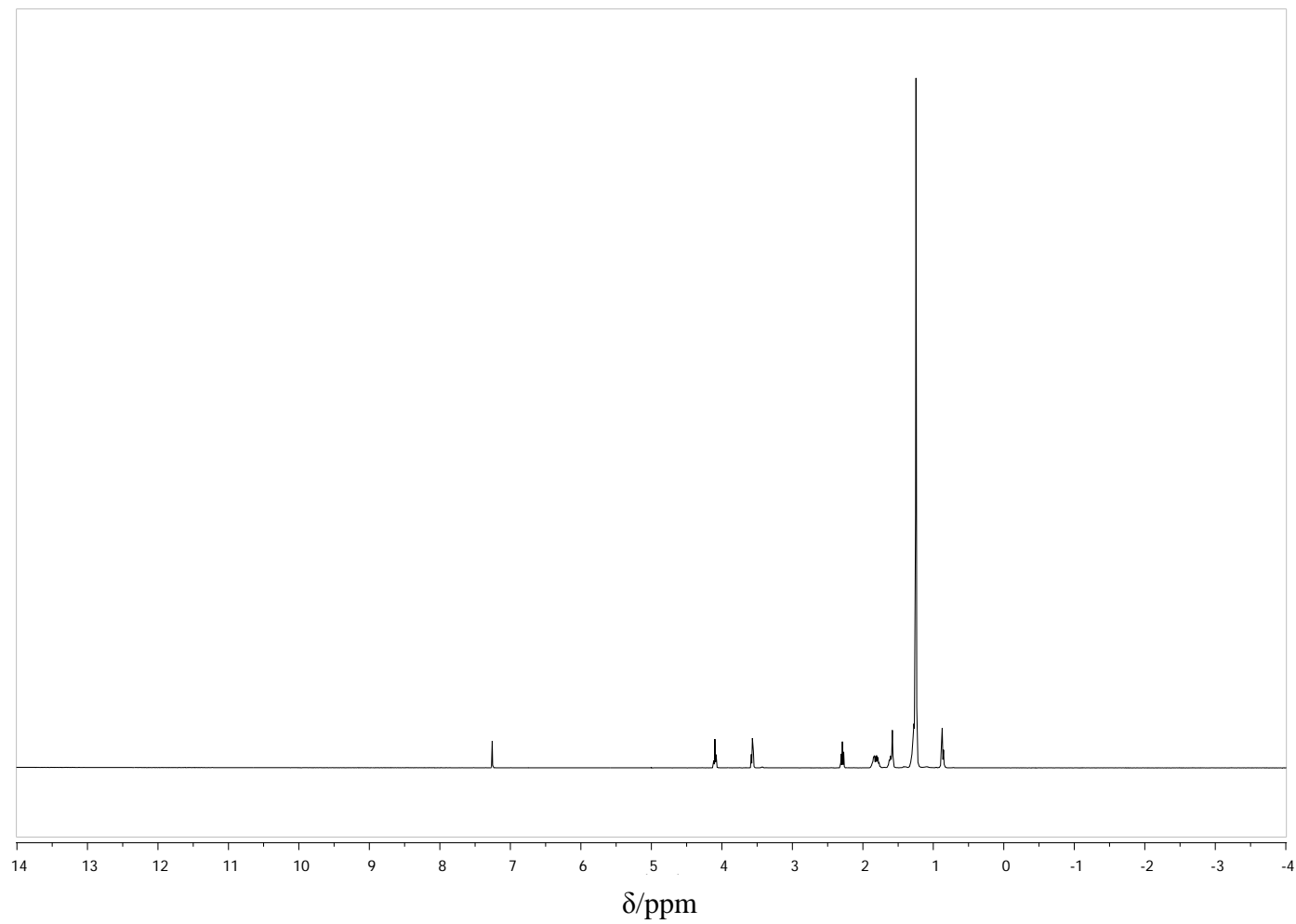


**Figure A-16:**  $^1\text{H}$ -NMR spectrum of compound **12**.

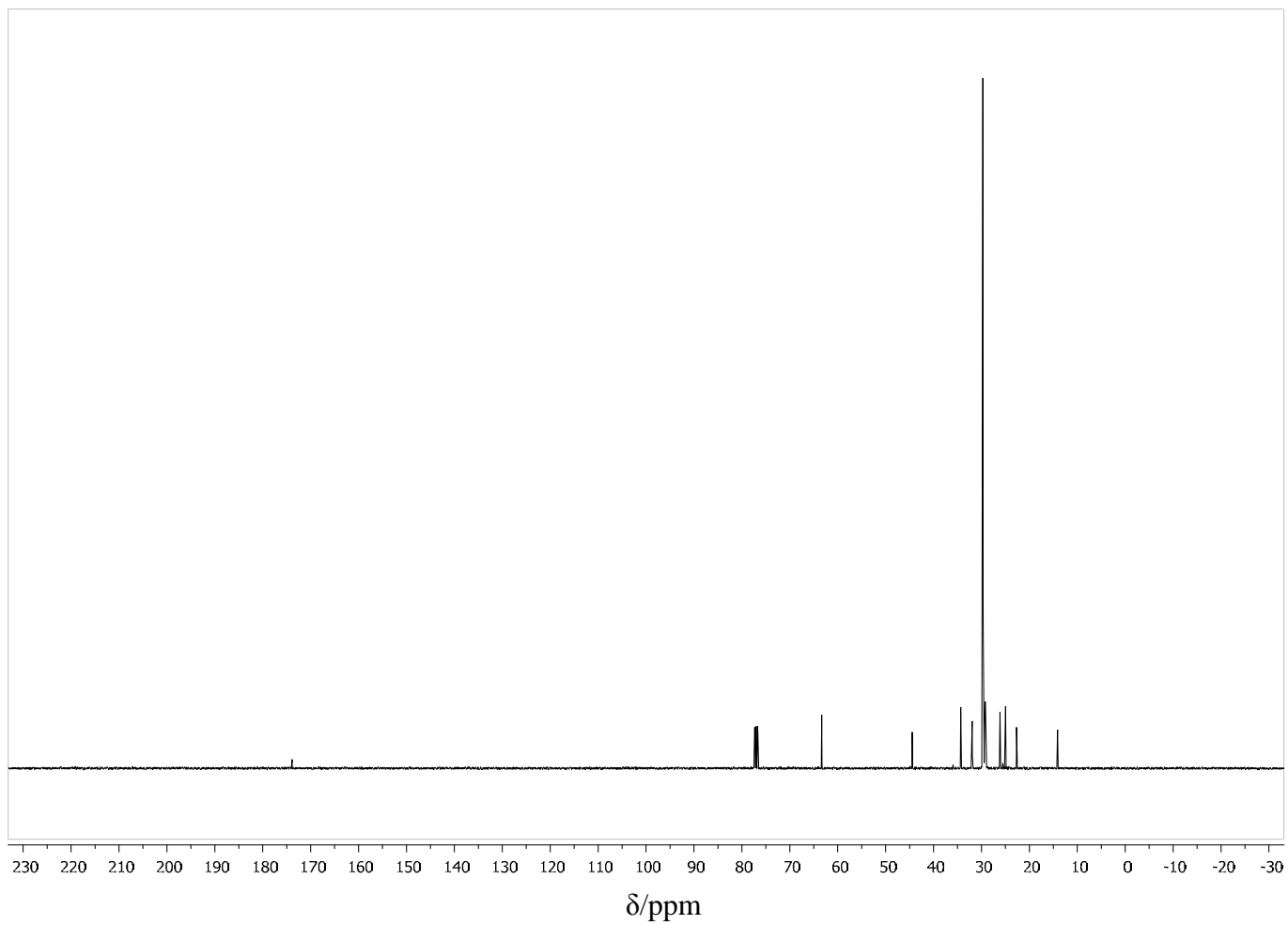


**Figure A-17:**  $^{13}\text{C}$ -NMR spectrum of compound 12.

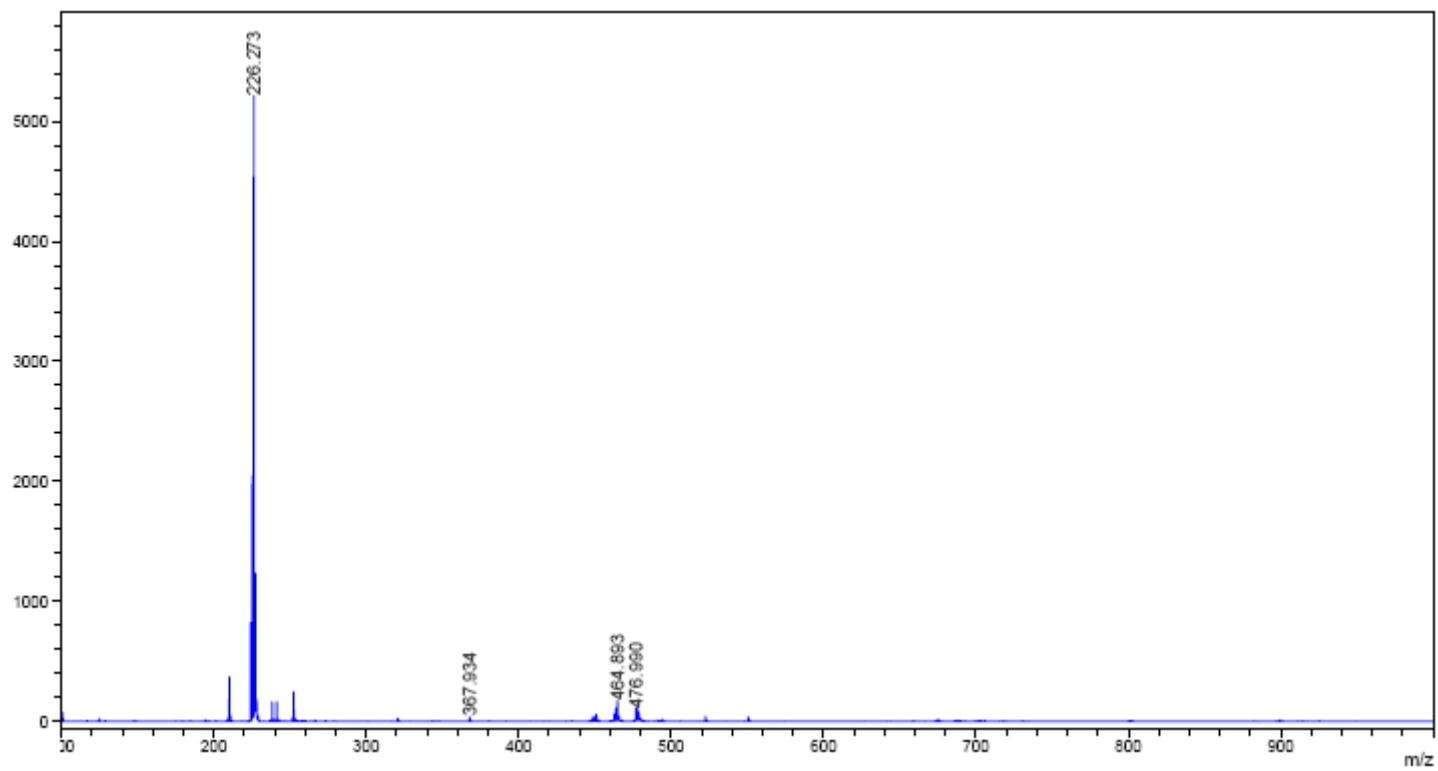


**Figure A-18:** Mass spectrum of compound **12**.

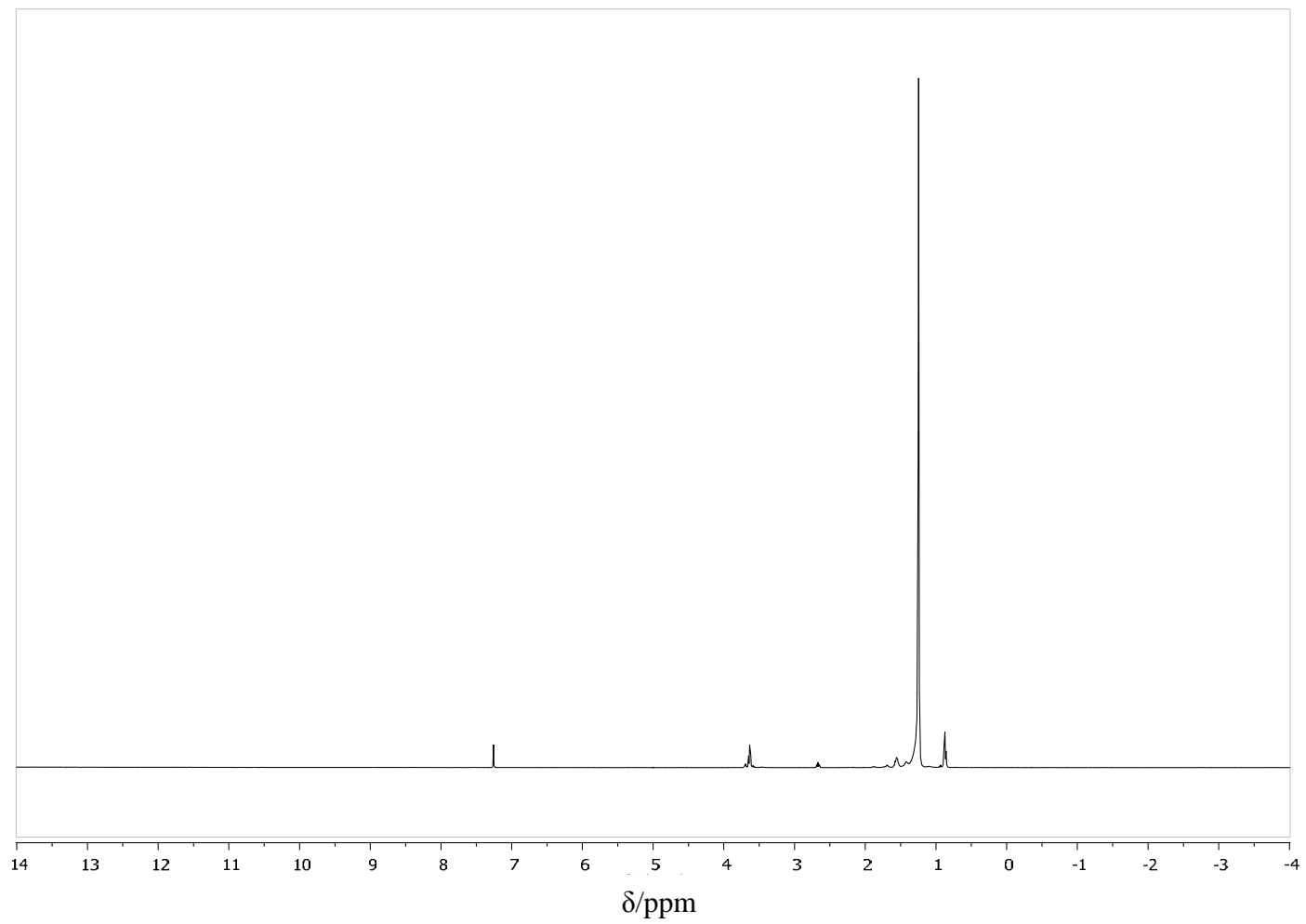


**Figure A-19:**  $^1\text{H-NMR}$  spectrum of compound 13.

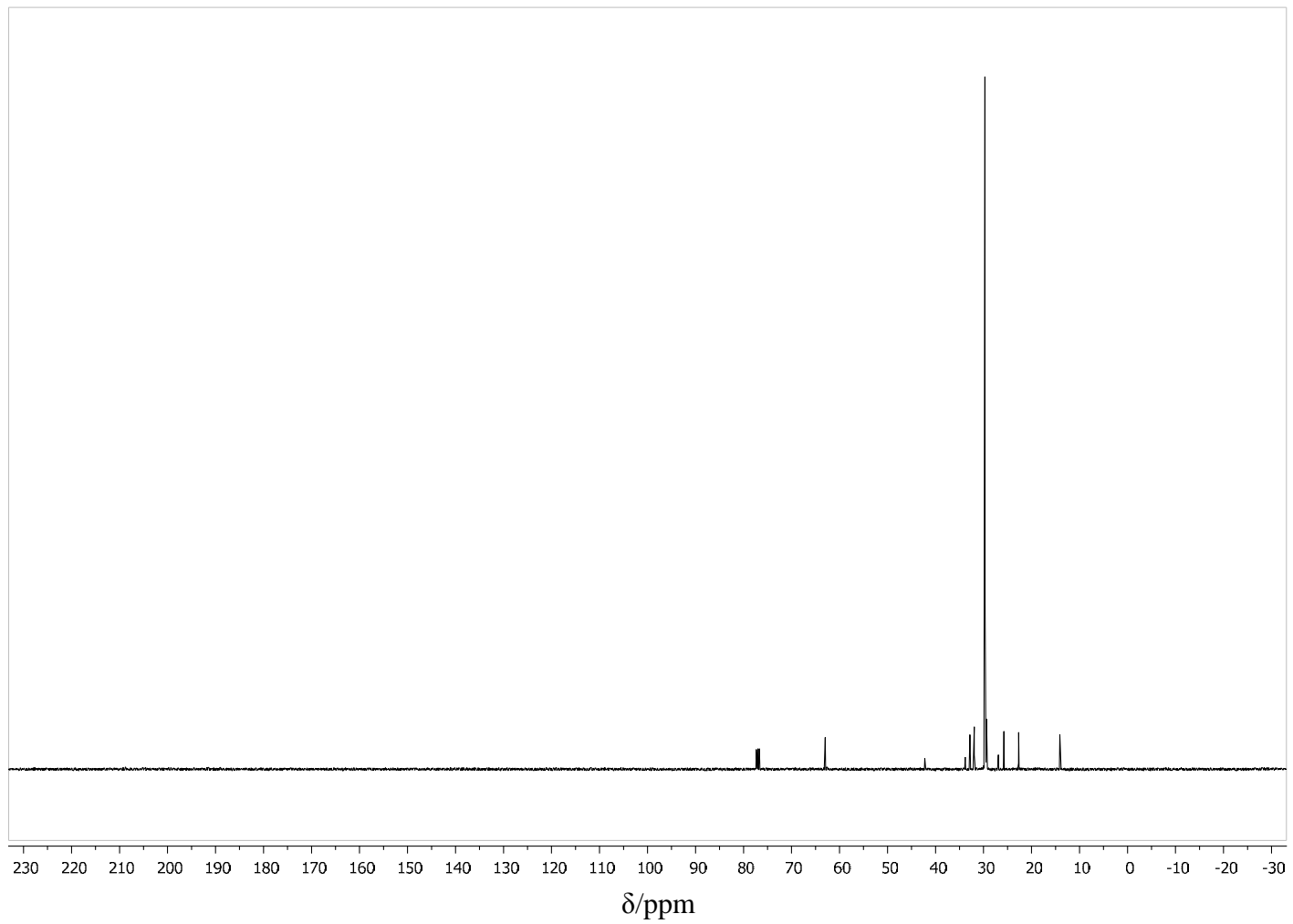


**Figure A-20:**  $^{13}\text{C}$ -NMR spectrum of compound 13.



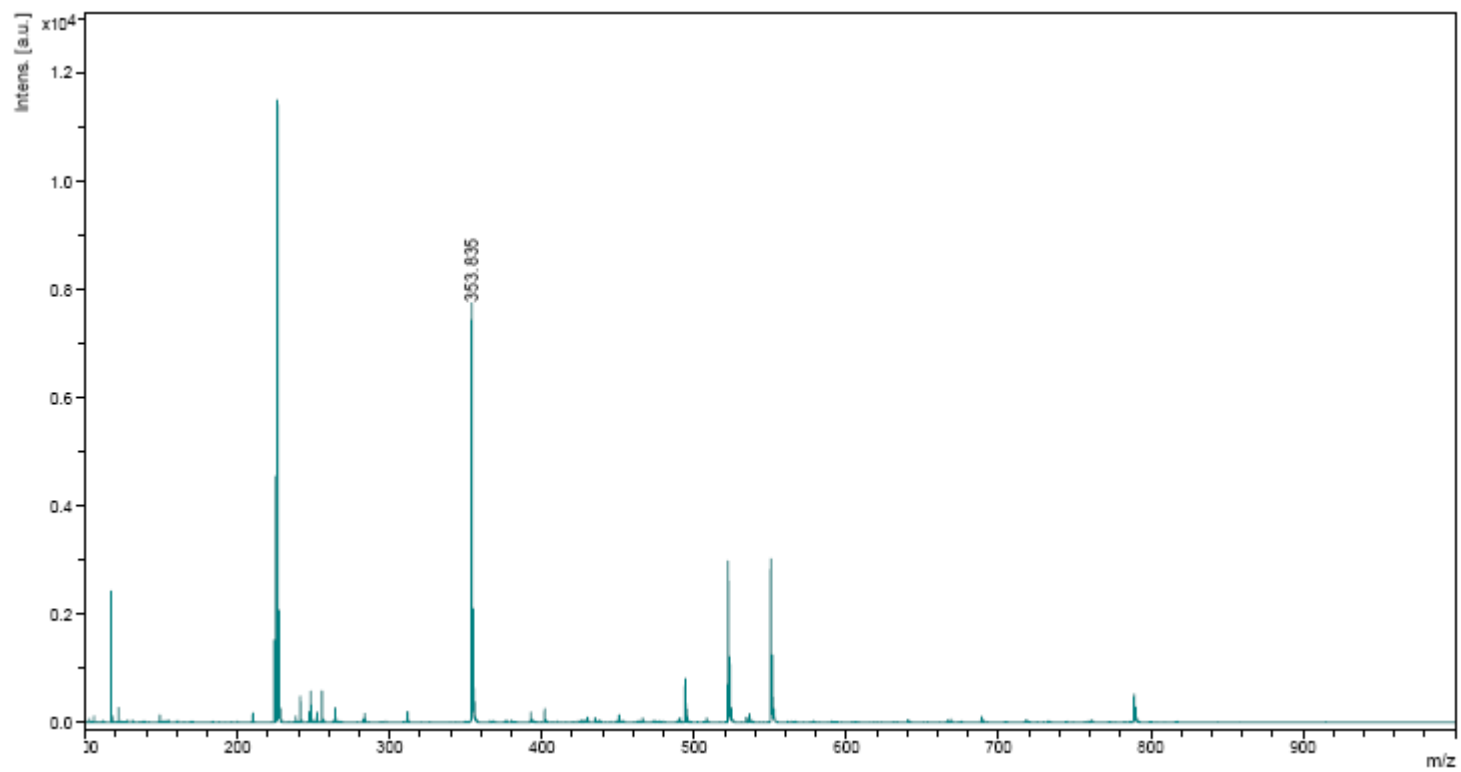


**Figure A-21:** Mass spectrum of compound **13**.

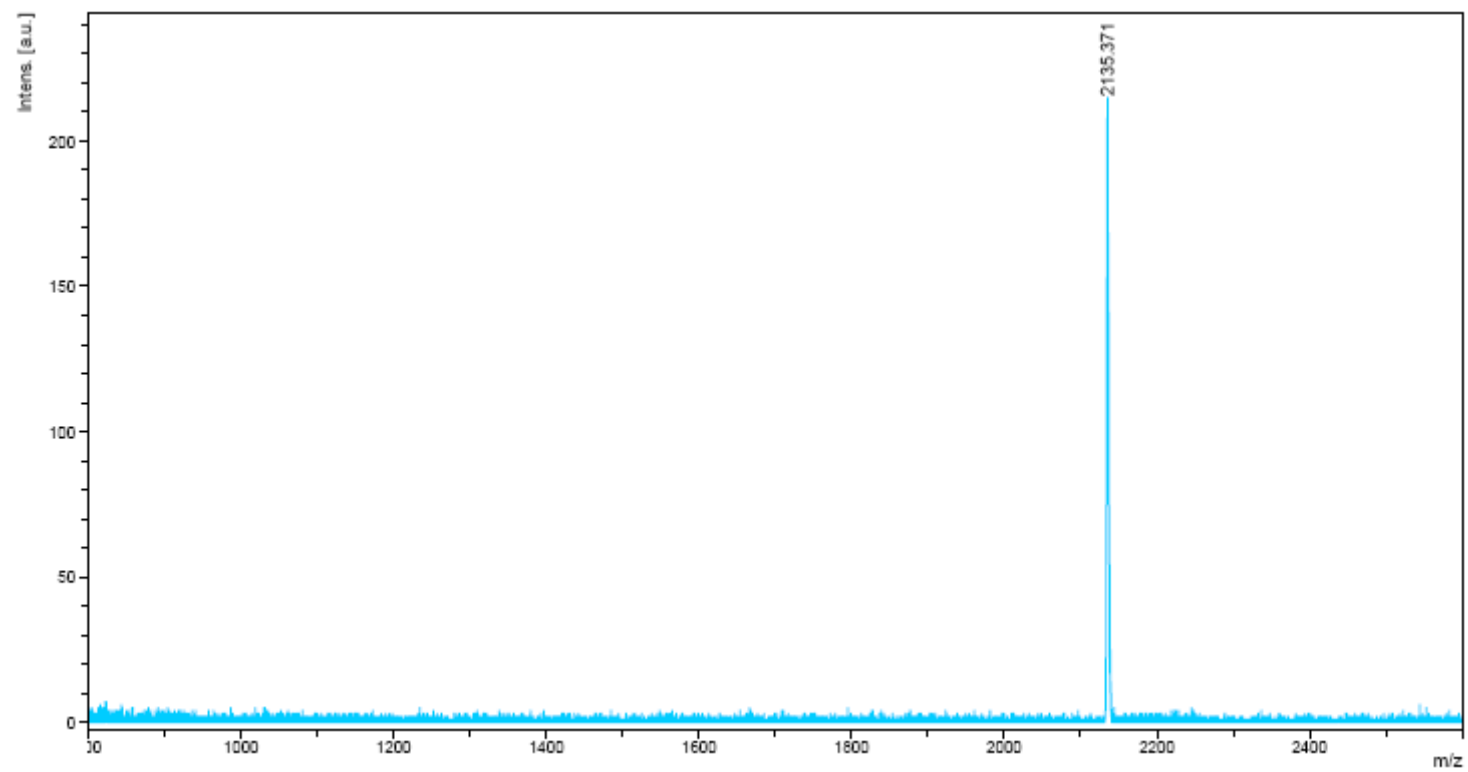


**Figure A-22:** Mass spectrum of compound **14**.

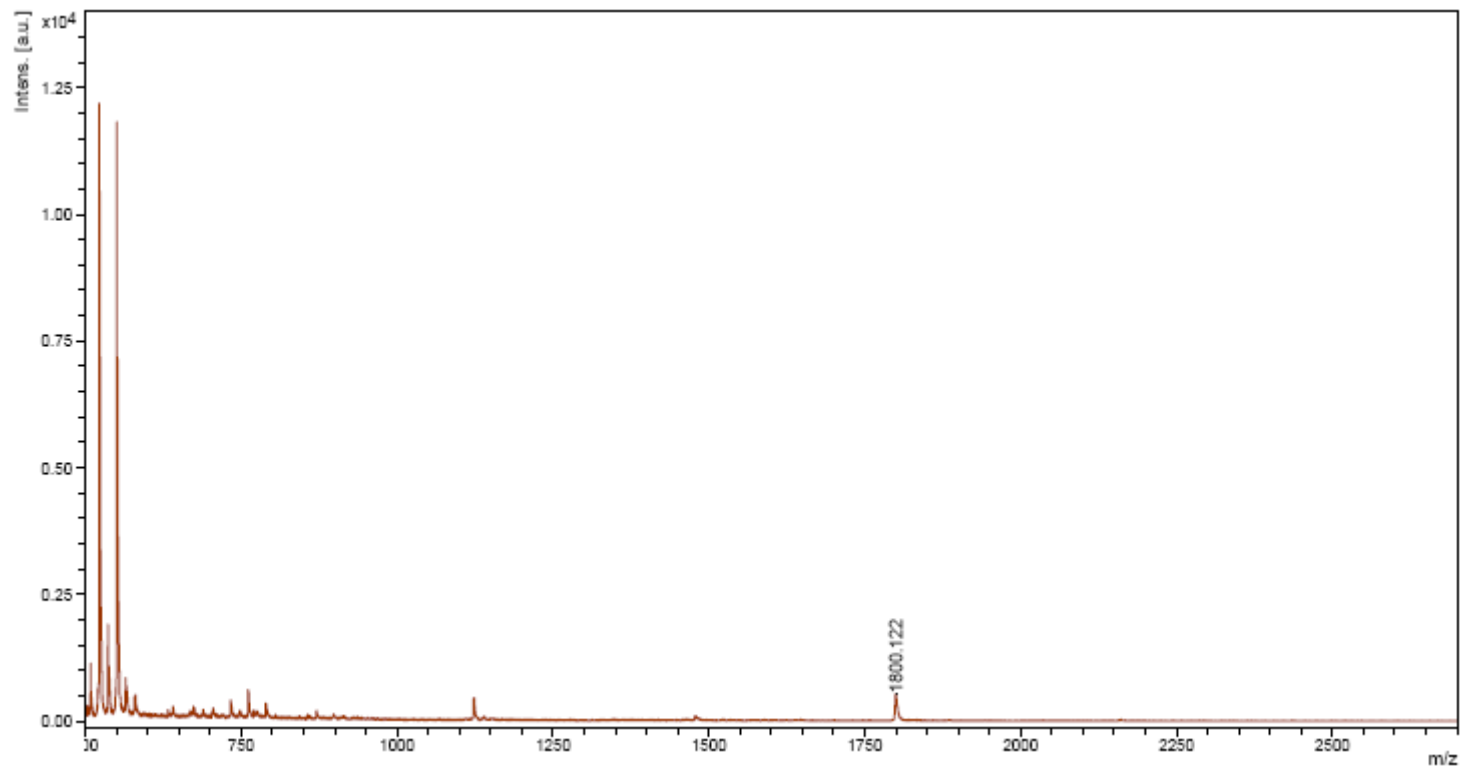


**Figure A-23:** Mass spectrum of compound **15**.

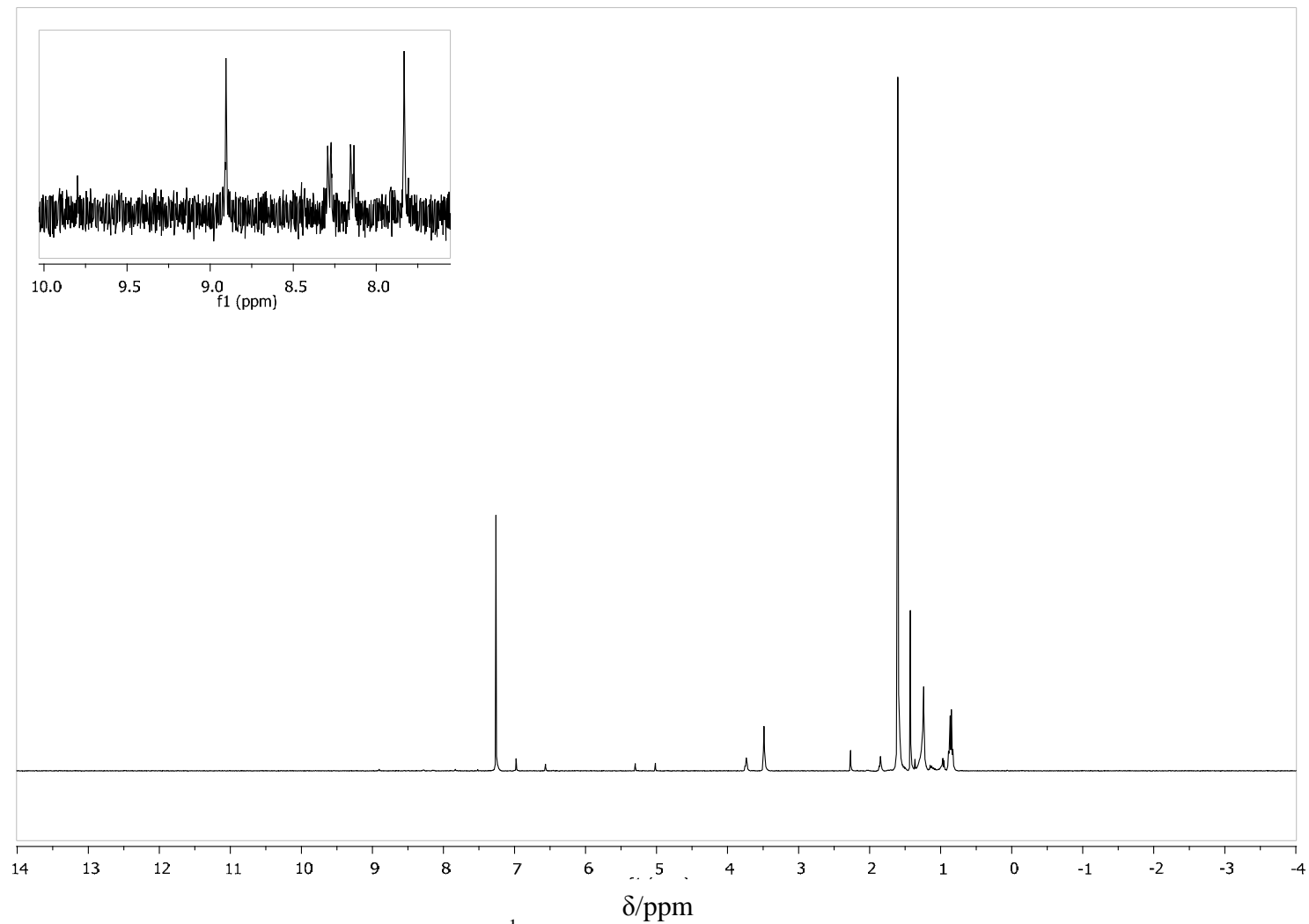


**Figure A-24:**  $^1\text{H-NMR}$  spectrum of compound **Zn-14**.

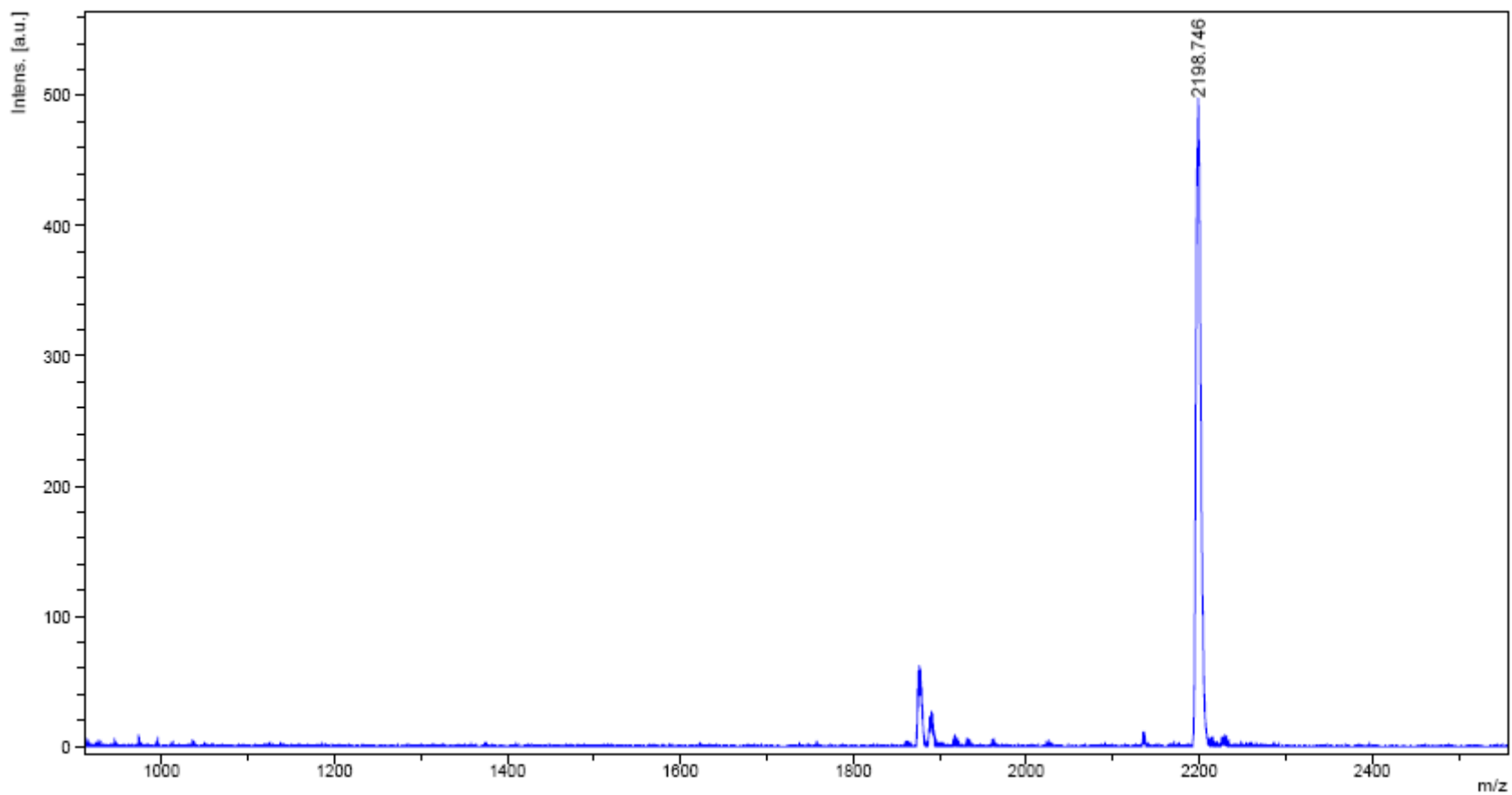
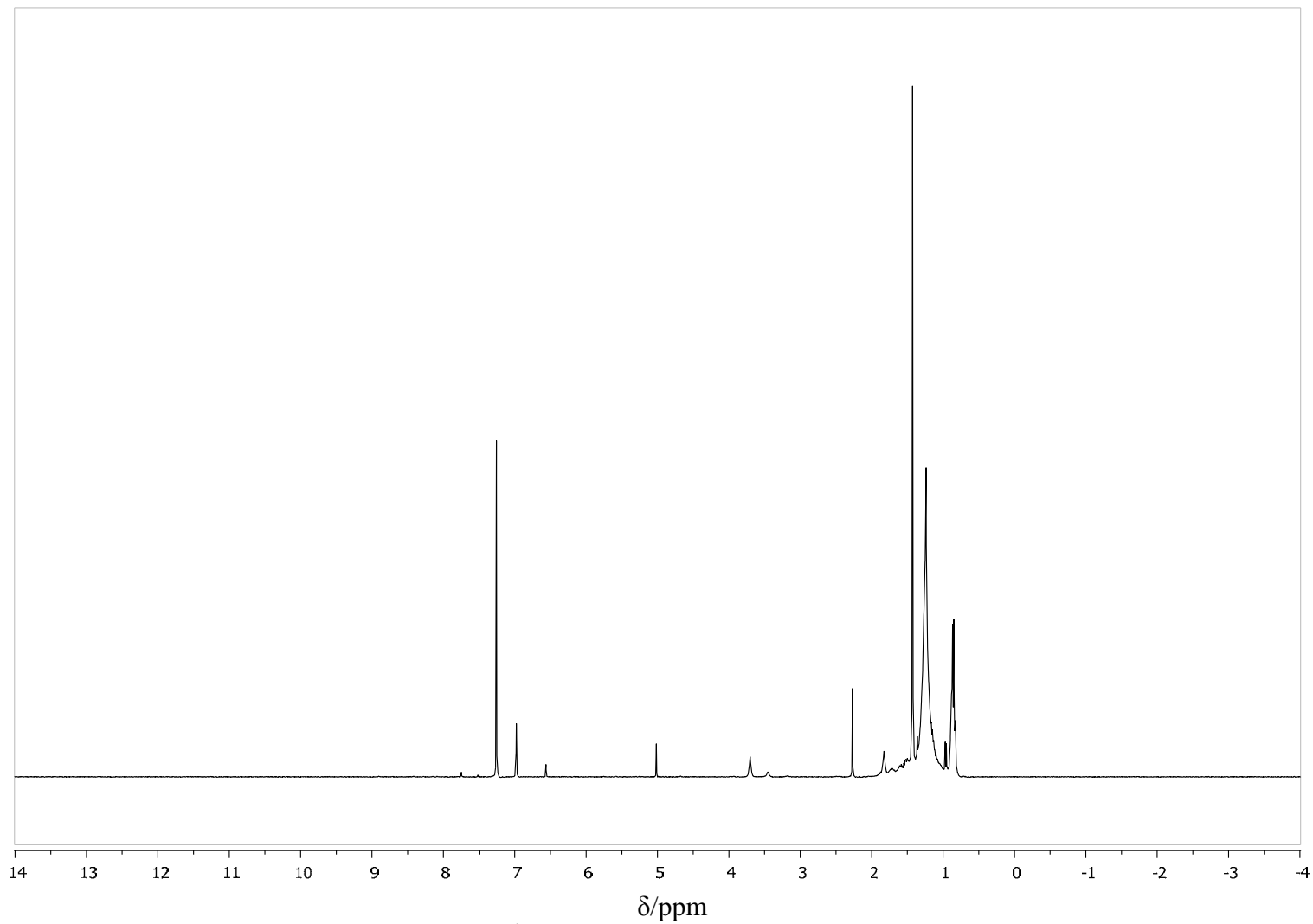


Figure A-25: Mass spectrum of compound Zn-14.



**Figure A-26:**  $^1\text{H-NMR}$  spectrum of compound **Zn-15**.

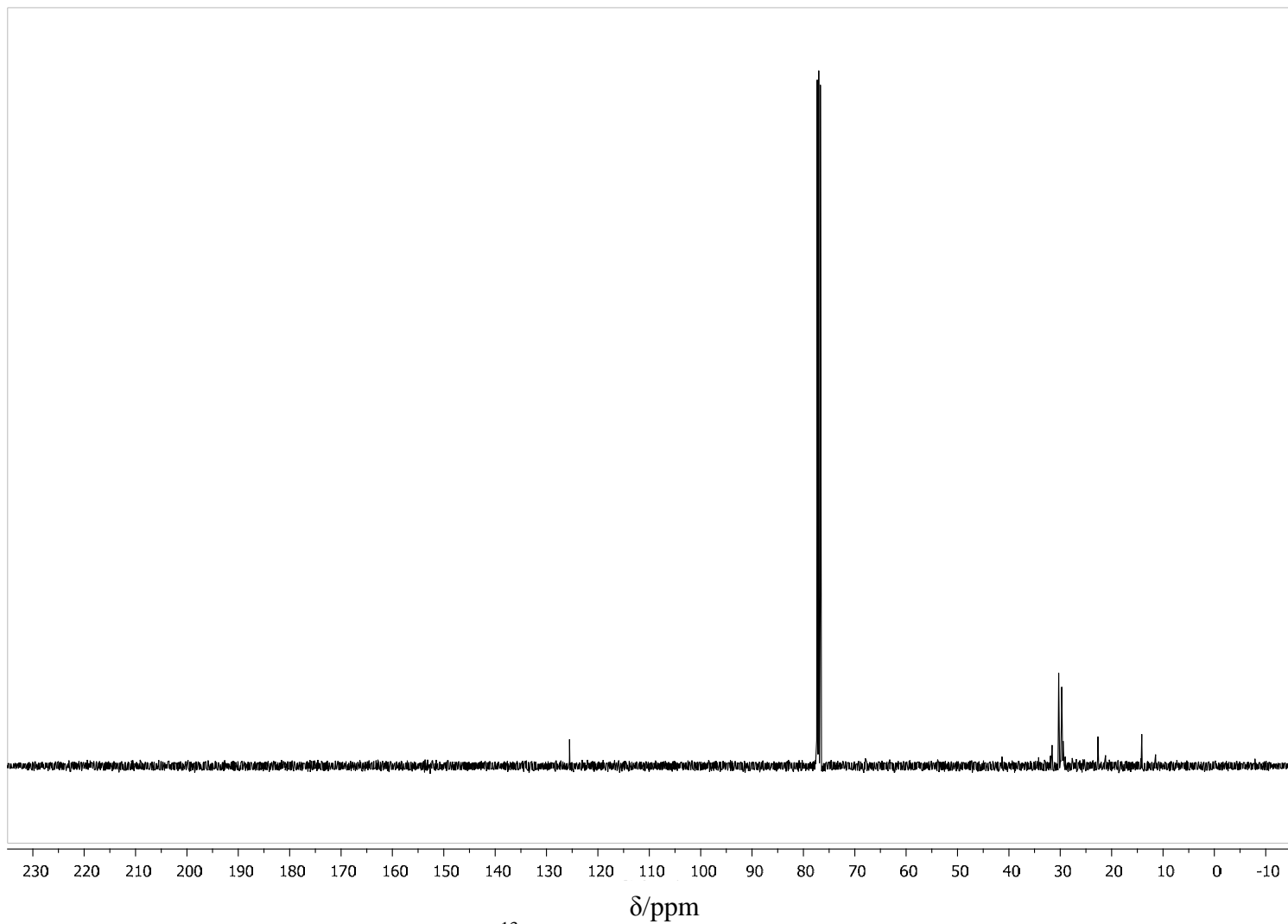
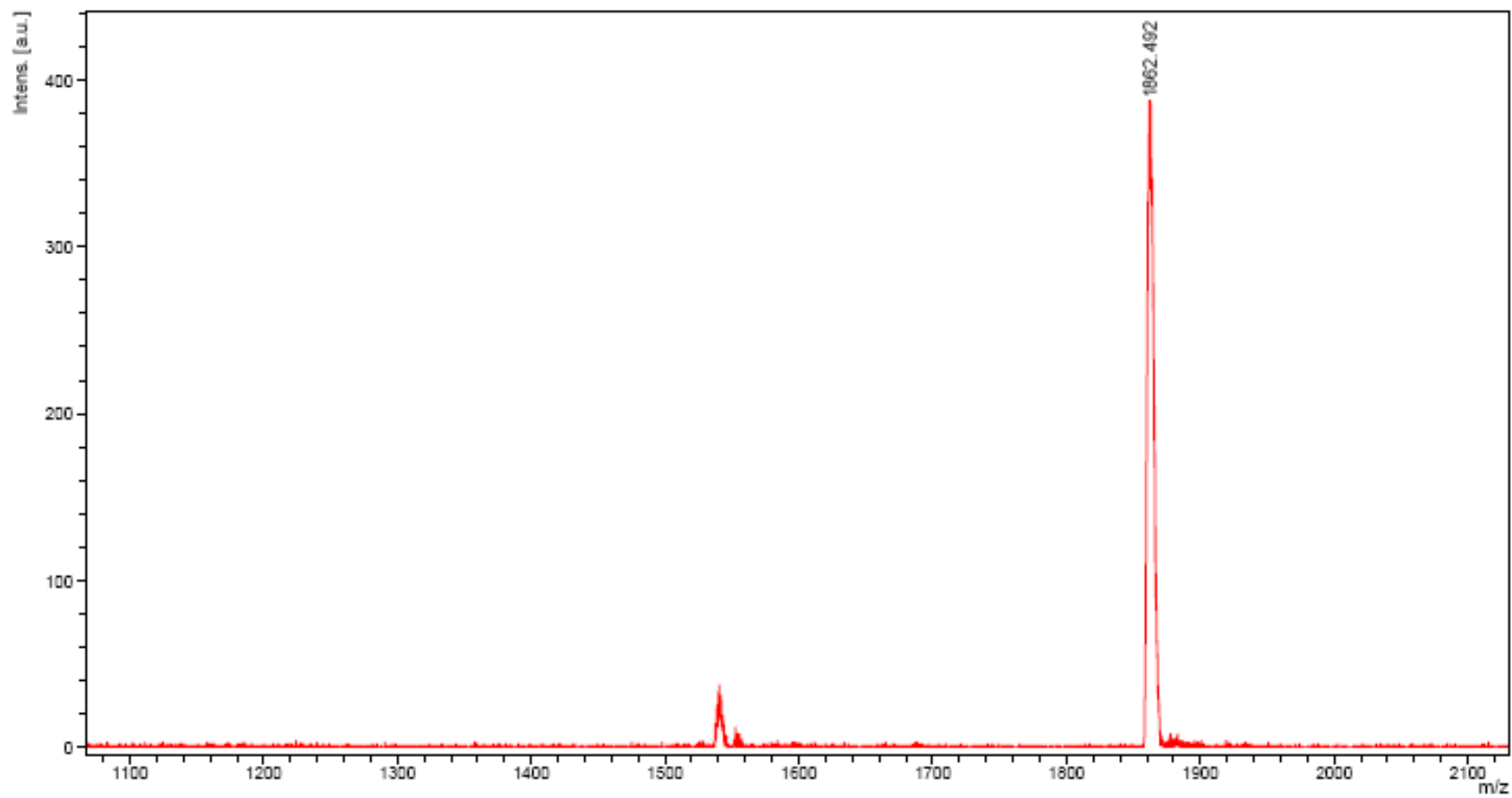


Figure A-27:  $^{13}\text{C}$ -NMR spectrum of compound Zn-15.



**Figure A-28:** Mass spectrum of compound **Zn-15**.



## **APPENDIX B**

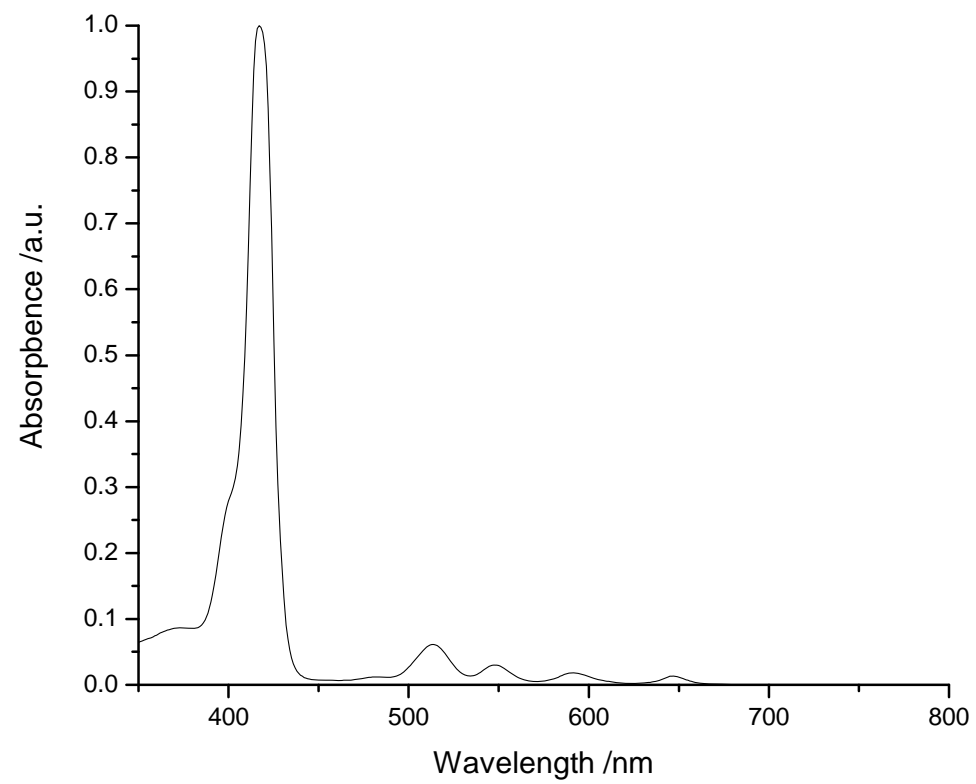


**Figure B-1:** Absorption spectrum of compound 1.

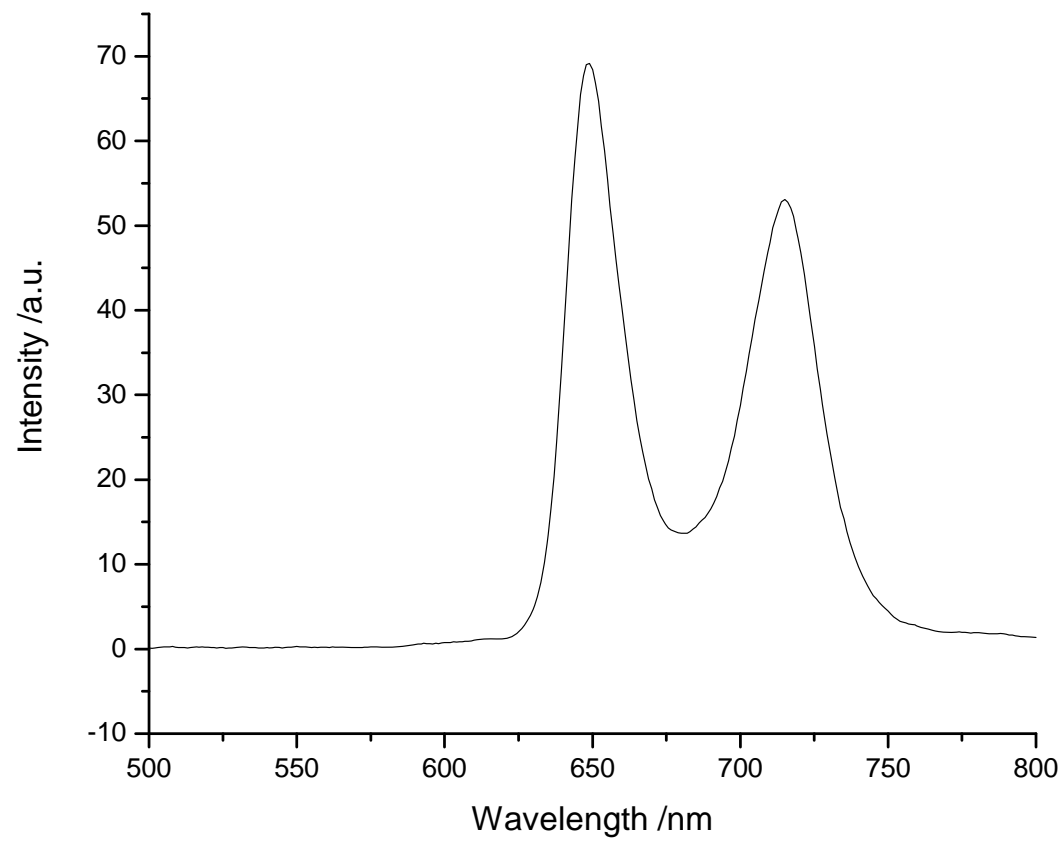


**Figure B-2:** Emission spectrum of compound 1.

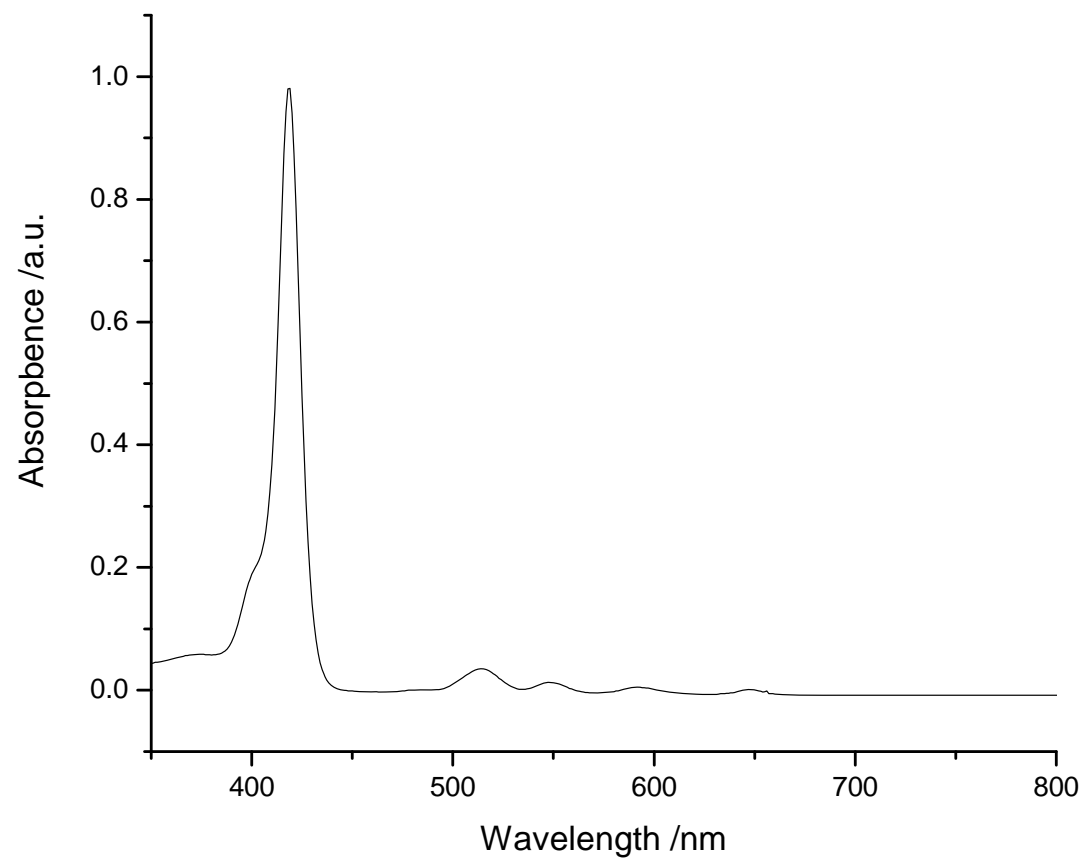


**Figure B-3:** Absorption spectrum of compound 2.

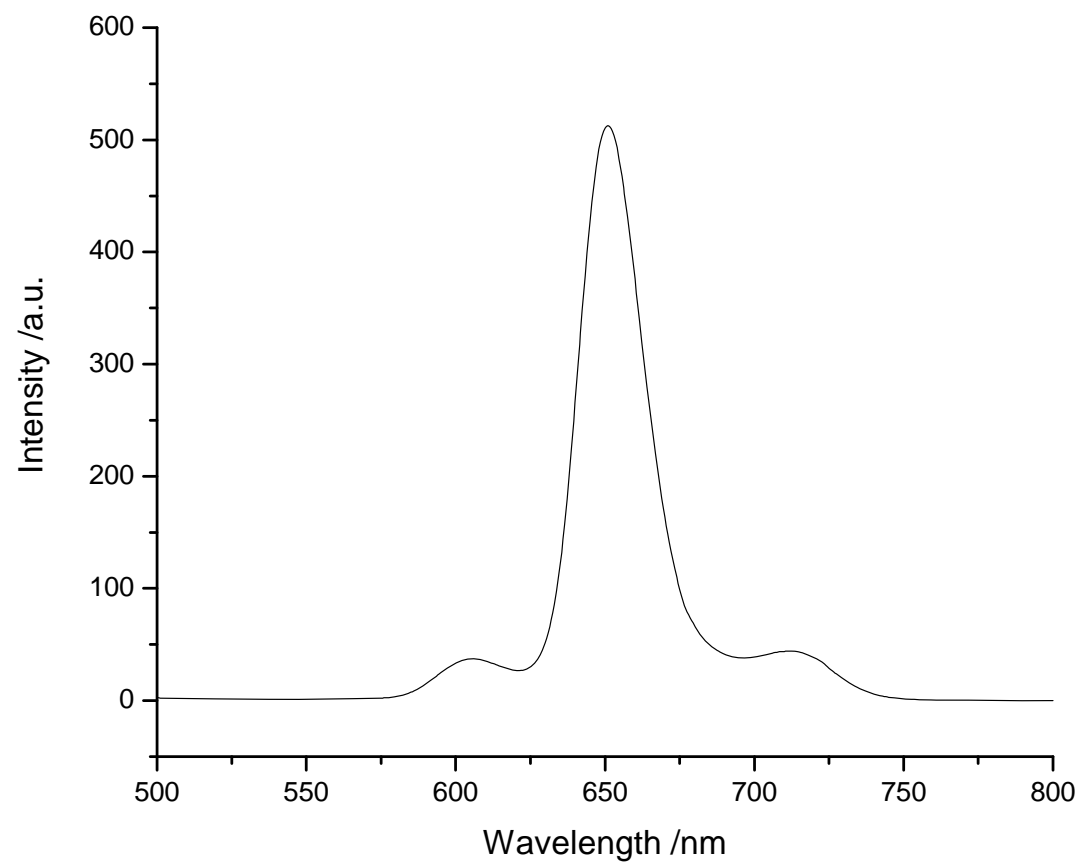


**Figure B-4:** Emission spectrum of compound 2.

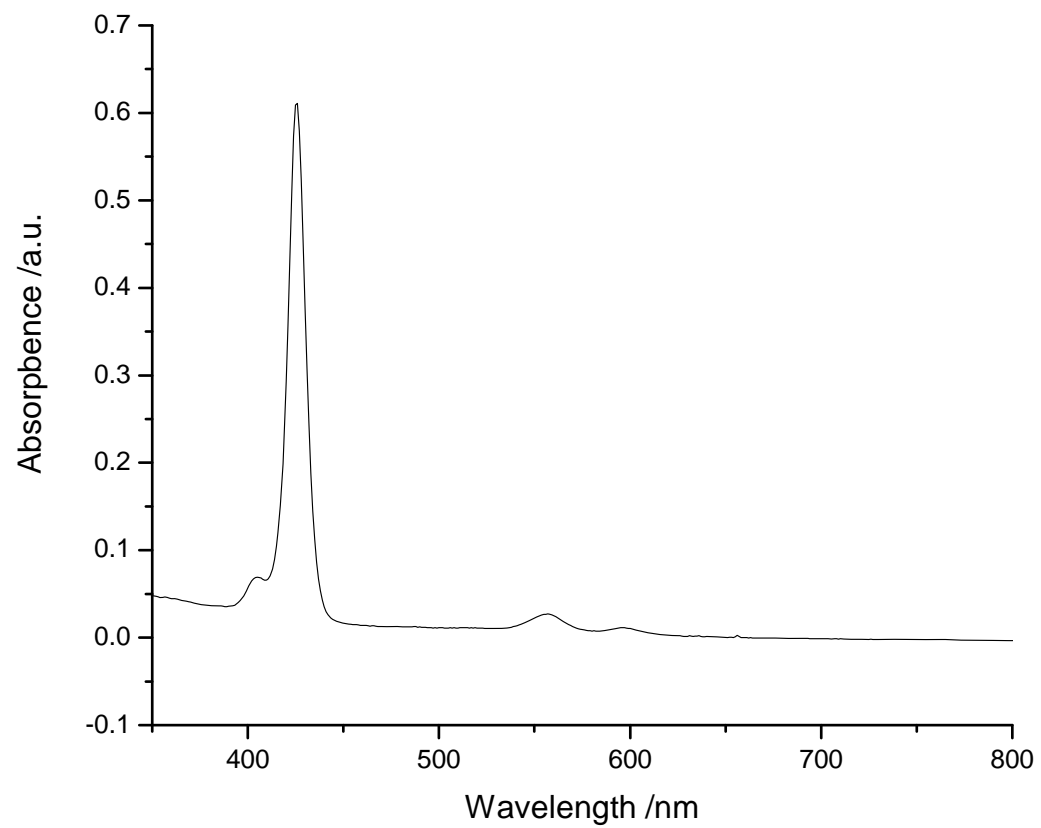


**Figure B-5:** Absorption spectrum of compound **Zn-1**.

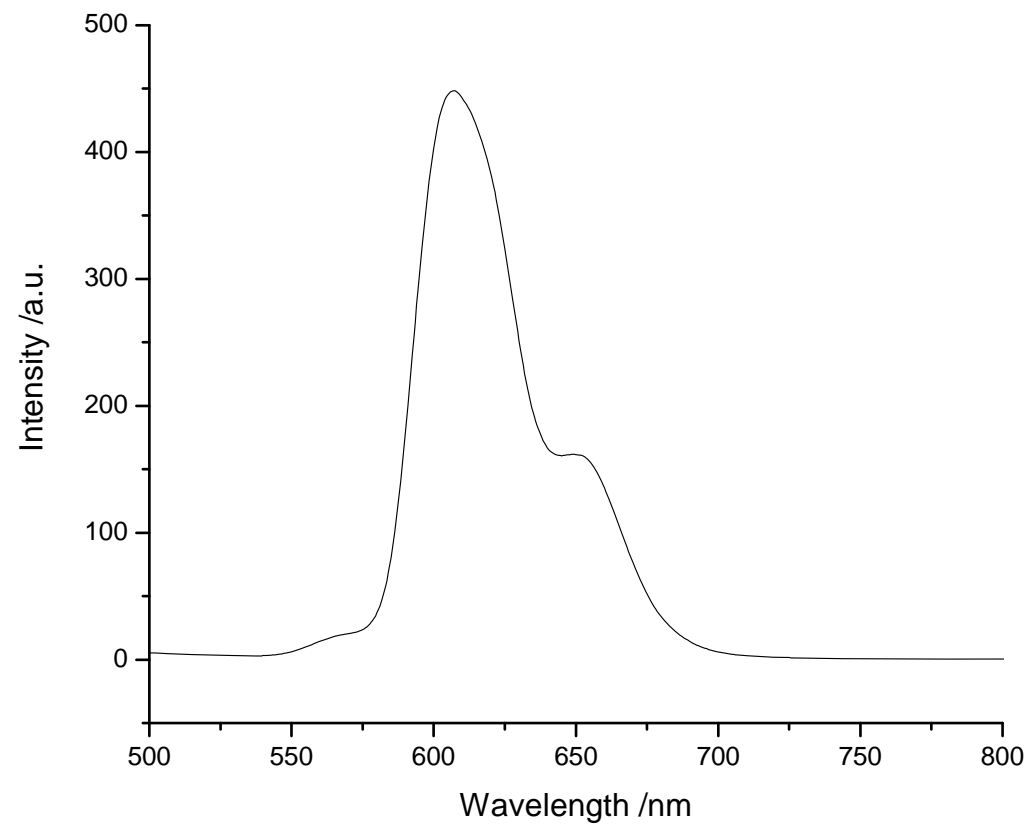


**Figure B-6:** Emission spectrum of compound **Zn-1**.

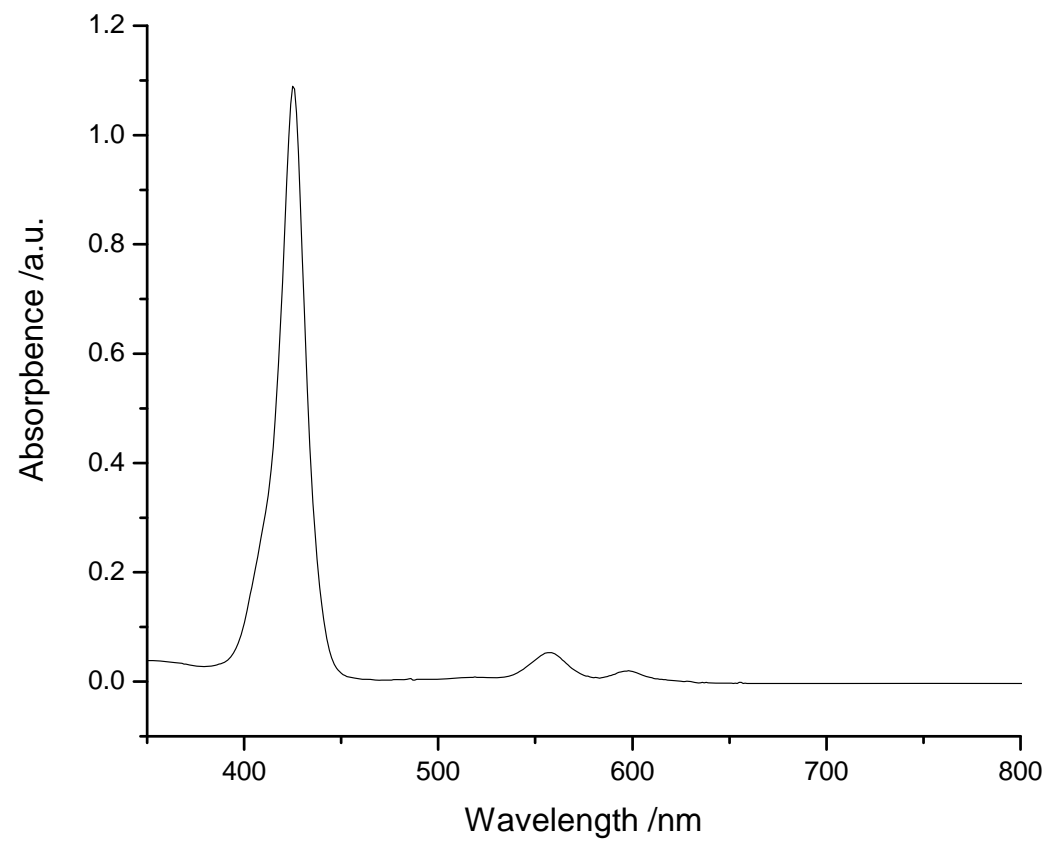


**Figure B-7:** Absorption spectrum of compound **Zn-2**.



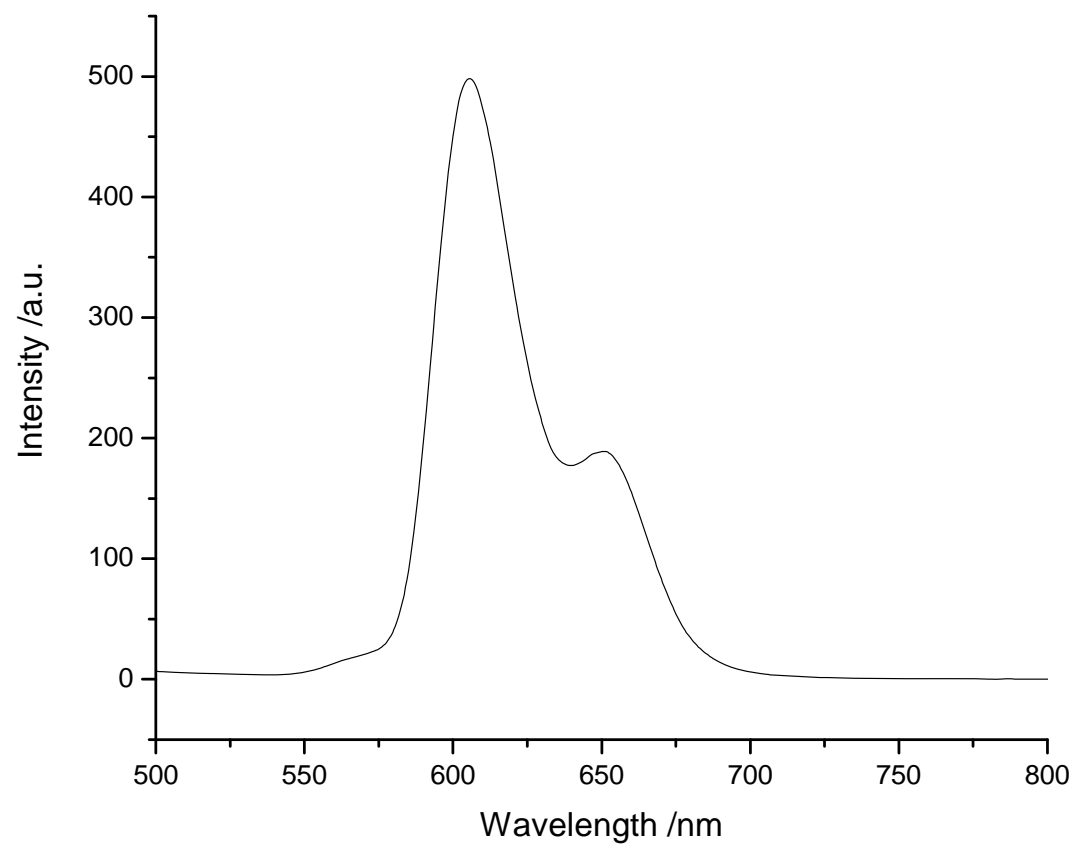


**Figure B-8:** Emission spectrum of compound **Zn-2**.

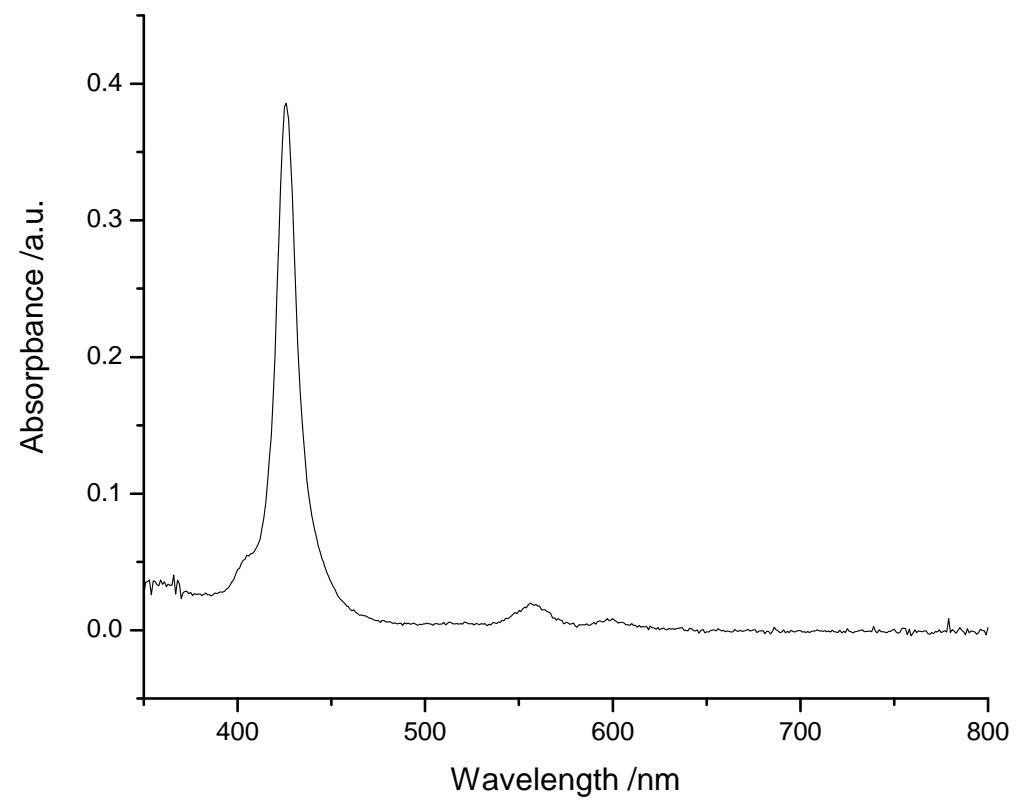


**Figure B-9:** Absorption spectrum of compound **Zn-14**.

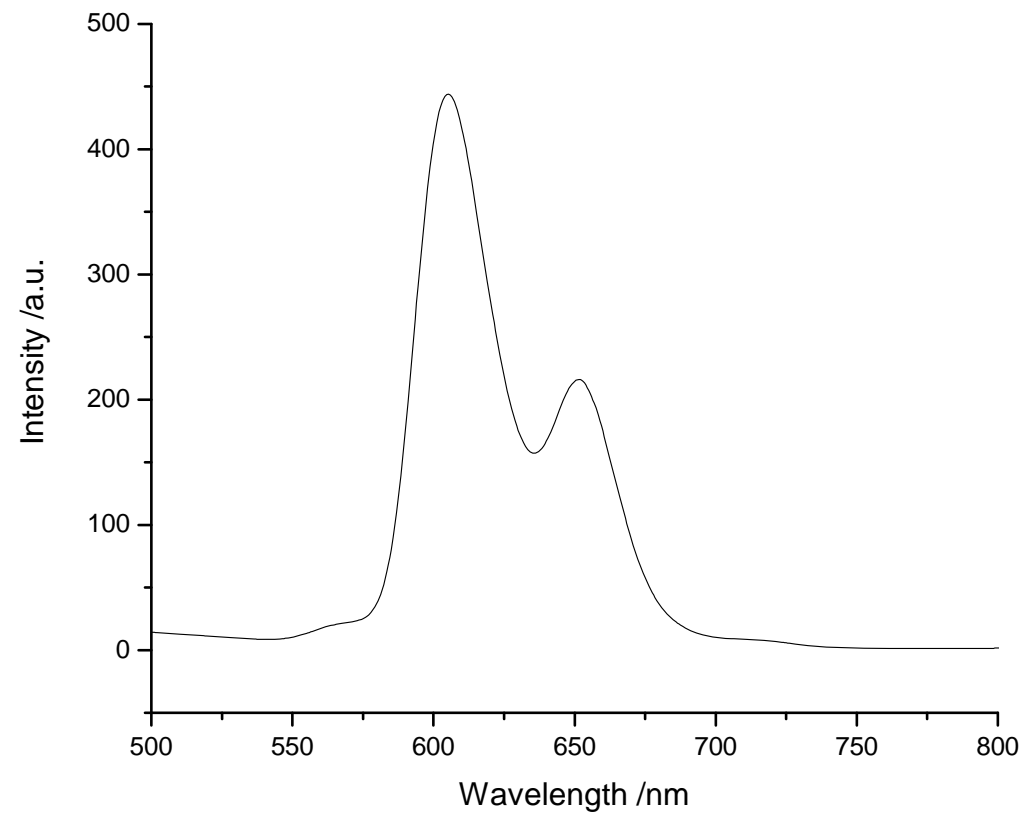


**Figure B-10:** Emission spectrum of compound **Zn-14**.

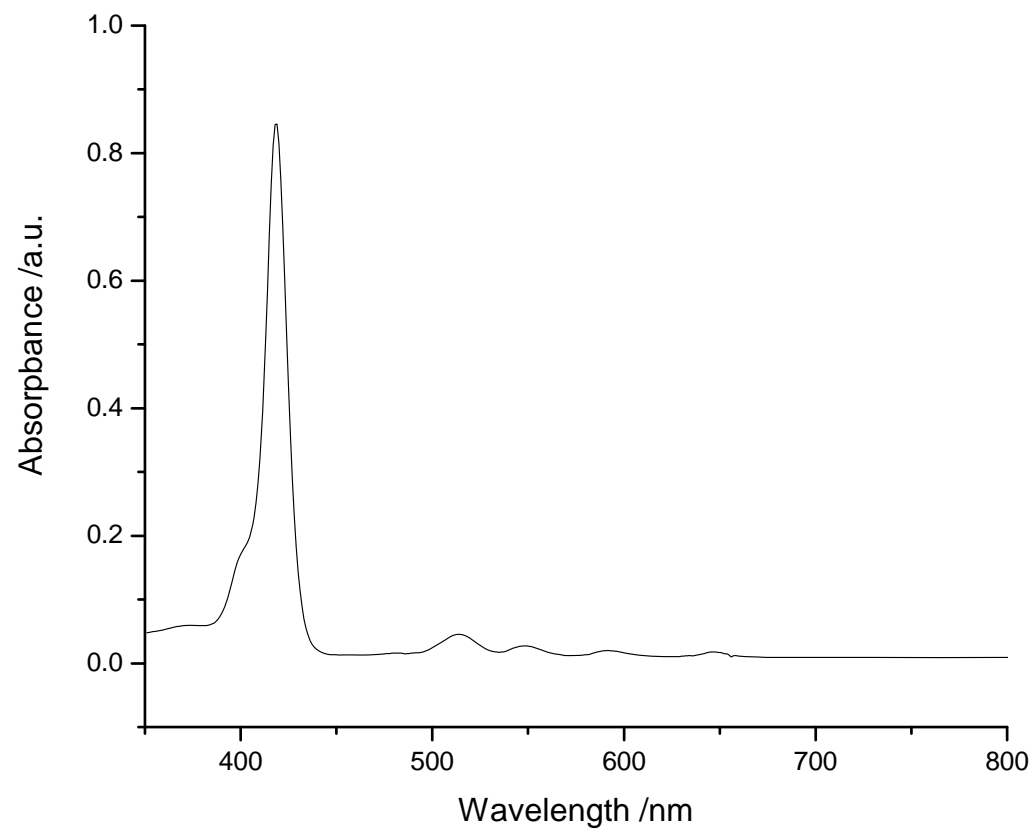


**Figure B-11:** Absorption spectrum of compound **15**.

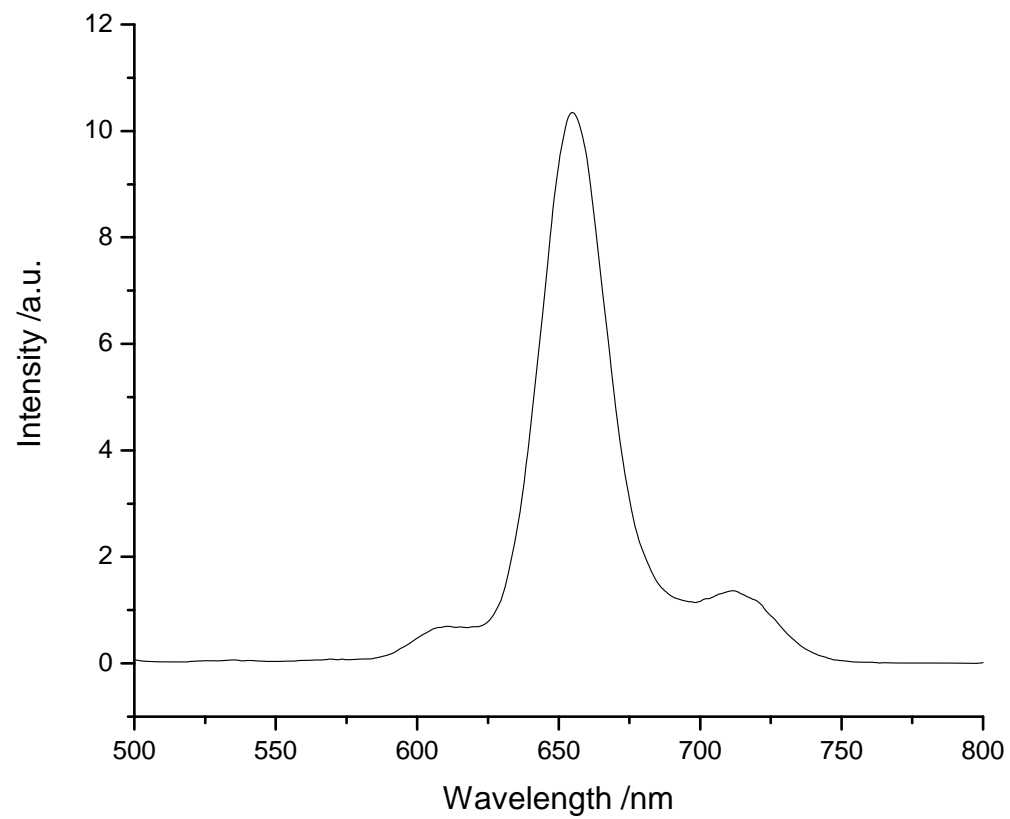


**Figure B-12:** Emission spectrum of compound **15**.

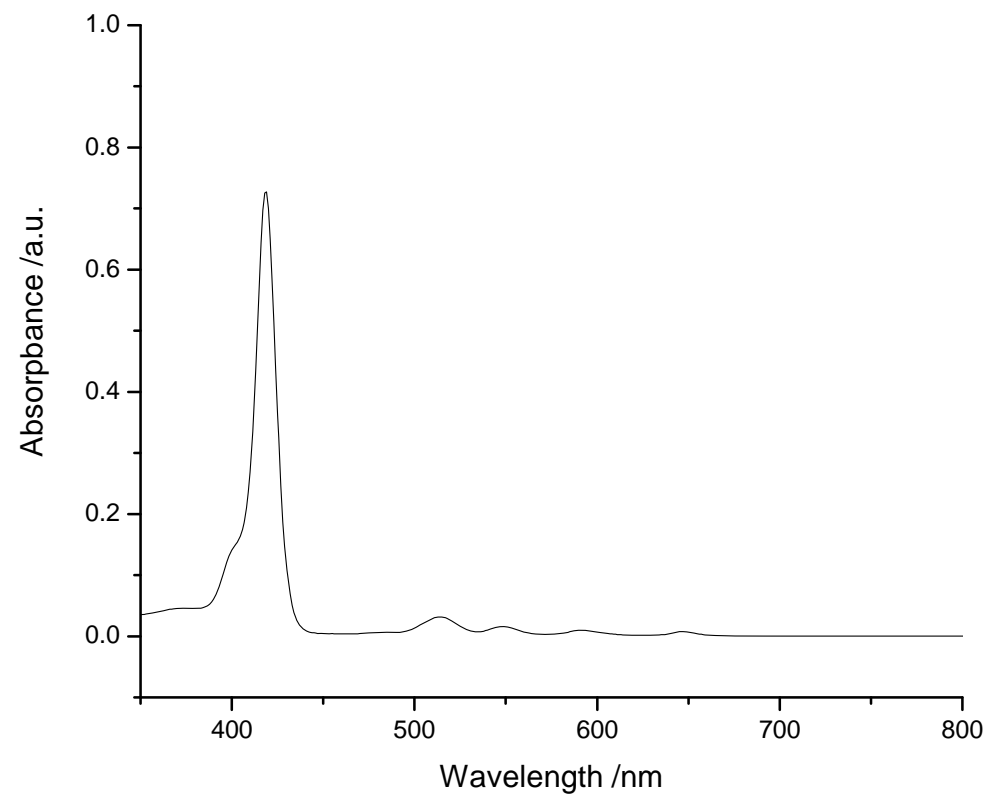


**Figure B-13:** Absorption spectrum of compound **Zn-15**.

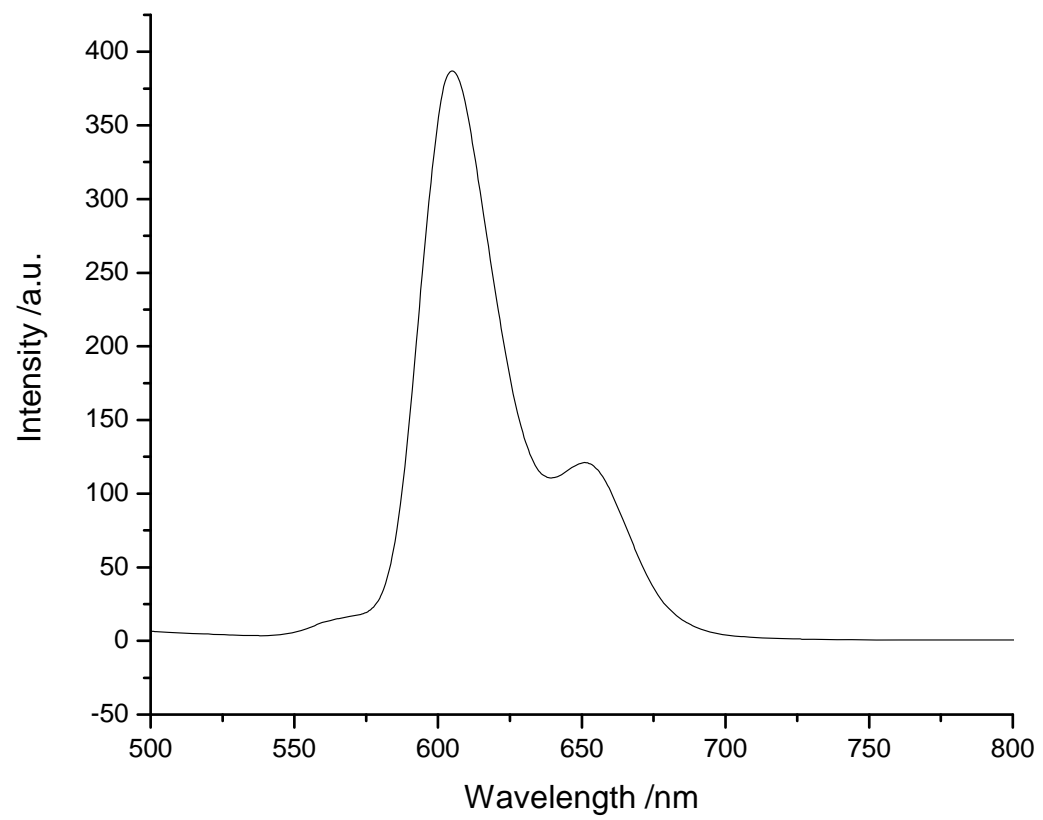


**Figure B-14:** Emission spectrum of compound **Zn-15**.

## VITA

Mr Chawanwit Reanprayoon was born on September 22, 1985 in Ratchaburi province, Thailand. He got a Bachelor's Degree of chemistry in Faculty of Science at Chulalongkorn University, Bangkok in 2007. After that, he was admitted into a Master Degree program in Petrochemistry and Polymer Science, Faculty of Science, Chulalongkorn University, Bangkok in 2007 and completed the program in 2011.